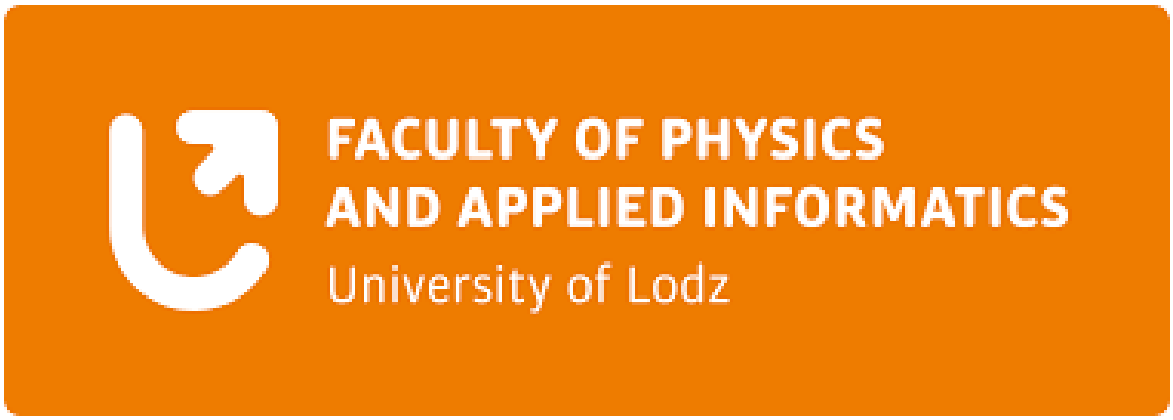

Study on the Application of Phototransferred Thermoluminescence to Reassessment of Radiation Dose Using the MCP-N and MTS-N Detectors

PhD Thesis

by

Hiba Musadaq Salim Al-Hameed

PhD Supervisor: DSc Andrzej Korejwo,
Professor of the University of Lodz

Department of Nuclear Physics and Radiation Safety

Łódź 2019

Acknowledgments

Undertaking this PhD has been a truly life-changing experience for me and it would not have been possible without the support and guidance that I received from many people.

I would like to express my special appreciation and thanks to my Supervisor, **DSc Andrzej Korejwo**, professor of the University of Lodz, for the guidance and encouragement of my research and for allowing me to grow as a research scientist. I have been extremely lucky to have a supervisor who cared so much about my work, and who responded to my questions and queries so promptly, you have been a tremendous mentor to me.

My sincere thanks and appreciation to, **Prof. Józef Andrzejewski**, DSc, for the supportive me along studying path.

In particular, I would like to thank **Dr Małgorzata Wrzesień**, your advice on both research as well as on my lab work have been great and valuable.

I would also like to thank all the **staff members in the University of Lodz,** Faculty of Physics and Applied Informatics, for helping me as my society even at times of hardship.

I would also like to say a heartfelt thanks to you to my **Mum**, **Dad**, for always believing in me and encouraging me to follow my dreams, and helping in whatever way they could during this challenging period.

I am very grateful to my husband **Eng. Forat Al-Sahar**, who has been by my side throughout this PhD, living every single minute with me, and without him, I would not have had the courage to embark on this journey in the first place.

Finally, to my sweetie **Maryam**, my little baby that past months, and she represented the light on my road and making it possible for me to complete what I started.

Table of contents

Abstract

The main topic of this work is an experimental study on the PTTL (PhotoTransferred ThermoLuminescence) phenomenon applying in dosimetry: an examination of the effect of UV and thermal stimulation parameters on the emission of thermoluminescence light, and as a consequence – the search for optimal stimulation conditions that determines the accuracy of the re-determination of dose. Measurements were performed with two types of dosimeters: MTS-N and MCP-N, using the RA'04 Reader-Analyser.

Radiation dose ranges reached up to 1000 mGy for MTS-N detectors and 25 mGy for MCP-N detectors, whose efficiency is 25–30 times higher than the efficiency of MTS-N detectors under standard measurement conditions. The dependence of PTTL data reading performance on UV wavelength, exposure time and temperature of detectors during UV irradiation was examined.

Analysis of the results obtained at three available UV wavelengths (254, 302 and 365 nm) showed that in the tested range the highest efficiency occurred at λ = 254 nm. Therefore, the subsequent search for optimal measurement conditions was conducted under UV stimulation with a wavelength of 254 nm.

The light emission efficiency of detectors was tested using the PTTL phenomenon in a wide range of stimulation parameters, such as UV exposure time combined with detector heating (from 30 min to 8 hours for MTS-N detectors and from 10 min to 4 hours for MCP-N detectors) and heating temperature during UV exposure (from 33 °C to 140 °C for MTS-N detectors and from 30 °C to 120 °C for MCP-N detectors).

The most important results relate to the usefulness of the PTTL method for the dose re-evaluation: indication of optimal conditions for UV exposure and thermal treatment of TL detectors within the limits of measurements performed, determination of PTTL reading performance and analysis of linearity of detector indications (the linear relationship between the number of counts and the dose is beneficial from a practical point of view). Studies have shown that the high sensitivity of MCP-N detectors in routine measurements of TL dosimetry is not reflected when the PTTL phenomenon is used: in repeated readings, MCP-N detectors proved to be similar or even less efficient than MTS-N, and also have a significant spread of performance.

Research Objective of the Present Study

Radiation dose control is extremely important, especially for people professionally exposed to ionising radiation. One of the most frequently used dosimeters is a personal dosimeter with thermoluminescence detectors (TLD). Doses registered by the detector are read in a special TLD reader. The dose information can be read once only: it is almost totally destroyed during the readout. To re-read the dose information, it is necessary, after the first reading of the detector, to perform optical stimulation by ultraviolet radiation with simultaneous heating. After such treatment, the detector can again become a source of luminescence light related to the primary exposure to ionizing radiation. Re-reading of the detector in the TLD reader is possible due to the phenomenon of UV light stimulated thermoluminescence (PhotoTransferred ThermoLuminescence: PTTL).

Obtaining at least some information during re-reading the detector is very helpful in situations such as loss of information about the dose in the event of measuring apparatus failure. The use of PTTL phenomenon to reassessing the dose may contribute to more complete results and this, in turn, is directly related to the safety of people exposed to ionising radiation.

Quality of the dose re-estimation while undergoing re-reading depends on some stimulation parameters. There is e.g. a wavelength of UV light, the temperature of detector heating during UV exposure, and time of UV exposure. Depending on these conditions, the re-reading performance and consequently also the accuracy of the dose measurement varies.

The main topic of this work is **searching for optimal conditions of TLD stimulation (with UV radiation and heating) to obtain the best results of dose re-estimation using PTTL phenomenon.** This requires testing a large set of parameters affecting detection performance. In this work, such studies were carried out using dosimeters with wide practical application: MTS-N and MCP-N.

1. Introduction

Thermoluminescence detectors, such as LiF:Mg,Ti and LiF:Mg,Cu,P, are widely used in the field of ionising radiation dosimetry because they are small in size, sensitive, tissue-equivalent for ionising radiation and do not require any power supply. Radiation and in particular ionising radiation occurs in a wide range of fields, covering medical applications in diagnosis via X-ray, in treatments via radiotherapy, as well as industrial applications, e.g. for defect control of materials and food sterilisation. Radiation protection is crucial for medical staff who conduct an X-ray, gamma and particle irradiation as well as for the workers at a nuclear plants and quality control. To allow appropriate protection, the extent of radiation exposure needs to be known. Therefore, collected and monitored data must be as accurate as possible. This is the aim of dosimetry.

The amount of ionising radiation (the dose) can be measured for a person at the workplace (personal dosimetry) or in a certain location (environmental dosimetry). Even though there is a variety of ways to achieve this, an increasingly frequent one is utilising the thermoluminescent properties of certain materials. These materials store the energy of incident ionising radiation for a certain amount of time and release the energy in the form of light once the material is heated. The amount of light emitted can be recorded and used to calculate the dose stored on the dosimeter containing the thermoluminescent crystal.

For this study the properties of a thermoluminescence material consisting of lithium fluoride doped with magnesium and titanium (LiF:Mg,Ti), and lithium fluoride doped with magnesium, copper and phosphorus (LiF:Mg,Cu,P) investigated using PTTL phenomenon.

2. Radiation Protection and Dosimetry

2.1. Ionising Radiation

Ionising radiation is increasingly used in a variety of applications in medicine, research and industry because of their known benefits for society. The radiation protection objective, therefore, is to keep the risks as low as reasonably achievable (ALARA) while maximising benefits [1].

Radiation is the emission or transmission of energy in the form of waves or particles through space or through a material medium [2].

Radiation is classified into two main categories:

- non-ionising radiation (cannot ionise matter because its energy is lower than the ionisation potential of a matter),
- ionising radiation (can ionise matter either directly or indirectly because its energy exceeds the ionisation potential of a matter).

Ionising radiation contains two major categories as shown in Fig. 2.1 [3].

- directly ionising radiation (charged particles): electrons, protons, alpha particles, heavy ions,
- indirectly ionising radiation (neutral particles): photons (X-rays, gamma rays), neutrons [4].

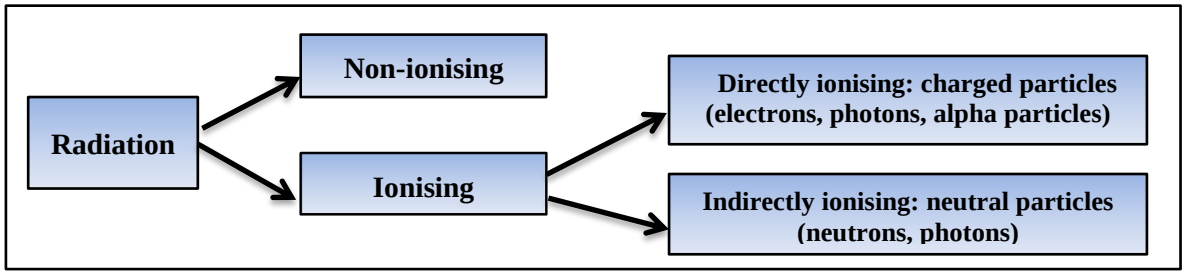

Fig. 2.1: Classification of radiation [4].

Both directly and indirectly ionising radiation is used in the treatment of diseases, mainly – but not exclusively – malignant diseases. The branch of medicine that uses radiation in the treatment of disease is called radiotherapy, therapeutic radiology or radiation oncology. Diagnostic radiology and nuclear medicine are branches of medicine that use ionising radiation in diagnosis of disease [4].

Both α and β particles are prominent examples of charged particle radiation. Neutrons and photons are both uncharged, the first is also counted among particle radiation while γ-rays and X-radiation are an electromagnetic radiation.

Before discussing radiation protection and dosimetry in more detail, some important dose quantities when working with radiation should be recalled.

2.2. Dose Quantities and Units

The dosimetric concepts and the definition of dose quantities for use in radiation protection for external irradiation were defined by the International Commission on Radiological Protection (ICRP) and the International Commission on Radiation Units and Measurements (ICRU) which regularly publish updates or revisions. Three types of quantities are of special relevance for radiation protection purposes against external irradiation: [5]

- physical quantities,
- protection quantities,
- operational quantities.

2.2.1. Physical Quantities

These important quantities are defined:

- kerma,
- absorbed dose,
- linear energy transfer (LET).

They are defined by the International Commission on Radiation Units and Measurements in ICRU Report 85 [6].

Kerma

The kerma is the quotient of sum of Kinetic Energy Released per MAss. It is defined by:

$$K = \frac{\mathrm{d}E_{\mathrm{tr}}}{\mathrm{d}m}, \tag{2.1}$$

where $\mathrm{d}E_{\mathrm{tr}}$ is the mean sum of the initial kinetic energies of all the charged particles liberated in a mass dm of a material by the uncharged particles incident on dm.

Therefore, kerma is defined only for uncharged particles (photons or neutrons). The unit of kerma is joule per kilogram ($\mathrm{J \cdot kg^{-1}}$) and is called gray (Gy).

Absorbed Dose

The absorbed dose is the quotient of $\mathrm{d}\bar{\varepsilon}$ by dm, where $\mathrm{d}\bar{\varepsilon}$ is the mean energy imparted to matter of mass dm:

$$D = \frac{\mathrm{d}\bar{\varepsilon}}{\mathrm{d}m}. \tag{2.2}$$

The unit of absorbed dose is joule per kilogram, and is called gray (Gy).

Linear Energy Transfer

The Linear Energy Transfer (LET, or L_{Δ}) describes the action of charged particle into the matter. It is the quotient of $\mathrm{d}E_{\Delta}$ energy by dl, where $\mathrm{d}E_{\Delta}$ is the mean energy lost by the charged particles due to electronic interactions in traversing a distance dl, minus the mean sum of the kinetic energies in excess of Δ of all the electrons released by the charged particles:

$$\mathrm{LET} = \frac{\mathrm{d}E_{\Delta}}{\mathrm{d}m}. \tag{2.3}$$

The unit of LET is joule per metre ($\mathrm{J \cdot m^{-1}}$), or, in practice, kiloelectronvolt per millimetre (keV/mm) of track length.

In general, the larger the mass or charge of the particle with the same energy, the greater the LET [7,8].

2.2.2. Protection Quantities

The important protection quantities are

- equivalent dose of an organ/tissue,
- effective dose for whole the body.

Protection quantities are defined by the International Commission on Radiological Protection in ICRP Publication 103 [9]. These quantities cannot be measured directly; therefore operational quantities are used to estimate the protection quantities.

Equivalent Dose of an Organ / Tissue

The equivalent dose (radiation weighted dose), $H_{T,R}$, in an organ or tissue, takes the biological effects of the absorbed dose depending on the type of radiation into account. The equivalent dose can then be calculated using the following equation:

$$H_T = \sum_R w_R D_{T,R} \,, \tag{2.4}$$

where w_R is a weighting factor for different types of radiation (R) and $D_{T,R}$ is the mean absorbed dose in a tissue T due to radiation of type R. The unit is the same as for the absorbed dose ($J \cdot kg^{-1}$) but it is named sievert (Sv) [9,10].

Effective Dose

The equivalent dose takes into account biological effects of different types of radiation on an organ or tissue through different weighting factors w_R. The effective dose goes one step further and also includes biological effects on a set of tissues. This is done by another set of weighting factors w_T related to tissues (T):

$$E = \sum_T w_T H_T = \sum_T w_T \sum_R w_R D_{T,R} \,, \tag{2.5}$$

where H_T is the equivalent dose in a tissue T, and w_T is the tissue weighting factor for tissue T. The unit of effective dose is joule per kilogram ($J \cdot kg^{-1}$) and it is also called sievert (Sv).

2.2.3. Operational Quantities

The operational quantities were determined by ICRU to give an estimate of the suitable protection quantities. These quantities are viable for both area and personal monitoring. Operational quantities are:

- ambient dose equivalent,
- directional dose equivalent,
- personal dose equivalent.

Three operational quantities are based on the concept of the dose equivalent, H, which is defined as the product of Q and D at a point in tissue, where D is the absorbed dose and Q is the quality factor according to equation:

$$H = Q \cdot D \tag{2.6}$$

The unit is joule per kilogram ($J \cdot kg^{-1}$) and it is again called sievert (Sv).

Although both, the dose equivalent and the equivalent dose, are derived from the absorbed dose, they differ as the respective weighting (or quality) factors are calculated differently. Where the weighting factor w_R for the equivalent dose depends only on the type of radiation from the outside, the quality factor Q for the dose equivalent includes secondary radiation from the inside, which is produced in the tissue itself in the course of the absorption process. It is a function of the linear energy transfer in water and can change in a body. All three types of dose equivalent are defined at a certain point at a depth d either inside a sphere (the ICRU sphere for the ambient dose equivalent and the directional dose equivalent) or inside a body (for the personal dose equivalent).

The unit is $J \cdot kg^{-1}$ for all three quantities and is called sievert (Sv) [11, 12].

Ambient Dose Equivalent

The ambient dose equivalent, $H^*(d)$, is the dose equivalent at a depth d in the ICRU sphere, produced by an expanded and aligned radiation field.

Directional Dose Equivalent

The directional dose equivalent $H'(d,\Omega)$ is similar to the ambient dose equivalent but with a specified direction in addition to the depth in the ICRU sphere.

Personal Dose Equivalent

The personal dose equivalent $H_p(d)$ is used in individual monitoring and it is the dose equivalent at a specified depth d in a body. The penetration depth radiation is specified as:

- for strongly penetrating radiation 10 mm (for whole the body),
- for weakly penetrating radiation 0.07 mm (for the skin),
- for weakly penetrating radiation 3 mm (for the eye).

Instruments, which are used to measure the ambient dose equivalent, shall have an isotropic response. Instruments, which are used to measure directional dose equivalent and personal dose equivalent, shall have a defined directional response. Examples of detectors that can measure the ambient dose equivalent are ionisation chambers and GM tubes. Also passive detectors, like TLDs, can be used [13].

2.3. Biological Effects of Ionising Radiation

When ionising radiation passes through tissue, the component atoms may be ionised or excited. As a result the structure of molecules may change and lead to cell damage. In particular, the genetic material of the cell, the DNA may be changed. Two categories of radiation-induced injury are recognised:

Non-stochastic effects: (deterministic) are associated with high doses and are characterised by a threshold. Above this threshold the damage increases with dose. This threshold depends on the material or organ in question. The threshold for tissue reactions is between 0.1 and 0.5 Gy.

Stochastic effects: are associated with lower doses and have no threshold. The main stochastic effect is cancer. As there is no minimal dose at which stochastic radiation effects start to occur, the lower limit at which radiation can be detected should be kept as low as possible, because small doses acquired over longer durations add up and can also have harmful effects.

The biological effect of ionising radiation depends on:

- radiation intensity,
- energy type of the radiation,

- exposure time,
- area exposed,
- depth of energy deposition.

Different quantities such as the absorbed dose, the equivalent dose, and the effective dose have been introduced to specify the dose received and the biological effectiveness of that dose [14, 15].

2.3.1 Quality or Weighting Factor

The biological effect of radiation is not directly proportional to the energy deposited by radiation in an organism. It depends, in addition, on the way in which the energy is deposited along the path of the radiation, and this, in turn, depends on the type of radiation and its energy. Thus the biological effect of the radiation increases with the linear energy transfer (LET) increasing. Thus for the same absorbed dose, the biological effect from high LET radiation such as α particles or protons is much greater than that from low LET radiation such as β or γ rays. The weighting factor w_R is introduced to take into account this difference in the biological effects of different types of radiation [9]. The weighting factors for the various types of radiation and energies are given in Table 2.1.

Table 2.1: The ICRP radiation weighting factors [9]

Radiation Type	Radiation Weighting Factor, w_R
Photons	1
Electrons and muons	1
Protons and charged pions	2
Alpha particles, fission fragments, heavy ions	20
Neutrons	5–20 (continuous function of neutron energy)

2.4. Radiation Protection Principles

Radiation protection is based on the three fundamental principles of justification exposure, keeping doses as low as reasonably achievable (optimisation) and the application of dose limits. The International Commission on Radiological Protection (ICRP) is responsible for the development of these principles. A rule for radiation protection is the so called ALARA principle, meaning As Low As

Reasonably Achievable. In accordance with this principle there are guidelines that control the amount of radiation human beings are allowed to be exposed to.

1. Justification

Justification needs to evaluate the benefits of radiation and doing so in an easy way especially in the case of radiotherapy. Assessment of the risks requires a knowledge of the dose received by persons.

2. Optimisation

Optimisation of the procedure is a crucial phenomenon. When radiation is to be used, the exposure should be optimised to minimise any possibility of detriment. An optimisation can be divided into two types. Firstly that, applied in the radiotherapy, optimising the doses for the tumour and other structures. The second one is optimising the protection of occupational workers, patients, and general public. Both the justification and optimisation are included in a part of strategies when handling the potential situations or procedure.

3. Dose limits

Dose limits are one of the three principles of protection as introduced by ICRP. Dose constraints are used in an optimisation process to guide treatment planning. Constraints and the importance thereof may be subject to change to achieve the optimum solution to a problem. The main idea of dose limitation is described in the phrases ‘No dose limitation for medical exposure of the patient it is always assumed that the benefits for the patient outweighs the risks’ and ‘Limits need to be applied for public and occupational exposures’ [9, 16, 17].

2.4.1. Radiation Protection Rules

The primary objective of radiological protection is to protect against radiation exposure or to reduce the amount of exposure to the extent that it minimises its risk.

Exposure to ionising radiation is accomplished either:

- through exposure to radiation from the source located outside the body and capable of penetrating the body,

or

• from within the body as a result of the entry of radioactive substances into the body through the digestive or respiratory system or through skin.

Radiation exposure from an external source of radiation may be achieved from a device for the production of radiation or from radioactive material, with different types and energy of the radiation.

Radiation from the x-ray tube or gamma ray sources or neutrons is capable of penetrating the body and affecting the insides. For comparison, the beta particles can penetrate the body and enter the internal tissues at a depth of a few millimetres.

To reduce the value of radiation exposure resulting from radiological practices, it is possible to employ three main principles to reduce the value of exposure from an external radiation source.

1. Time

Exposure time is a key factor in the exposure to an external radiative source or during the period of taking radioactive nuclides into the internal radiation exposure.

Reduction of the exposure time causes a reduction of radioactive dose. When a dose limit is established and a dose rate is known, we can determine the limit of time to deal with the source of radiation, to ensure that the dose limit is not exceeded, using the following formula:

$$\text{Time Limit} = \frac{\text{Dose Limit}}{\text{Dose Rate}}. \qquad (2.7)$$

Time is an important factor in the medical and industrial applications of radiation.

2. Distance

Distance plays a key role in radiation protection. The greater the distance from the source of radiation, the lower the amount of radiation exposure. The effect of distance on the intensity is similar as in the case of light emitted from a point source. The closer the light source is, the greater the intensity and vice versa. This applies exactly to the amount of radiation exposure: the farther away from the source of radiation, the lower the radiation exposure. Additionally, the absorption of radiation in the air reduces the dose, insignificantly for electromagnetic radiation at small distances, strongly for charged particles.

3. Shielding

When the radiation passes through material, it deposits energy in this material through the production of ions and the excitation of atoms, and thus the material absorbs the radiation energy. The ability of the material to absorb radiative energy depends on several factors, such as the type of radiation, its energy and the type of material.

The principles of radiation protection to reduce the amount of radiation doses from an external radioactive source include:

- reduce the time needed to deal with the radiation source,
- increase the time before dealing with sources of decay able radiation to ensure that the amount of radiation activity is reduced if possible,
- work to increase the distance from the source of radiation as far as possible,
- use appropriate shields depending on the type and energy of the radiation,
- use one or more factors or all available to reduce the amount of radiation exposure whenever we were to keep the radiation exposure rate as low as possible,
- work to study the efficiency of workers in reducing radiation exposure and avoid wasting money and time on procedures that do not affect the process of reducing the amount of radiation exposure [18].

2.5. Radiation Dosimeters

A dosimeter is a radiation detection device used to measure doses from ionising radiation. For a person who works with radiation it is necessary to monitor and record the amount of radiation received. Therefore, it should be possible to measure a dose received in a short time as well as to determine the entire dose received in a long time.

Dosimeters are classified into two general categories:

- a passive dosimeter produces a radiation-induced signal, which is stored in the device; the dosimeter is then processed and the output is analysed;
- an active dosimeter produces a radiation-induced signal and displays direct reading of the detected dose or dose rate in real time [19].

2.6. Thermoluminescence Dosimetry

The sensitive volume of a thermoluminescence dosimeter (TLD) consists of a small mass of crystalline dielectric material containing suitable activators to make it perform as a thermoluminescent phosphor. Thermoluminescence dosimetry is used in many scientific applications and applied in radiation protection, radiotherapy, industry, environmental and space research, using many different materials. They use the ability to store the energy of ionising radiation and release this energy as light when the crystal is heated. Thermoluminescence dosimeters and difficulties arising with their usage will be described in more detail in the following chapters. The properties of thermoluminescence phenomenon are described in the chapter 3, and application of TLD systems – in chapter 5.

3. Thermoluminescence Theory

3.1. Luminescence Phenomena

The luminescence is defined as the emission of optical light from a matter following the absorption of energy. According to Stokes' law, the wavelength of emitted light exceeds a wavelength of incident radiation. The wavelength of emitted light is characteristic for the luminescent substance, not for incident radiation. The light emitted should be visible light, ultra-violet, or infrared light [20].

3.1.1. Luminescence and Stokes' Law

This special cold light emission, luminescence, does not include the emission of blackbody radiation, and involves two steps:

- the excitation of single atoms, single molecules, combinations of molecules, or a crystal of a solid material to higher energy state,
- subsequent emission of photons or simply light [21].

The different types of luminescence are named according to the radiation that leads to luminescence. They are described and summarised below:

- photoluminescence: excitation by ultraviolet or optical light,
- radioluminescence: excitation by ionising radiations (x-rays, γ-rays and charged particles).

In addition to excitation by radiation, luminescence can also be generated from other types of energy [22]:

- chemiluminescence: chemical energy,
- triboluminescence: mechanical energy,
- electroluminescence: electric field,
- bioluminescence: biochemical energy,
- sonoluminescence: sound waves.

Light emission can be subclassified into two types:

- phosphorescence (delayed emission) where time of the light emission exceeds 10^{-8} s (this process is temperature dependent),
- fluorescence (prompt emission) where time of the light emission is smaller than 10^{-8} s (temperature independent process) [22, 23].

These types depend on features of lifetime or time delay τ_c between the absorption of energy and emission of light. Phosphorescence is hence characterised by a delay between energy absorption and light emission. Phosphorescence also continues for some time after the excitation has been removed, from about 10^{-3} second to days or even years.

The family tree of luminescence phenomena is shown in figure below.

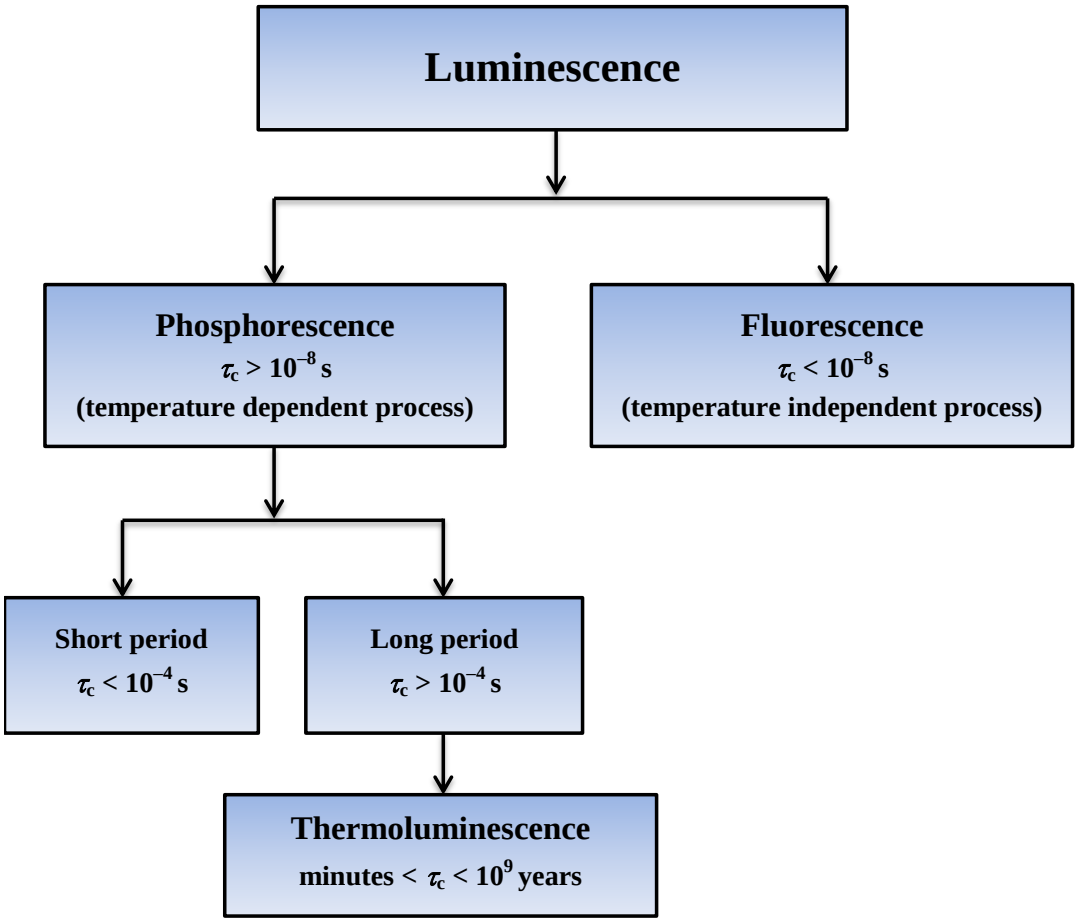

Fig. 3.1: The family tree of luminescence phenomena [21].

3.2. Concepts of Thermoluminescence

3.2.1. Definition of Thermoluminescence

The phenomenon of thermoluminescence of minerals was known as early as in 1663. It was at that time when sir Robert Boyle, upon warming a diamond in contact with his body in the dark, saw a glimmering light. Wiedman and Schmidt are the first who used the term ‘thermoluminescence’ in literature in 1895 for the observation of excess light emission over the thermal background [19].

Thermoluminescence (TL) is thermally stimulated emission of stored energy in the form of radiation (light) by insulator or semiconductor material. The energy can be stored by exposing the material to ionising or non-ionising radiation (ultraviolet light). The thermoluminescence dosimetry is used to measure the dose of ionising radiation.

3.2.2. Mechanism of the Process

The phenomenon of thermoluminescence can be explained in terms of the band theory of solids. Before irradiation, electrons are located in the valence band inside the crystal. When the ionising radiation interacts with thermoluminescence material, free electrons are produced and transferred from the valence band to the conduction band. Therefore, a hole (absence of an electron) remains in the valence band and can also move inside the crystal. Due to impurities used to increase the number of traps in the lattice and to increase the number of luminescence centres and doping of the crystal, electron and hole traps are created in the band gap between the valence and the conduction band. Thus electrons and holes are trapped at defects. Many hole centres are thermally unstable and may decay rapidly at normal room temperature. If these traps are deep, the electrons and holes will not have enough energy to escape. During the heating of crystal their energy is increased, they leave the traps and recombine at the luminescence centres. The effect of such heating is shown in Fig. 3.2 [24, 25]. The production of free electrons is associated with the production of free positive holes which may also migrate, in energy terms, via the valence band [26].

A TL detector can be considered as an integrating detector in which the number of electrons (e^-) and holes (h), which are trapped, is the number of the e^-/ h pairs which are produced during the exposure. Preferably, every trapped e^-/ h emits one photon. Consequently, the number of emitted photons is equal to the number of charged pairs, which are also proportional to the dose which is absorbed by the crystal.

By increasing the temperature, the escape rate is increased and the mean half-life of e^-/ h is reduced. This rate, as it is increased, reaches a maximum at a specific temperature and then is rapidly reduced. But as the intensity of the emitted light is proportional to this rate, it could be realised, that there would be a creation of a peak in the graph of intensity versus temperature, called glow peak, and the graph called glow curve [27, 28].

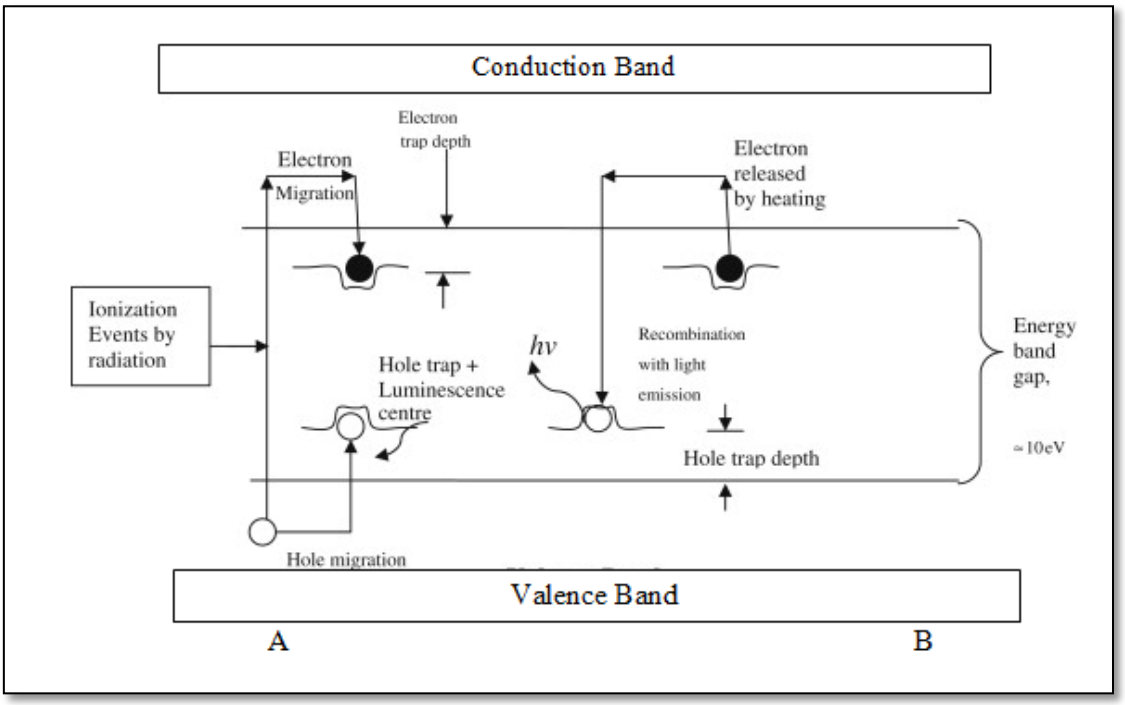

Fig. 3.2: Energy-level diagram of the thermoluminescence process: (A) ionisation by radiation, and trapping of electrons and holes; (B) heating to release electrons, allowing luminescence production [25].

In total, thermoluminescence can be described by two stages:

- the first stage is the change of the system from equilibrium to the metastable state by absorption of energy from UV or ionising radiation,
- the second stage is the relaxation of the system back to the equilibrium by energy release such as light with the help of thermal stimulation.

Thus, thermoluminescence is the thermally stimulated emission of light following the previous absorption of energy from radiation [29].

These stages and light emission will be discussed briefly.

1. Energy Storage

There are two processes for the basis of this absorbed energy:

- electronic excitation,
- displacement damage.

At the end of these processes, radiation-induced defects are formed in the material structure. Radiation-induced defects are localised electron states occupied by the non-equilibrium concentration of electrons [30].

Before irradiation, materials have electron energy states and after irradiation, some of these states are occupied by a non-equilibrium concentration of electrons. Therefore, these occupied states are called radiation-induced defects. According to McKeever, the cause of defect creation is electron excitation rather than non-ionising displacement damage.

Energy storage caused by electron excitation takes place by the electron-hole pair production and excitation creation. Electron-hole pair production is the formation of mobile holes and electrons in the crystal structure of the material after radiation. In addition, there exists a mid-gap state caused by defects which may be created by pre-existing impurities or radiation-induced defects. This gap is found between the two energy bands, called conduction band and valence band. The valence band is the outermost energy level and contains electron-hole pairs in the ground state of the solid. On the other hand, in the conduction band, electrons are free to move and have the ability to produce electric current.

According to thermoluminescence phenomena, it is assumed that there are two kinds of imperfections called electron trap and hole trap in the crystal which are localised at mid gap states [29, 31, 32].

In the mid-gap, the electron trap is located close to the conduction band and the hole trap is close to the valence band.

Figure 3.2 illustrates the energy storage mechanism. After irradiation, the electrons pass from valence band to conduction band and hole becomes positively charged area in the valence band. When the electron reaches the conduction band, electron find its way into an electron trap and hole occupies its associated trap. Hole traps are called luminescence centre in this process in the mid gap, the electron trap is close to the conduction band and the hole trap is far from the valence band.

After irradiation, the electrons pass from valence band to conduction band and positively charged objects in the valence band – holes – are created. When an electron reaches the conduction band, this electron finds its way into an electron trap and, moreover, a hole occupies its associated trap. Hole traps created in this process are called *luminescence centres* [29, 31–33].

2. Energy Release

Excitation can be removed by heating the material to suitable temperature (in TL dosimetry) or by light (as in X-ray phosphor plates). The deexcitation results in the release of the stored energy. The state of the material changes from metastable to ground.

When temperature increases, the electron trapped in the electron trap is released to the conduction band. After that electron is free to re-trap or recombine with the hole found in the hole trap. The recombination of the electron with the hole in hole trap results in the emission of photons. In this case, hole trap is called as *recombination centre* [29].

3. Glow Curve

After the energy release, the output of the emitted light as a function of temperature is called *thermoluminescence glow curve*. The shape of the glow curves contains of one or more peaks of emitted light and some of them may overlap. The magnitude and form of the glow curves depends on the spectral response of the light sensitive device, different filter usage between the sample and the detector and heating rate. In addition, when the sample is irradiated it has only ‘one shot effect’. A second thermoluminescence emission cannot be recorded by cooling and reheating it unless it is not irradiated again. Figure 3.3 shows glow curve examples of some thermoluminescent materials.

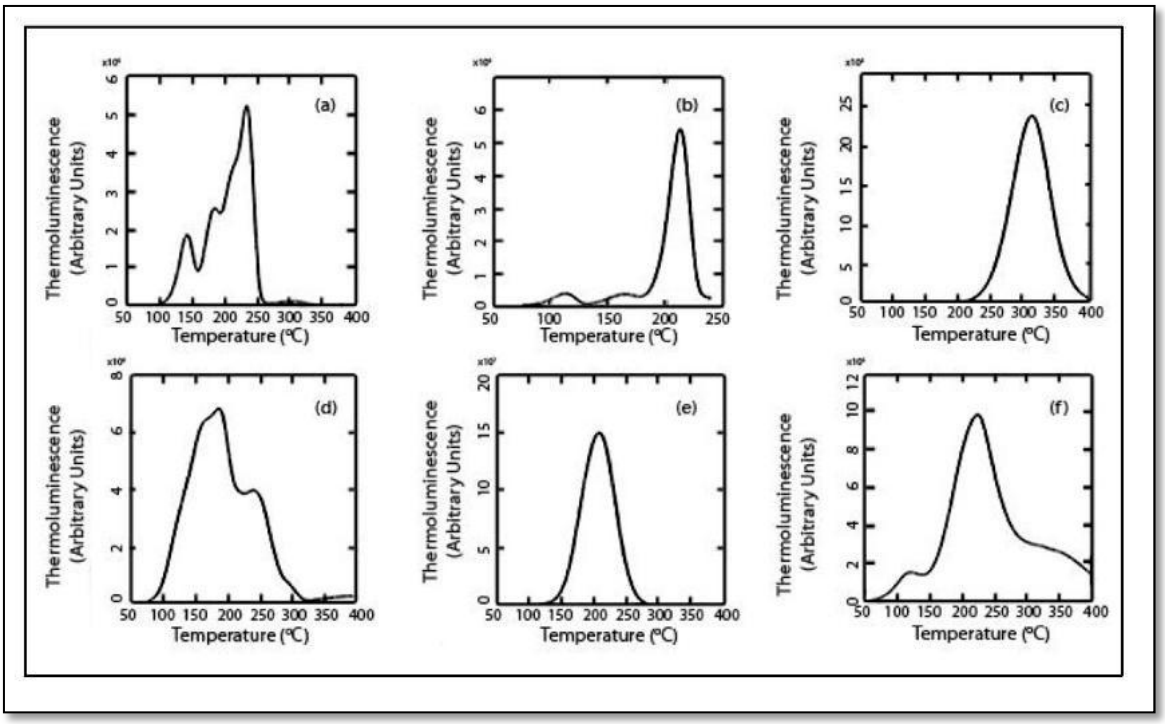

Fig. 3.3: Some representative examples of glow curves of some of the main TLD materials: (a) LiF:Mg,Ti; (b) LiF:Mg,Cu,P; (c) CaF_2:Mn; (d) CaF_2:Dy; (e) Al_2O_3:C; (f) $CaSO_4$ [31].

First studies of the thermal stability and preparation a mathematical description of the TL phenomenon has been performed by Randall and Wilkins.

Their model, describing the probability of electron to escape from traps, was named as an electron-hole recombination model. First-order model describes the TL glow peak [29].

An explanation of the observed TL properties can be obtained from the energy band theory of solids. In an ideal crystalline semiconductor or insulator most of the electrons reside in the valence band. The next highest band that the electrons can occupy is the conduction band, separated from the valence band by the so-called forbidden band gap. The energy difference between the valence and conduction bands is called energy band gap (E_g). However, whenever structural defects occur in a crystal, or if there are impurities within the lattice, there is a possibility for electrons to possess energies which are forbidden in the perfect crystal. In a simple TL model two levels are assumed, one situated below the bottom of the conduction band and the other situated above the top of the valence band. The highest level indicated by T (Fig. 3.4) is situated above the equilibrium Fermi level (E_F) and thus empty in the equilibrium state before the exposure to radiation and the creation

of electrons and holes. It is therefore a potential electron trap. The other level (indicated by *R*) is a potential hole trap and can function as a recombination centre. The absorption of radiant energy with $h\nu > E_g$ results in ionisation of valence electrons, producing energetic electrons and holes which will, after thermalisation, produces free electrons in the conduction band and free holes in the valence band. The free charge carriers recombine with each other or become trapped.

In the simple model the energy needed to release an electron from the trap into the conduction band. Figure 3.4 illustrates the simplest possible model known (one trap / one centre model). If the trap depth $E \gg kT_0$, where T_0 is the temperature at irradiation, then any electron that becomes trapped will remain so for a long period of time. It means that after exposure to the radiation there will exist a substantial population of trapped electrons. Furthermore, because the free electrons and holes are created and annihilated in pairs, there must be an equal population of trapped holes at level *T*. Because the normal equilibrium Fermi level E_F is situated below level *T* and above level *R*, these populations of trapped electrons and holes represent a non-equilibrium state.

The reaction path for a return to equilibrium is always open, but because the perturbation from equilibrium (during exposure to ionising radiation) was performed at low temperatures (compared to *E/k*), the relaxation rate as determined by Eq. (3.1), is slow. Thus, the non-equilibrium state is metastable and will exist for an indefinite period, governed by the rate parameters *E* and α.

The return to equilibrium can be speeded up by raising the temperature of the TL material above T_0. This will increase the probability of de-trapping and the electrons will now be released from the trap into the conduction band. The charge carrier migrates through the conduction band of the crystal until it undergoes recombination at recombination centre *R* [34].

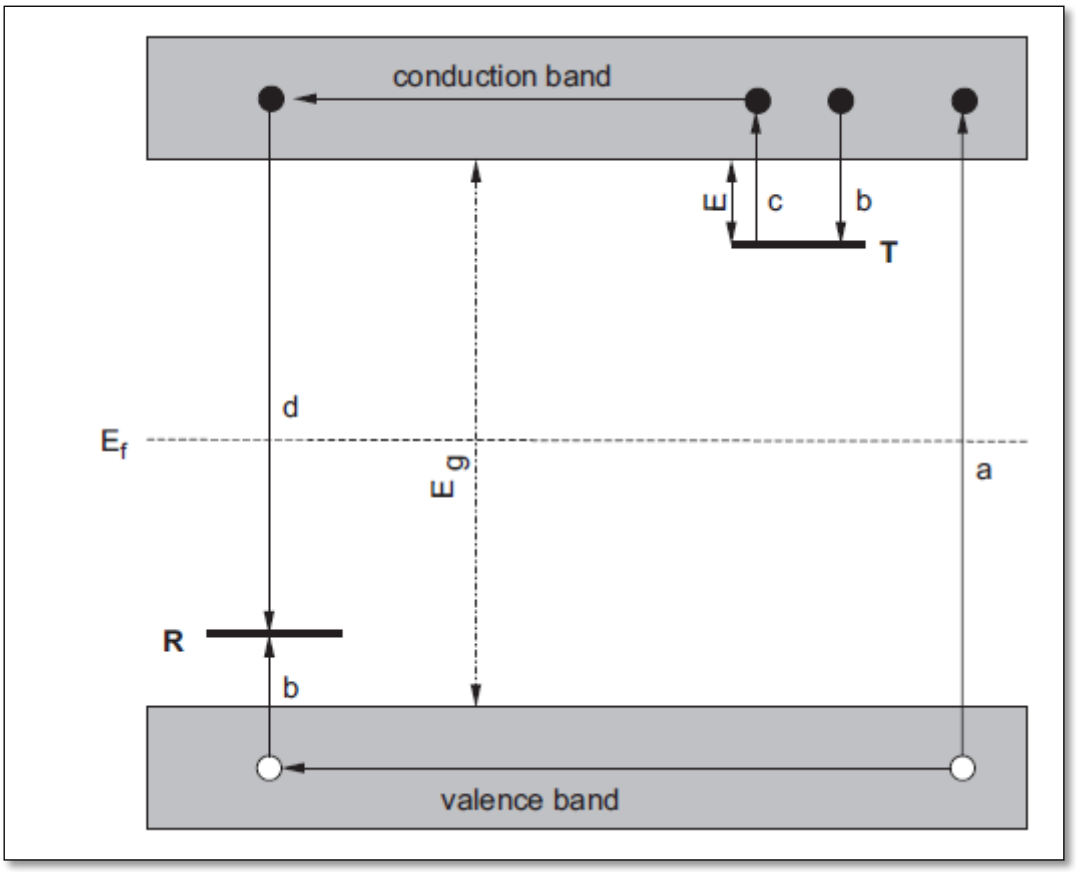

Fig. 3.4: Energy transition for the simple one trap / one centre model [34].
(a) generation of electrons and holes;
(b) electron and hole trapping;
(c) electron release due to thermal stimulation;
(d) recombination.
Solid circles represent electrons, open circles represent holes.

The probability of thermal emission of electron from an electron trap per unit time (p) is given by theory using the equation:

$$p = \frac{1}{\tau} = \alpha \mathrm{e}^{-E/kT}, \qquad (3.1)$$

where:

τ: mean lifetime of a charge carrier in a trap,

α: frequency factor associated with the particular lattice defects,

E: energy of the trap,

k: Boltzmann constant; $k = 8.62 \times 10^{-5}$ eV/K,

T: temperature.

The next equation determines the electrons' escape rate from the metastable trap, depending on the energy of the trap E and temperature T:

$$-\frac{\mathrm{d}n}{\mathrm{d}t} = n\alpha \mathrm{e}^{-E/kT}, \tag{3.2}$$

where n is the number of electrons remained and t is the time of escape [35, 36].

If all the electrons escaping from the traps cause light emission (i.e., we can omit secondary trapping), the intensity of thermoluminescence glow I (precisely, I is a physical value proportional to the light intensity) depends on the rate of release of electrons from traps and their rate of arrival at luminescence centres:

$$I = -C\frac{\mathrm{d}n}{\mathrm{d}t} = Cn\alpha \mathrm{e}^{-E/kT}, \tag{3.3}$$

where C is a constant relating to the efficiency of luminescence.

When the material is heated, we can express the temperature growing rate R by the formula

$$R = \frac{\mathrm{d}T}{\mathrm{d}t}. \tag{3.4}$$

Then:

$$\frac{\mathrm{d}n}{\mathrm{d}t} = \frac{\mathrm{d}n}{\mathrm{d}T}\cdot\frac{\mathrm{d}T}{\mathrm{d}t} = R\frac{\mathrm{d}n}{\mathrm{d}T}. \tag{3.5}$$

By substitution of (3.5) into Eq. (3.2) we obtain

$$-\frac{\mathrm{d}n}{\mathrm{d}t} = \frac{1}{R}n\alpha \mathrm{e}^{-E/kT} \tag{3.6}$$

Applying the linear heating, with the linearly time-dependent temperature:

$$T = T_0 + \beta t,$$

where T_0 is the initial temperature and β is a constant value equal to $1/R$, and calculating the intensity of emitted light, Eq. (3.7) gives the expression for the glow intensity from electrons trapped at a single trapping level:

$$I(T) = Cn_0\frac{\alpha}{\beta}\exp(-E/kT)\exp\left(-\int_{T_0}^{T}\alpha\beta^{-1}\exp(-E/kT)\,\mathrm{d}T\right), \tag{3.7}$$

where n_0 is a number of electrons trapped at the time $t = 0$.

A large number of different defects in a crystal leads to the appearance of different peaks in the glow curve. The size of the peaks in the glow curve is determined by the amount of incident radiation.

For the second-order model TL glow curve becomes:

$$I(T) = C\frac{n_0^2}{N}\cdot\frac{\alpha}{\beta}\exp(-E/kT)\left[1+\frac{n_0^2}{N}\cdot\frac{\alpha}{\beta}\int_{T_0}^{T}\exp(-E/kT)\mathrm{d}T\right]^{-2}. \qquad (3.8)$$

The second-order model describes the probability of recombination and re-trapping of electrons being trapped in the metastable state or recombine in the ground state [29, 37].

3.3. Properties of Thermoluminescence Materials

Although there are more than 2000 TL materials available, only 8 are used as they are more appropriate for measuring in radiation dosimetry. Four of them have a low atomic number (*Z*) and are characterised as tissue-equivalent materials, as they are applied in medical, personal and industrial applications. These include:

- lithium fluoride(LiF),
- lithium borate ($Li_2B_4O_7$),
- magnesium borate ($B_2Mg_3O_6$),
- beryllium oxide (BeO).

And also, following four materials have a high atomic number and are non-tissue equivalent materials, but due to their high sensitivity they are used for environmental monitoring. These include:

- calcium sulphate ($CaSO_4$),
- calcium fluoride (CaF_2),
- aluminium oxide (Al_2O_3),
- magnesium orthosilicate (Mg_2SiO_4) [38, 39].

The TLDs may be used in an extended range of occupational exposures from low level as in conventional radiography, angiography, nuclear medicine to those of high risk such as radiotherapy. In addition, any decisions made by regulatory

bodies for workers are based on the results of personal dosimeters in comparison with different dose limits.

Some important properties of thermoluminescence phosphors are listed below.

1. Annealing of the detectors

It should be noted that dosimeters have to be annealed before use for removal the thermoluminescence memory effect. In the reading process, the traps are emptied, except for the deepest ones, which form the ‘memory’ of the read dose. In order for the detector to be used again, the traps must be emptied. For this purpose, TLDs are subjected to a thermal treatment called annealing. This process is carried out by heating the detectors under controlled conditions. The duration and temperature of the annealing process depend on the chemical composition and are suggested by the manufacturer. Annealing removes any residual signal from previous radiation exposure and sets the sensitivity of all TLD in a uniform level. It guarantees optimal and reproducible properties of the detector during repeated use. In other words, it ensures that the TL material is restored to a ‘blank state’.

There are two types of annealing:

- pre-irradiation: prepares detectors to exposure, cleans ‘memory’ of the detector;
- post-irradiation: eliminates a harmful light production during readout by unreliable shallow traps (low-temperature peaks).

Usually the pre-exposure annealing is carried out at a temperature between 200 °C and 400 °C. In some cases it is completed by additional heating at lower temperature. The post-exposure annealing is needed for some TLDs and is carried out at relatively lower temperature.

2. Absorbed Dose Response

It is useful for a phosphor to have a linear TL absorbed dose response over measurement and calibration ranges of the absorbed dose. The response of TL phosphor is usually linear at low absorbed dose values, it becomes supralinear when the dose increases, and finally saturated at high values.

The sensitivity of a phosphor may also change with different grain sizes and often most markedly with photon energy or LET of the radiation.

The LiF:Mg,Ti and LiF:Mg,Cu,P show different dose responses. The dose response of LiF:Mg,Ti is linear, supralinear and sublinear while dose response of LiF:Mg,Cu,P with standard concentrations of impurities is linear and sublinear, as shown in Fig. 3.5 and 3.6.

The normalised TL dose response for the glow peak can be defined in equation:

$$f(D) = \frac{S(D)/D}{S(D_*)/D_*}, \tag{3.9}$$

where $S(D)$ is the TL intensity of the glow peak at an irradiated dose D, and $S(D_*)$ is the TL intensity of the peak at standard or low dose, preferably in the linear response region. This is illustrated in Fig. 3.5.

The region is defined as a linear where $f(D) = 1$, supralinear where $f(D) > 1$, and sublinear where $f(D) < 1$.

The main dosimetric peaks of LiF:Mg,Ti and LiF,Mg,Cu,P are shown in the Fig. 3.6 for the photon induced TL dose response. For LiF:Mg,Ti the peak 5 is in the accurately linear region of constant TL efficiency: from the lowest measurable dose levels approximately 10^{-6} Gy up to a dose level of about 1 Gy, $f(D)$ is equal to 1. The region above 1 Gy is supralinear; therein the $f(D)$ value reaches maximum approximately between 3–4 at level dose in the range (300–400) Gy.

In contrast, LiF:Mg,Cu,P does not exhibits supralinearity [40, 41].

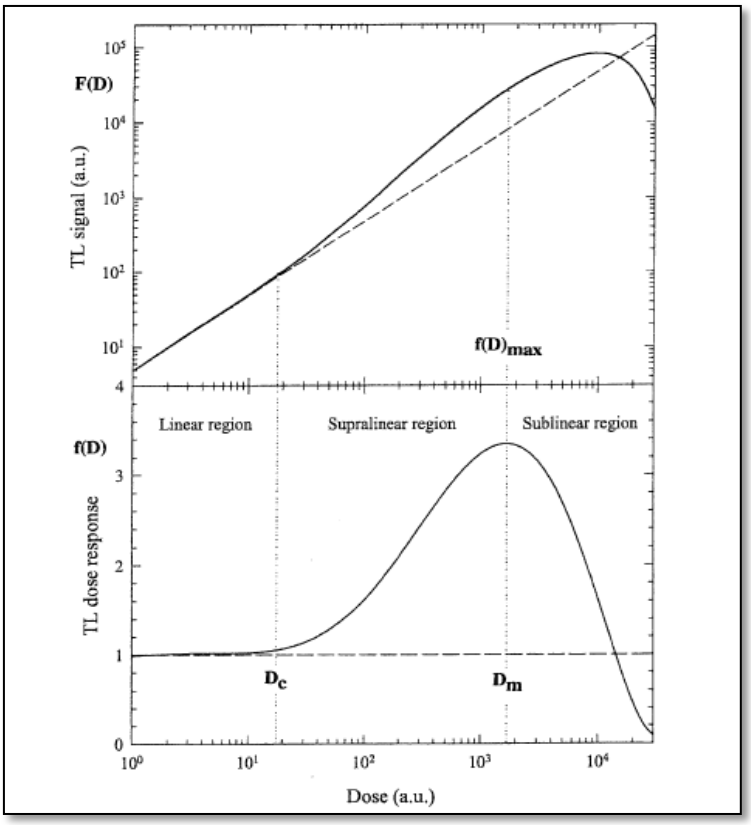

Fig. 3.5: The TL output, $F(D)$, as a function of dose at constant photon energy, and TL dose response function, $f(D)$, as a function of dose illustrating linearity ($f(D) = 1$), supralinearity and sublinearity. The maximum supralinearity, $f(D)_{max}$, occurs at the dose D_m; D_c represents a critical dose [42].

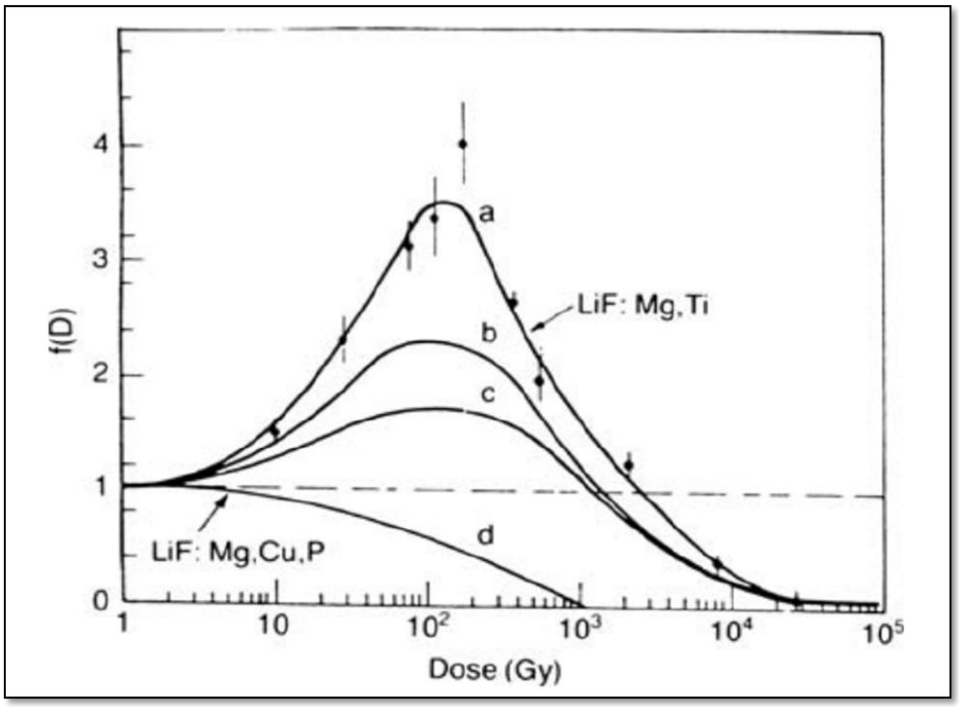

Fig. 3.6: $f(D)$ of composite peak as a function of photon energy in Li:Mg,Ti: (a) ^{60}Co photons, (b) X-rays 50 kV_p, (c) X-rays 20 kV_p; (d) $f(D)$ of peak in LiF:Mg,Cu,P following ^{60}Co irradiation [43].

3. Relative Energy Response

The photon mass absorption coefficient of an element is a function of photon energy and is dependent on the main photon absorption and other interaction processes, such as the photoelectric effect, Compton scattering, pair production and (of relatively minor importance) Rayleigh (elastic) scattering. All coefficients and cross sections are dependent on the atomic number Z of the target atoms and on the photon energy E. The total photon interaction cross section per atom:

$$\sigma_{\text{tot}} = \sigma_{\text{pe}} + \sigma_{\text{cs}} + \sigma_{\text{pp}}. \tag{3.10}$$

For elements of low atomic number the photoelectric effect is dominant for photon energies up to approximately 15 keV. For high atomic numbers the photoelectric effect is dominant up to several hundred keV.

Compton scattering in a tissue is very important in the energy range between 20 keV and 10^4 keV approximately.

The approximate dependence of these interaction cross sections as functions of atomic number Z and photon energy E is shown in below in Table 3.1.

Table 3.1: Approximate dependence of photon interaction cross sections on the atomic number (Z) of the absorber [44]

Interaction	Approximate dependence
Photoelectric effect	$\sigma_{\text{pe}} \propto Z^4$ for low-energy photons $\sigma_{\text{pe}} \propto Z^5$ for high-energy photons
Compton scattering	$\sigma_{\text{cs}} \propto Z$
Pair production	$\sigma_{\text{pp}} \propto Z^2$ ($E > 1.02$ MeV)

The photon energy response of a TL phosphor may be expressed in different methods and a commonly used method is to compare the response of the phosphor normalised at a particular photon energy, usually ^{60}Co gamma rays energy (1.25 MeV mean), with that of air or tissue. The relative energy response (RER) of the phosphor at photon energy E is:

$$\text{RER}(E) = \frac{\left[\mu_{\text{m(TLD)}} / \mu_{\text{m(air)}}\right]_E}{\left[\mu_{\text{m(TLD)}} / \mu_{\text{m(air)}}\right]_{1.25\,\text{MeV}}}, \tag{3.11}$$

where μ_{m} is the mass energy absorption coefficient.

The plot of relative energy response shows the relative detector response at the same kerma, normalised at 1.25 MeV. Under conditions of electronic equilibrium, the plots are based on absorbed dose [45].

4. Fading

Fading is a TL signal loss with time after exposure of the material to ionising radiation. It is a process in which the latent information is unintentionally lost before readout. The fading is mainly due to thermally or optically stimulated release of electrons from traps or a combination of both. This process has a negative impact, especially for long-term measurements.

In 2004, Al-Haj and Lagarde described the process of glow curve evaluation and the change in the glow curve over time due to the phenomenon of fading (shown in Fig. 3.7), and the distortion of the glow curve due to anomalies in routine practice resulting in the assignment of incorrect doses. The rate of signal loss is described in Eq. (3.1). Fading of the peaks at lower temperature occurs over time and can be used to estimate for how long a TLD was deployed.

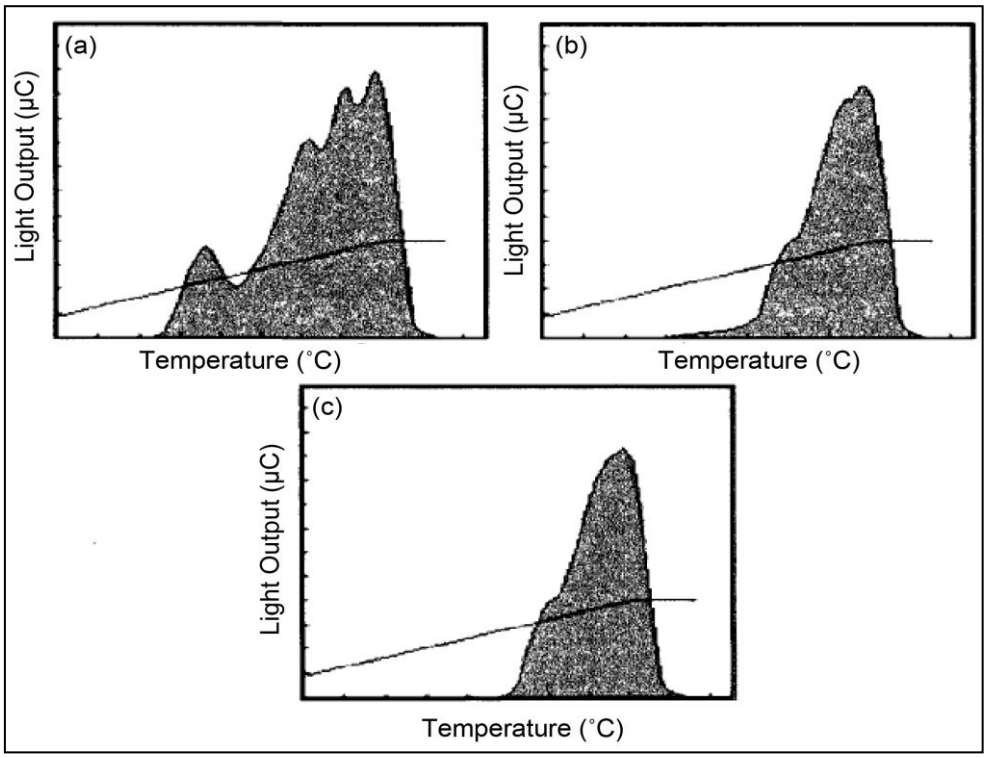

Fig. 3.7: Glow curve for LiF:Mg exposed to equal doses of radiation and read at different times post exposure. The solid line depicts the temperature of the TL crystal as a function of time.
(a) The glow curve measured shortly after irradiating.
(b) TLD was read one month post exposure.
(c) TLD was read three months after exposure [46].

5. Distortions at the Reading

The distortions of a glow curve are anomalies of reading related to an incomplete TLD readout, the presence of a contaminant on the TLD, light-induced peaks, and electrical spikes. Defects can be generated during production of the TLD pellets, damages are possibly due to mishandling or prolonged use. This type of anomaly will result in the readout dose being lower than that was actually received. Some TLD contaminants result in the read dose being larger than that actually received. Contaminants can be anything present in the environment that will glow when heated. Common contaminants are dirt, chemicals, and fat from a human body. Light-induced anomalies also result in overestimation of the dose. This occurs when the TLD is exposed to light between annealing and reading. During the reading of the illuminated detectors, quanta of light are generated, the source of which is not the process of exposure by ionising radiation of the phosphor. This is an undesirable effect, creating the so-called non-reader background, often called a zero reading. Electrical spikes result in spurious peaks leading to an overestimation of dose. These capricious instabilities can be due to reader electronics or the fluctuations in the electrical power line. How these impact the glow curve is shown in Fig. 3.8.

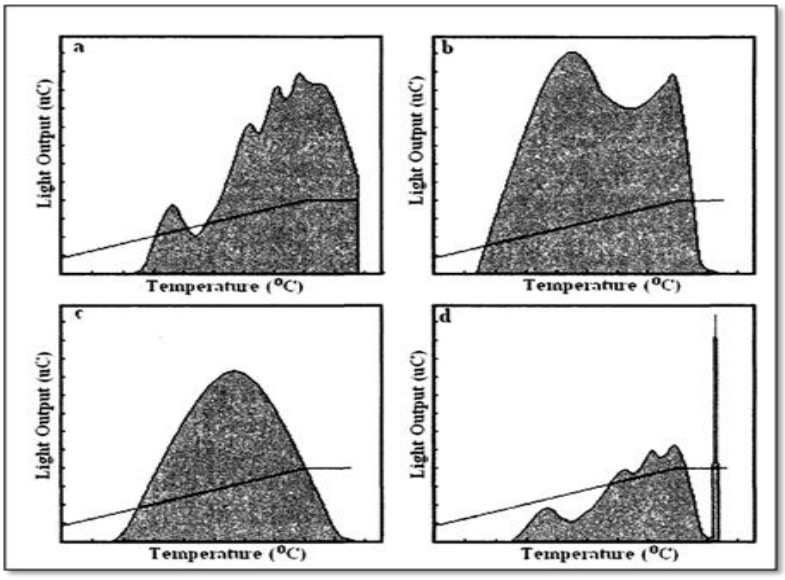

Fig. 3.8: Glow curves showing different anomalies that can occur during the readout of a TLD. The solid black line shows the temperature as the TLD is heated as a function of time.
(a) An incomplete readout is shown; it can be seen how some signals are cut-off.
(b) There is a peak caused by the presence of a contaminant that obscures the glow curve from the TLD.
(c) The glow curve is light-induced from the exposure of the TL to light.
(d) The result of an electrical spike; might be due to reader electronics fault or to the fluctuations in the electrical power line [46].

3.3.1. TL Holders and Filters

TL material is placed in holders when it is taken for dose measurement. When it is placed in a holder, the assembly is called a thermoluminescence dosimeter (TLD). The holder serves to protect the TL crystal from contamination and mechanical damage. The holder also allows placement of different filters in front of the TL crystals. The purposes of using filters are to correct the energy dependence of TL material, obtain equivalent doses inside a material (used to obtain deep dose rates inside a human body), to filter out unwanted particles, and to correct for backscatter.

The TLD issued to radiation workers is typically composed of four different TL phosphors and filters:

1. The first filter is a thin Mylar window which provides insignificant attenuation to incident radiation and keeps the TL crystal from being exposed to sunlight. The skin dose to an individual is measured by this TL phosphor.

2. The second filter is usually a tissue-equivalent plastic with a density thickness equal to 1 cm of tissue. This phosphor is used to determine the deep dose to an individual.

3. The third filter TL phosphor is usually a neutron sensitive TL material. It has a filter containing hydrogenous material, to thermalise neutrons by elastic scattering making them more likely to be absorbed by the TL phosphor.

4. The fourth filter usually contains a low *Z* metal such as copper to attenuate any beta particles to measure only the dose contribution coming from photons [47, 48].

Commercial TLD holder (badge) is shown in Fig. 3.9. It is very important that a worker wears correctly the badge as well as keeping it clear and dry.

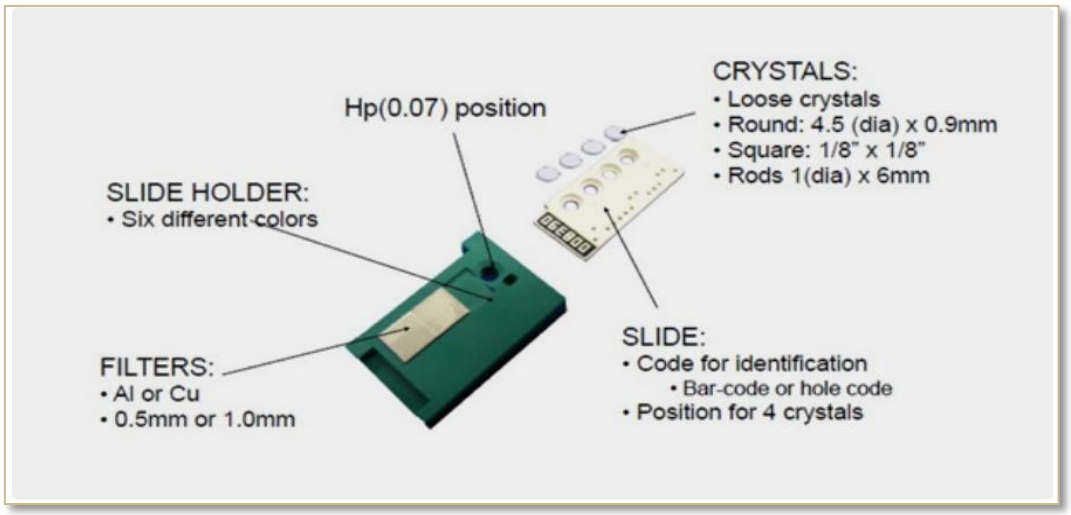

Fig. 3.9: Commercially available TLDs holders [47].

3.3.2. Lithium Fluoride Family (LiF)

LiF is recognised universally as an excellent TL material widely used in dosimetric applications for personnel monitoring, especially if used in the form of solid pellets. Due to its properties such as high sensitivity, low background, tissue equivalence (with atomic number equal to 8.2 – close to 7.4 of the human tissue), LiF is the most common phosphor used in the TL dosimetry. This phosphor is a kind of a pattern because its properties are best known and used as a standard to comparing with different TL materials.

The two most distinguished varieties used are LiF doped either with magnesium and titanium (LiF:Mg,Ti) or with magnesium, copper, and phosphor (LiF:Mg,Cu,P). First of these – LiF:Mg,Ti – is the older one, dating back to the 60 s, and today most commonly used for dosimetry. The compound LiF:Mg,Cu,P is a more recent development and has a much higher sensitivity compared to LiF:Mg,Ti [31, 49].

3.3.3. Physical Characteristics of MTS-N and MCP-N Dosimeters

Two important features of the detectors used for clinical dosimetry are defined as follows:

1. Precision is a term associated with the random uncertainties of the measurement, i.e. the uncertainties that have been derived by statistical methods from a number

of repeated readings. Commonly used measure of statistical dispersion is a standard deviation

2. Accuracy defines the effect of both systematic and random uncertainties. And it is a statement of the closeness with which a measurement is expected to approach the true value. The value of a quantity is understood to be considered as 'true' either by theoretical considerations or by comparison with a fundamental measurement. The indicated value is the value of a quantity as indicated by the relevant measuring device, sometimes also called 'reading' or 'measured' value.

The precision and accuracy of TL dosimeters in the dose estimations is composed of several parameters [50, 51].

In order to achieve optimal properties, to the thermoluminescent crystal additive impurities are introduced to create defects that form the trapping and luminescence centres. The impurities and their typical concentrations of both LiF:Mg,Ti and LiF:Mg,Cu,P are shown in Table 3.2. These elements play a key role in the emergence of the phenomenon of the TL, since they are responsible for the creation of traps in the band gap crystal.

Table 3.2: Ranges of admixtures concentrations typically reported for LiF:Mg,Ti and LiF:Mg,Cu,P [52].

LiF:Mg,Ti	LiF:Mg,Cu,P
Mg 0.01 %	Mg 0.2 %
Ti (10–15) ppm	P (1–4) %
	Cu (0.02–0.05) %

Due to the traps in the crystal of LiF, the TL intensity, as a function of the temperature, has a number of glow peaks. Initially it is raised exponentially, reaches a maximum and then reduces producing a peak. As there are many traps, many glow peaks are produced. The height and the number of the peaks in a glow curve of a crystal depend on the:

- number of the impurities,
- defects of the material,
- thermal history.

3.4. Advantages and Disadvantages of TLD

The most important advantages and disadvantages of the TLD are shown in Tab. 3.3 and 3.4 [53, 54].

Table 3.3: Advantages of TLD.

No	Advantages
1.	Available in many forms, namely chips, pellets, rods, powder, single crystals, ribbons and gel
2.	Wide useful dose range
3.	Dose rate independence and linear response to dose received
4.	Small size and therefore a possibility for point dose measurements
5.	Large availability of TLDs and readers from many manufacturers
6.	Reusability: by using annealing procedures they can be reused many times before they are completely damaged from radiation
7.	Passive energy storage
8.	Tissue equivalence
9.	In a single exposure many TLDs can be exposed
10.	The read-out is quick and it does not require any wet chemicals
11.	Readout convenience
12.	High precision manifested by small standard deviation of the signal
13.	Possibility of dose measuring over a long period (months or even a year)
14.	Excellent resistance to environment (i.e. temperature, humidity)
15.	Can distinguish between types of radiation by using different lithium isotopes
16.	Cheap to use and maintain

Table 3.4: Disadvantages of TLD.

No	Disadvantages
1.	Susceptibility to lose the information
2.	Sensitivity to light
3.	The storage in a TLD is not stable: annealing heating cycle is needed
4.	It is not recommended for beam calibration
5.	The signal is read only once: it is erased during the readout cycle
6.	Fading: loss of TL signal with time
7.	The sensitivity is decreased or increased after a large dose received by a TLD; an additional anneal procedure is then needed
8.	The lack of uniformity for different dosimeters made from a given batch of phosphors; to avoid this problem calibration of the batch is necessary to achieve proper accuracy and precision
9.	Instability of the storage
10.	TLD sensitivity can vary with time in some phosphors due to the migration of trapping centres in the crystals at room temperature. However, annealing of the TLD can usually restore them to some reference condition again.
11.	Readout and calibration time consuming

4. Phototransferred Thermoluminescence Phenomenon (PTTL)

4.1. Ultraviolet Radiation (UV)

'Ultraviolet' means 'beyond violet' (from Latin *ultra*: 'beyond'). Ultraviolet (UV) is electromagnetic radiation with a frequency higher than violet light. UV radiation is used in a variety of applications such as medical therapy, sterilisation of food, water, air and medical products, and polymerisation of dental fillings. Exposure to ultraviolet radiation is harmful and it needs to be monitored [55].

4.1.1. Sources of UV and Biological Effects

A wavelength of ultraviolet extends from about 10 nm to 400 nm, and it is shorter than that of visible light but longer than X-rays.

Although the divisions between the spectral regions are not necessarily rigid, it would seem sensible to adopt international recommendations. Ultraviolet radiation can be classified into three regions:

- UVA: (315–400) nm (long wave or 'black light'),
- UVB (280–315) nm (middle wave or 'erythemal'),
- UVC (100–280) nm (shortwave or 'germicidal').

Exposure to UV occurs from both natural and artificial sources. Most artificial sources of UV, except for lasers, emit a spectral continuum of UV containing characteristic peaks, troughs and lines. These sources include various lamps used in medicine, industry, commerce, research and at home.

UV-induced biological effects depend on the wavelengths of the radiation emitted by the source. For determination of hazard it is necessary to have information on the spectral form (range of wavelength) of emission. This requires spectral irradiance ($W\,m^{-2}\,nm^{-1}$) measurements at the examined object. The biological or hazard weighted irradiance ($W\,m^{-2}$ effective), commonly called the

effective UV irradiance or dose rate (exposure), is determined by multiplying the spectral irradiance at each wavelength by the biological or hazard weighting factor (which quantifies the relative efficacy at each wavelength for causing the effect) and summing over all wavelengths. Such factors or weighting functions are obtained from action spectra [56, 57, 58].

The Sun is the largest source of UV radiation; the sunlight that reaches the Earth's surface consists mainly of UVA radiation, with a smaller component of UVB. All of the UVC is filtered by the ozone layer, and thus no UVC reaches the Earth's surface [59].

4.2. Phototransferred Thermoluminescence (PTTL)

Phototransferred Thermoluminescence (PTTL) is an interesting feature of TL detectors and is useful for dose reassessment. The PTTL efficiency is very suitable for those applications requiring a high degree of confidence in the dose results, such as personal dosimetry. PTTL is a phenomenon observed in many thermoluminescent materials such as insulators or semiconductors. PTTL is caused by the optically stimulated transfer of electric charge from deep traps to shallow traps, resulting in the generation of TL peaks at lower temperatures. A PTTL phenomenon is a useful technique in dating and radiation dosimetry. PTTL yield is proportional to the initial absorbed dose. The phenomenon of light-induced thermoluminescence is closely related to the structure of the phosphor, which must contain at least three types of electron traps: shallow traps (acceptor), deep traps (donor) and piercing traps (recombination centre). The electrons found in donor traps are not released in the process of reading the detector, however, they play a key role in the emergence of the PTTL phenomenon.

To observe the PTTL phenomenon some additional factors are necessary: the heating and ultraviolet exposure of detectors. These factors cause vibrations of the crystal lattice which facilitates the transfer of electrons from deep electron traps to shallower ones [60].

PTTL phenomenon gives the opportunity to ‘reread’ the TL signal from LiF after the first heating. The PTTL properties lead to receiving useful information regarding the optical energies likely to be most efficient in transferring charge between centres and help to identify the mechanisms involved in the optically stimulated and thermally stimulated luminescence processes.

The UV radiation stimulates the material of the phosphor, through to which electrons from deeper electron traps are transferred to more shallow traps. UV radiation releases the electron from the deep trap (I) to the conduction band (see Fig. 4.1 which illustrates the first stage of PTTL phenomenon). The electron travels in the conduction band (K) until it is intercepted by one of the shallower traps (L). In order to obtain information on what part of the electrons was trapped in the effect of the PTTL phenomenon, the material should be heated in the same way as in the case of a classic thermoluminescent material reading. In situations where re-evaluation of the dose is necessary, it is possible to reuse the thermoluminescence detector, which has already been heated in the reader by applying additional heat combined with the preceding exposure to ultraviolet radiation. After UV exposure, the detector should be placed back in the thermoluminescent material reader and read at settings typical for the type of thermoluminescence detector used [61].

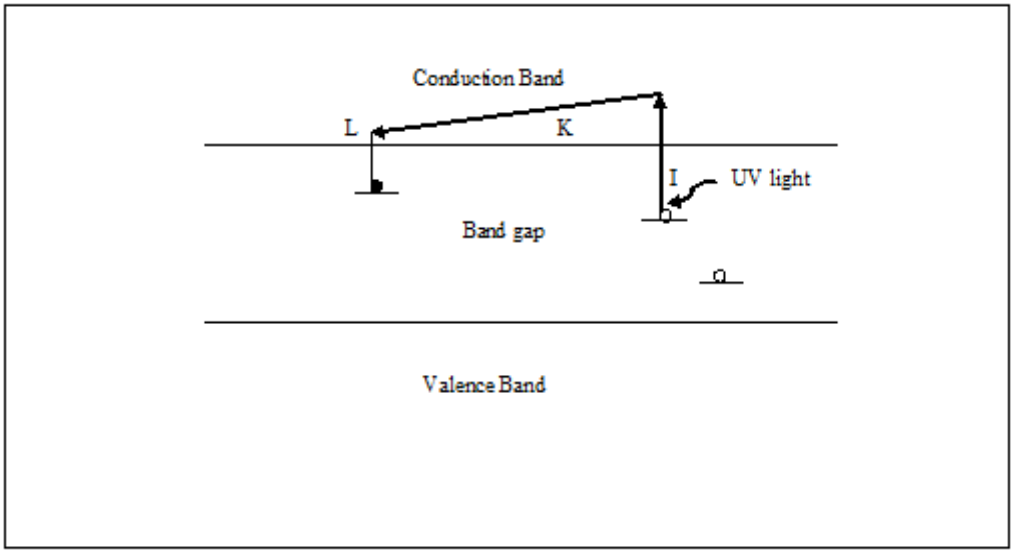

Fig. 4.1: Scheme of PTTL phenomenon [62].

4.3. PTTL Model

The mechanisms of phototransfer and PTTL production at a more fundamental level are described in this chapter basing on [34].

4.3.1. Simple Model (two traps / one centre)

The simplest model to describe PTTL assumes two traps and one luminescence centre: one deep trap from which the charge is excited (donor trap), one shallow trap into which the charge is transferred (acceptor trap), and one recombination centre (hole trap: luminescence centre). Fig. 4.1 shows possible transfer of electrons in the model. The transfer of charge from the donor traps into the acceptor traps during illumination may be described by the following set of rate equations [29, 61]:

$$\frac{\mathrm{d}n_\mathrm{a}}{\mathrm{d}t} = A_\mathrm{a}(N_\mathrm{a} - n_\mathrm{a})n_\mathrm{c} - f_\mathrm{a}n_\mathrm{a} \tag{4.1}$$

$$\frac{\mathrm{d}n_\mathrm{d}}{\mathrm{d}t} = A_\mathrm{d}(N_\mathrm{d} - n_\mathrm{d})n_\mathrm{c} - f_\mathrm{d}n_\mathrm{d} \tag{4.2}$$

$$\frac{\mathrm{d}m}{\mathrm{d}t} = -A_m m n_\mathrm{c} = \frac{m}{\tau}, \tag{4.3}$$

where:

N_a: concentration (m^{-3}) of shallow acceptor traps,

N_d: concentration (m^{-3}) of deep donor traps,

n_a, n_d: concentration (m^{-3}) of electrons or holes trapped at these centres respectively

[the condition supposed for PTTL is the initial condition that $n_{\mathrm{a}0} = 0$ and $n_{\mathrm{d}0} = m_0$ after irradiation and immediately before illumination],

n_c: the concentration of free electrons,

m: sum of concentrations n_a, n_d and n_c:

$$m = n_\mathrm{a} + n_\mathrm{d} + n_\mathrm{c}, \tag{4.4}$$

A_a and A_d: probabilities ($\mathrm{m}^3\ \mathrm{s}^{-1}$) for trapping of free charges in the empty traps,

A_m: probability of a free electron recombining with a trapped hole at the recombination centre,

τ: recombination lifetime,

$f_\mathrm{a} = \phi(\lambda)\ \sigma_\mathrm{a}(\lambda)$: rate at which electrons are lost from shallow acceptor traps,

$f_d = \phi(\lambda)\,\sigma_d\,(\lambda)$: rate at which electrons are lost from deep donor trap

[f_a and f_d are optical detrapping terms, $\phi(\lambda)$ is the intensity of excitation light, σ_a and σ_d – the photoionisation cross section from the deep donor traps and shallow acceptors traps respectively] [37].

During heating the sample the electrons will thermally escape from shallow acceptor traps and either recombine with the trapped holes to yield PTTL signal or be re-trapped in the deep donor traps. This process can now be represented by the following rate equations:

$$\frac{\mathrm{d}n_c}{\mathrm{d}t} = \frac{\mathrm{d}m}{\mathrm{d}t} - \frac{\mathrm{d}n_d}{\mathrm{d}t} - \frac{\mathrm{d}n_a}{\mathrm{d}t}\,. \tag{4.5}$$

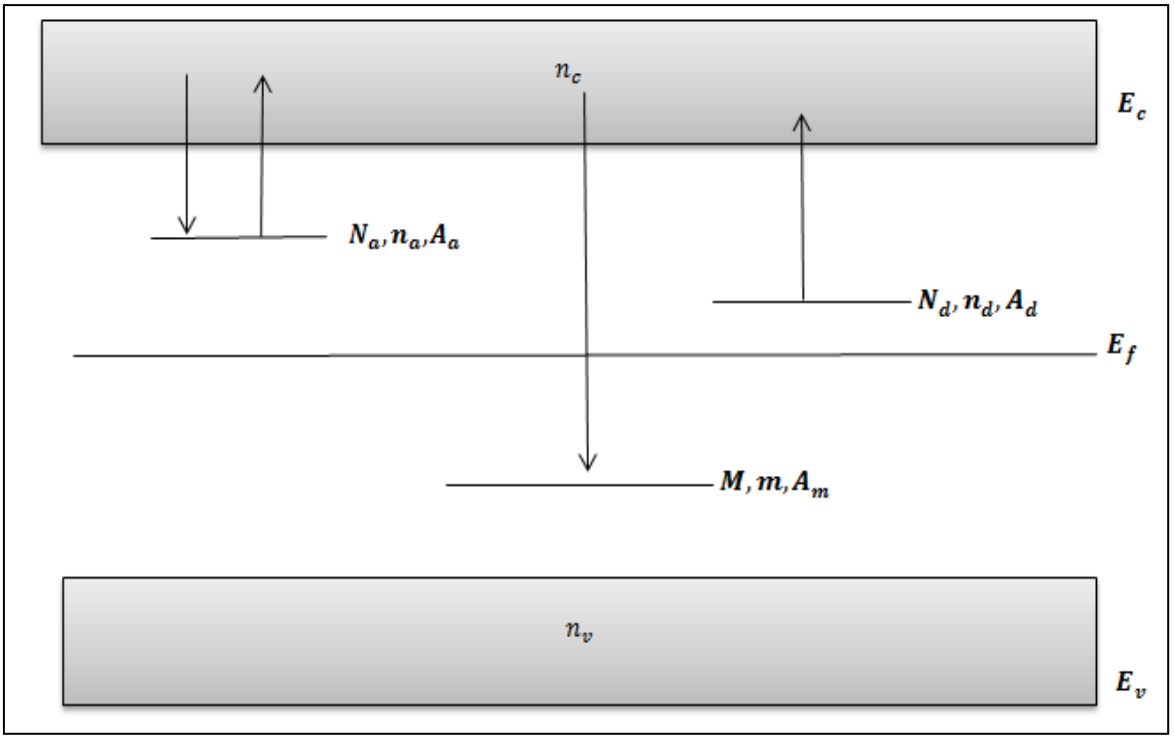

Fig. 4.2: Simple model of PTTL. E_c and E_v are the conduction band and valence band respectively, E_f is the Fermi level, the arrows represent possible transition of electron, M is the concentration (m^{-3}) of the recombination centres [37].

For a description of the processes occurring during heating, both f_a and f_d are equal 0 since heating is done in the dark. Equations (4.1)—(4.3) are transformed with replacing the optical detrapping term f_a by the thermal detrapping term γ_a. Additionally, the thermal emptying of the donor traps is negligible, so in the Eq. (4.6) the term γ_d corresponding to f_d is skipped:

$$\frac{\mathrm{d}n_\mathrm{a}}{\mathrm{d}t} = A_\mathrm{a}(N_\mathrm{a} - n_\mathrm{a})n_\mathrm{c} - \gamma_\mathrm{a} n_\mathrm{a} \tag{4.6}$$

$$\frac{\mathrm{d}n_\mathrm{d}}{\mathrm{d}t} = A_\mathrm{d}(N_\mathrm{d} - n_\mathrm{d})n_\mathrm{c} \tag{4.7}$$

$$\frac{\mathrm{d}m}{\mathrm{d}t} = -A_m m n_\mathrm{c} = \frac{m}{\tau}. \tag{4.8}$$

The thermal excitation term has the form:

$$\gamma_\mathrm{a} = s_\mathrm{a}\,\mathrm{e}^{-E_\mathrm{a}/kT}, \tag{4.9}$$

where:

s_a: frequency factor of the acceptor trap,

E_a: energy depth of the acceptor trap,

T: temperature,

k: Boltzmann constant.

Assuming quasi-equilibrium and no re-trapping into the source trap

$$\gamma_\mathrm{a} n_\mathrm{a} \gg A_\mathrm{a}(N_\mathrm{a} - n_\mathrm{a})n_\mathrm{c},$$

the solution of Eq. (4.5)—(4.8) gives a form of PTTL intensity:

$$I_\mathrm{PTTL} = -\frac{\mathrm{d}m}{\mathrm{d}t} = \gamma_\mathrm{a} A_m F(m), \tag{4.10}$$

where:

I_PTTL: value proportional to the intensity of the TL emission during heating (PTTL glow curve),

F_m: expression (evaluated by Alexander and Mackeever) [61]:

$$\begin{aligned} F(m) = {} & \left[(n_{\mathrm{a}0} + n_{\mathrm{d}0} - m_0 - N_\mathrm{d}) + m + (N_\mathrm{d} - n_{\mathrm{d}0})(m/m_0)^{A_\mathrm{d}/A_m}\right] \\ & \times \left[A_\mathrm{a}(N_\mathrm{a} + N_\mathrm{d} - n_{\mathrm{a}0} - n_{\mathrm{d}0} + m_0) + (A_m - A_\mathrm{a})(N_\mathrm{d} - n_{\mathrm{d}0})(m/m_0)^{A_\mathrm{d}/A_m}\right]^{-1} \end{aligned} \tag{4.11}$$

Equations (4.10) and (4.11) can be simplified by the introduction of an additional assumption of quasi-equilibrium and solved by using a linear heating rate $\beta = \mathrm{d}T/\mathrm{d}t$. Equation (4.10) can be written with a change of variable from t to T as follows:

$$I_\mathrm{PTTL} = -\beta\frac{\mathrm{d}m}{\mathrm{d}T} = \beta\gamma_\mathrm{a} A_m F(m). \tag{4.12}$$

The integrated area under the PTTL glow curve between the initial temperature T_0 and the final temperature T_f, marked as S_PTTL, is defined by the formula:

$$S_\mathrm{PTTL} = \int_{T_0}^{T_\mathrm{f}} I_\mathrm{PTTL}\mathrm{d}T \tag{4.13}$$

During heating under the conditions of re-trapping into the donor trap, basing on Eq. (4.5), (4.6) and (4.8), and with the assumption that $n_{a0} \ll N_d - n_{d0}$, the S_{PTTL} becomes:

$$S_{PTTL} \approx \frac{A_m m_0 n_{a0}}{A_d (N_d - n_{d0})} \tag{4.14}$$

Taking into account associated processes, the S_{PTTL} is not simply proportional to the electron concentration n_{a0} in the acceptor traps at the illumination period. If would take the assumption that re-trapping in to donor traps was negligible ($dn_d/dt \ll dm/dt$ and $dn_d/dt \ll dn_a/dt$), the S_{PTTL} can be expressed in this form

$$S_{PTTL} = \beta \int_{T_0}^{T_f} \frac{dm}{dT} dT = m_0 - m_f \,, \tag{4.15}$$

where the proportionality is distorted. However, the observation of PTTL suggest, that Eq. (4.15) is not a good assumption [60].

To use Eq. (4.14) to determine the dependence of the PTTL signal as a function of the illumination time, the variability of $n_{a0}(t)$, $n_{d0}(t)$ and $m_0(t)$ with illumination time t has to be known.

The function of illumination time is assumed by Wintle and Murray [63]. The rate equations describing the process are as follows:

$$\frac{dn_d}{dt} = -f_d n_d \tag{4.16}$$

$$\frac{dn_a}{dt} = a f_d n_d - f_a n_a \,, \tag{4.17}$$

where f_a and f_d are defined as before. The solution of Eq. (4.16) and (4.17) is

$$n_a = \frac{a f_d n_{d0}}{f_a - f_d} \left[\exp(-f_d t) - \exp(-f_a t) \right]. \tag{4.18}$$

Combining Eq. (4.15) and (4.18) and assuming that $f_a = 0$, the S_{PTTL} can be expressed as

$$S_{PTTL} = C n_{d0} [1 - \exp(-f_d t)], \tag{4.19}$$

where C is a proportionality constant.

The shape of the function described by Eq. (4.18) is characterised by an increase followed by a decrease to an eventual zero level. Illumination is not only a factor filling the acceptor traps, but also emptying these traps.

However, it is uncertain whether illumination does in fact optically empty the acceptor traps in all materials. Therefore, the validity of Eq. (4.18) is dependent upon the particular system being examined experimentally.

4.3.2. Complex Model (two traps / two centres)

The principle of this model of PTTL is described by Alexander and McKeever [61]. In the simple model, the PTTL versus time curve initially increases then decreases to zero after long illumination. A long, slow decrease is inevitable as long as some recombination takes place during the illumination period. But some experimental data showed a different relationship.

For cases where the curve first increases, then decreases, and follows a steady state level that is not zero at long illumination times, the simple model described above does not hold. In an attempt to explain experimental data for quartz which obviously show a stable equilibrium value at long illumination times after an initial decrease in the PTTL signal, the authors introduced a second recombination centre that was assumed to be non-radiative and an additional deep trap. The deep trap is not optically active and it was introduced to explain sensitivity changes [64]. Recombination at the second centre produces only phonons.

The rate equations describing the possible processes are as follow:

$$\frac{\mathrm{d}n_\mathrm{c}}{\mathrm{d}t} = R - \frac{\mathrm{d}n_\mathrm{a}}{\mathrm{d}t} - \frac{\mathrm{d}n_\mathrm{d}}{\mathrm{d}t} - A_{m_1} m_1 n_\mathrm{c} - A_{m_2} m_2 n_\mathrm{c} \tag{4.20}$$

$$\frac{\mathrm{d}n_\mathrm{a}}{\mathrm{d}t} = A_\mathrm{a}\left(N_\mathrm{a} - n_\mathrm{a}\right)n_\mathrm{c} - \gamma_\mathrm{a} n_\mathrm{a} \tag{4.21}$$

$$\frac{\mathrm{d}n_\mathrm{d}}{\mathrm{d}t} = A_\mathrm{d}\left(N_\mathrm{d} - n_\mathrm{d}\right)n_\mathrm{c} - f_\mathrm{d} n_\mathrm{d} \tag{4.22}$$

$$\frac{\mathrm{d}m_1}{\mathrm{d}t} = A_{h_1}\left(M_1 - m_1\right)n_\mathrm{v} - A_{m_1} m_1 n_\mathrm{c} \tag{4.23}$$

$$\frac{\mathrm{d}m_2}{\mathrm{d}t} = A_{h_2}\left(M_2 - m_2\right)n_\mathrm{v} - A_{m_2} m_2 n_\mathrm{c} \tag{4.24}$$

$$\frac{\mathrm{d}n_\mathrm{v}}{\mathrm{d}t} = R - A_{h_1}\left(M_1 - m_1\right)n_\mathrm{v} - A_{h_2}\left(M_2 - m_2\right)n_\mathrm{v}, \tag{4.25}$$

where:

R: rate ($\mathrm{m^{-3}\,s^{-1}}$) of generation electron-hole pairs,

A_{m_1}, A_{m_2}: respective probabilities of free electrons recombining with trapped holes at the two recombination centres ($m^3\,s^{-1}$),

m_1, m_2: respective concentrations (m^{-3}) of electrons or holes at these centres,

n_v: free hole concentration (m^{-3}) in the valence band,

A_{h_1}, A_{h_2}: respective probabilities for the hole trapping ($m^3\,s^{-1}$),

M_1, M_2: concentration (m^{-3}) of the radiative recombination centres and the non-radiative recombination centres respectively.

All other terms are defined as in the simple model. At the beginning of the illumination the number of electrons in the shallow traps (n_a) will be less than the number of holes in the radiative centre (m). When the recombination occurring at the radiative centre, the PTTL is produced, thus, the PTTL intensity is given by:

$$I_{\mathrm{PTTL}} = -\beta \frac{\mathrm{d}m_1}{\mathrm{d}T} = \beta A_{m_1} m_1 n_c \,. \tag{4.26}$$

Using the quasi-equilibrium assumption and substitution, n_c can be obtained. Assuming that re-trapping into the acceptor trap is slow and that re-trapping into the donor trap is the dominant during heating (i.e. during PTTL signal readout), Alexander and McKeever [64] obtained for the integrated PTTL:

$$S_{\mathrm{PTTL}} = m_{10}\left[1-\left(1-\frac{n_{a0}}{m_{20}}\right)^{A_{m_1}/A_{m_2}}\right]. \tag{4.27}$$

If recombination into the non-radiative centre is the main mechanism for the production of luminescence then:

$$S_{\mathrm{PTTL}} = m_{10}\left[1-\left(1-\frac{n_{a0}}{m_{20}}\right)^{A_{m_1}/A_{d}}\right]. \tag{4.28}$$

4.3.3. Wavelength Dependence

An important characteristic of the PTTL effects in TLD materials is wavelength dependence. The PTTL signal as function of the wavelength of illuminating light is introduced via $f_d = \phi(\lambda)\sigma_d(\lambda)$. Assuming deep donor traps and parabolic bands the photo-ionisation cross section for the deep donor traps is given by:

$$\sigma_d = K\sqrt{E_0}\,\frac{(h\nu - E_0)^{3/2}}{h\nu(h\nu - \delta E_0)^2}, \tag{4.29}$$

where:

h: Planck constant,

E_0: optical ionisation energy of the donor traps,

ν: frequency of light,

K: constant,

$\delta = 1 - m_e/m^*$ is a constant dependent on the free electron mass m_e and the electron effective mass m^*.

To measure the PTTL wavelength dependence, the usual procedure is to illuminate the material in use for a fixed time at a given wavelength and monitoring how the resulting PTTL signal ($S_{PTTL}(\lambda)$) depends on the wavelength. The true wavelength response can be obtained by taking the initial slope of the $S_{PTTL}(t)$ curve [64]. Therefore, plotting the initial slope of the PTTL against wavelength ($S_{PTTL}(\lambda)$), a curve shape corresponding to the photo-ionisation cross section $\sigma(\lambda)$ is obtained.

5. Applications of TLD Systems in Medical Physics and Other Fields

Thermoluminescence dosimeters achieved very high application potential in different fields. The modernisation and development of the instrumentation and better understanding of TL has helped professionals to solve their problems in many areas. The applications of the TLD are summarised in the following are shown in the Fig. 5.1.

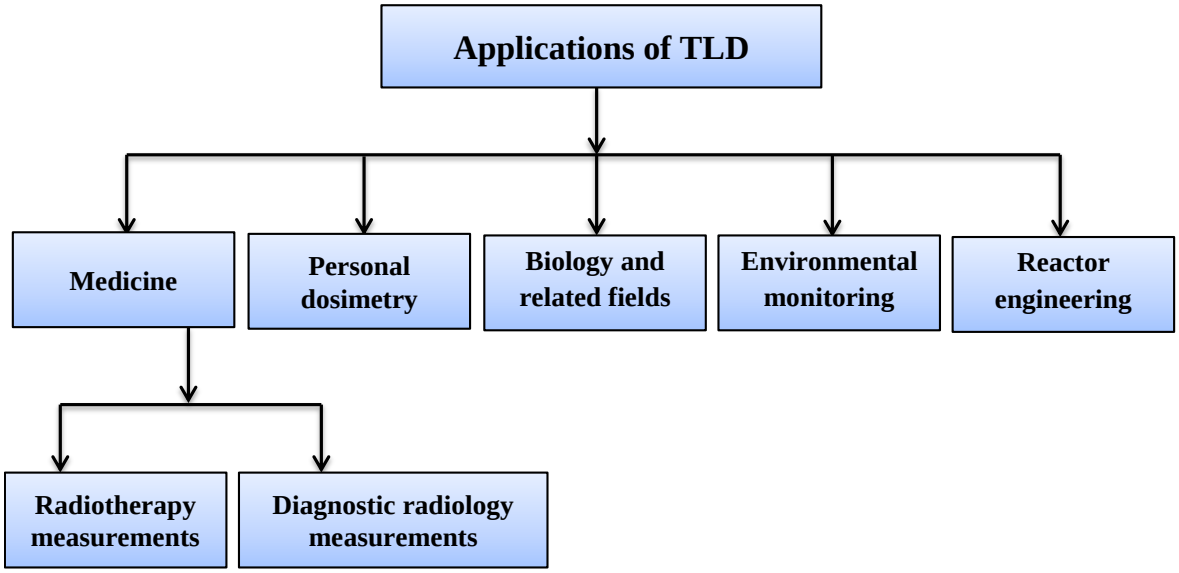

Fig. 5.1: Applications of TLD [65].

5.1. Applications in Medicine

5.1.1. Radiotherapy Measurements

In the past, radiotherapy has encountered the difficulties in accurate prediction of absorbed dose. This led to the development of in vivo measurement techniques. In radiotherapy it is very important to deliver the dose to the tumour with high accuracy. If the absorbed dose is high, the complications appear: damages to the healthy tissue surrounding the tumour. If the dose is too low, tumours may not be completely destroyed. This results in increased patient morbidity and mortality.

While the radiologist prescribes the absorbed dose, the physicist's task involves a designing how the dose should be delivered so that the requirements are met. Another task of physicist is a measurement of a volume distribution of the dose. TLD is suitable and useful for measurements for a variety of purposes in radiotherapy, including measurements of therapy machine output, beam uniformity checks and the measurement of absorbed dose in phantoms and in vivo for both internally and externally applied fields.

Professor Farrington Daniels of the University of Wisconsin-Madison is the first who developed TLD as a practical method of assessment ionising radiation exposure [66]. He pointed that the technique could be applied in the field of clinical measurement.

The arrangement of radiotherapy treatment fields is conventionally carried out using a combination of calculations involving standardised geometries together with depth dose and transverse dose measurements in phantoms. The final check on the absorbed dose delivered to the patient can be carried out by in vivo dosimetry. Similarly, absorbed doses to organs not involved in the treatment, which should be kept to the minimum, can be measured.

TL dosimeters are highly precise, provide rapid retrieval of information (using on-site readers), have good environmental stability, have good water or tissue equivalence and have a wide range of sensitivities. The last characteristic is particularly important for in vivo measurements of absorbed dose. Because of their small size, thermoluminescence dosimeters also give good spatial resolution. This is of particular value in many radiotherapy techniques where the absorbed dose has a high spatial variability. Thermoluminescence dosimeters may also be used to measure the absorbed dose to experimental animals [67].

TLD has proved to be a useful method in the comparison of patient absorbed dose from these new techniques as well as from the traditional ones.

5.1.2. Diagnostic Radiology Measurements

Diagnostic absorbed dose measurements are important for:

- improving the design of equipment to reduce patient absorbed dose,
- providing a measurement database epidemiological analysis of population radiation absorbed dose from diagnostic radiology,
- improving radiographers' techniques in the use of equipment to reduce the patient absorbed dose [22].

5.2. Application of TLD to Personal Dosimetry

The first aim of individual monitoring of external radiation is to assess radiation doses for individual employees and compare the doses with dose limits. In addition, the tasks include supplying information about the trends of these doses and about the conditions in places of work and delivering information about the event of accidental exposure.

The following quantities should be measured in personnel monitoring:

- skin dose or the surface absorbed dose to assess the dose equivalent to the basal layer of the epidermis at a depth of (5–10) mg cm^{-2},
- whole body dose or the dose equivalent at a depth of (400–1000) mg cm^{-2} below the surface of the body to assess or overestimate the effective dose or the average dose equivalent in the critical organs,
- extremity dose to assess the maximum value of the dose equivalent (skin dose) in tissue to any part of the hands, forearms, feet or ankles [22].

The role of TLD for an individual monitoring service is based on the following features:

- TL phosphors are available in solid form as chips, rods, powder,
- dose reading is practically independent of dose rate and of the angle of radiation incidence,
- in some TL materials, the fading at room temperature is small, especially after a post irradiation annealing,
- TL detectors are convenient to wear, suitable for postal service, flexible in issue period, can be evaluated in less than 1 minute and can be re-used.

5.3. Biology and Related Fields

Applications in the following fields are given as:

- animal experiments,
- bone dosimetry,
- photon radiation quality measurements,
- general biology and biochemistry,
- ecology,
- animal habitats studied.

5.4. Environmental Monitoring

TLD systems are widely used to environmental monitoring programmes near nuclear installations.

The increasing use of artificial sources of ionising radiation causes a need for the collection of well-documented data on radiation doses in the environment. An environmental dose monitoring system must be capable of measuring a man-made contribution approximately one tenth of the natural background under unfavourable field conditions such as sunlight, extreme temperatures, high humidity, etc. Thermoluminescence dosimeters can satisfy these requirements and therefore they play a very important role in environmental monitoring. Various high sensitivity dosimeter systems based on LiF:Mg,Cu,P, LiF:Mg,Ti and Al_2O_3:C were investigated in laboratory and field tests. TLD systems were involved in intercomparisons based on different protocols.

Performance Specification TLD systems for environmental monitoring have to fulfil high requirements, such as:

- reproducibility of measurement over the exposure range, and good precision,
- low fading over the field exposure period (3–12 months),
- insensitivity to environmental parameters, i.e. temperature, moisture, humidity, light,
- approximate tissue equivalence in dose reading,

- low self-irradiation due to natural radio nuclides in the TLD phosphor or holder,
- encapsulation in a plastic holder to provide secondary electronic equilibrium, shielding against rays and light as well as water tightness,
- calibration techniques for each field cycle to guarantee the highest precision for the conversion to exposure and to correct for fading, transit exposure and zero-dose reading [50, 68].

5.5. TLD in Reactor Engineering

Thermoluminescence dosimeters based on lithium fluoride are the most commonly used in dose measurements. Due to the special properties of lithium, LiF dosimeters are used not only with directly ionising radiation, but also with neutron fields, e.g. in nuclear reactors. Lithium has two stable isotopes: ^{6}Li (7.4 %) and ^{7}Li (92.6 %). The ^{6}Li isotope is a nuclide sensitive to neutrons due to ^{6}Li (n, α) reaction, which delivers directly ionising charged particles. Value of cross section of ^{6}Li (n, α) reaction for thermal neutrons is very high: approximately 940 b. For comparing, the corresponding cross section of ^{7}Li (n, α) reaction is equal only 45.4 mb.

In order to separate doses induced by neutrons and photons, LiF dosimeters containing different percentage of ^{6}Li are applied. The LiF chip enriched in ^{6}Li is very sensitive to thermal neutrons. In contrary, the LiF chip depleted in ^{6}Li has a negligible neutron response, so it is an effective gamma dosimeter.

Because the cross section of interaction with neutrons is highly dependent on their energy, the detector efficiency strongly depends on the neutrons' energy. Thus making a dosimeter with small energy dependence of effectivity on the neutrons' energy would be very difficult. However, TL neutron dosimeters are useful for thermal neutron dose measurement [69–71].

6. Equipment and Methodology of Measurement

During the measurements, a number of devices were used to prepare the measurements with two types of detectors. MTS-N type detectors were exposed in the Nicolaus Copernicus Hospital in Lodz using medical linear accelerator, and MCP-N type detectors were exposed using X-ray equipment located in the Laboratory of Nuclear Radiation and Dosimetry at the Faculty of Physics and Applied Informatics, the University of Lodz.

6.1. Measuring Equipment

In this chapter all elements of the equipment used for irradiation, reading, annealing and UV stimulation of TLD and for dose measuring are described:

- sources of radiation,
- TL detectors,
- TLD reader/analyser,
- annealing furnaces,
- UV lamp for TLD stimulation,
- X-ray and γ-ray multimeter.

6.1.1. Medical Linear Accelerator (LINAC)

The LINAC located at the facility of Nicolaus Copernicus Voivodeship Multidisciplinary Centre of Oncology and Traumatology in Lodz was the main source of radiation utilised for this study. The LINAC utilised for this study is a CLINAC (Fig. 6.1), manufactured by the Varian Corporation. The CLINAC contains an electron source, a set of controlled by radio frequency generator electrodes generating an electric field which accelerate electrons in the gaps between electrodes. The accelerated electrons are bent through magnets that redirect them to hit a target plate that delivers high energy X-rays (Bremsstrahlung). In the electron therapy mode, the electrons pass through thin window separating the

vacuum volume from the atmospheric air and the electron beam is directed to a patient [72].

Fig. 6.1: Irradiation device: linear accelerator CLINAC.

6.1.2. X-Ray Source: Mobile Radiographic Unit Intermedical Basic 4003

The mobile radiographic unit Intermedical Basic 4003 [73] allows the selection of exposure parameters with 2-point and 3-point techniques. Essential parameters of device are listed below:

- voltage (40–110) kV,
- anode current (25–70) mA,
- exposure time 7 ms – 5 s,
- power up to 3 kW.

The unit is shown in Fig. 6.2.

Fig. 6.2: Mobile radiographic X-ray unit Intermedical Basic 4003.

6.1.3. Thermoluminescence Detectors

The MTS-N (LiF:Mg,Ti) and MCP-N (LiF:Mg,Cu,P) detectors are sintered pellets of diameter 4.5 mm and 0.9 mm thick. Their characteristic properties are shown in the Tab. 6.1 and 6.2.

MTS-N Dosimeters

The LiF:Mg,Ti was one of the sensitive LiF based phosphors used in personal dosimetry. Its symbol (MTS-N) indicates the natural abundance of lithium. It is used to measure whole body, eye lens and skin equivalent doses. MTS-N is a LiF crystal doped with magnesium and titanium. Magnesium is used to increase the number of traps in the lattice and titanium is used in order to increase the number of luminescence centres.

Table 6.1: Characteristics of MTS-N dosimeters [74].

Main features of MTS pellets	Value or information
Atomic number Z	8.2
TL emission spectrum wavelength [nm]	400
Detection threshold [μGy]	10
Linearity range [Gy]	$5 \times 10^{-5} - 5$
Repeatability	< 2 %
Photon energy dependence 30 keV – 1.3 MeV	< 30 %
Thermal fading at room temperature	< 5 % / year
Fluorescent light effect on fading and zero reading	negligible at laboratory light intensity
Reusability	unlimited
Dose rate influence	independent

MCP-N Dosimeters

This TL material: lithium fluoride doped with magnesium, copper, and phosphorus (denoted as LiF:Mg,Cu,P) was discovered at the end of the seventies. Its sensitivity to γ-rays was found to be about 30 times that of standard LiF:Mg,Ti (TLD-100). Due to its stability and low background it is possible to measure reliably doses as low as 200 nGy. These properties made LiF:Mg,Cu,P the most favourable new TL dosimetric material [75].

Table 6.2: Characteristics of MCP-N dosimeters [74]

Main features of MCP pellets	Value or information
Atomic number Z	8.2
TL emission spectrum wavelength [nm]	385
Detection threshold [μGy]	0.1
Linearity range [Gy]	$10^{-6} - 10$
Repeatability	< 2 %
Photon energy dependence 30 keV – 1.3 MeV	< 20 %
Thermal fading at room temperature	< 5 % / year
Fluorescent light effect on fading and zero reading	negligible at laboratory light intensity
Reusability	unlimited
Dose rate influence	independent

6.1.4. TLD Reader-Analyser RA'04 (Manual TLD Reader)

The RA'04 TLD Reader-Analyser is a produced in Poland and is a modern versatile device for measuring the light emitted by the TL detectors during their heating. It is designed for the analysis, testing, and measurement of thermoluminescent materials. The reader contains a photomultiplier tube (PMT), heater, amplifier and recorder. The output charge received from photomultiplier tube is proportional to the absorbed dose. Parameters of the measurement are controlled with a computer. Data are saved in a computer memory and can be evaluated, visualised, transferred etc. using computer applications.

The reading takes place in the atmosphere of inert gas such as argon. The gas is continuously pumped to decrease spurious phenomena and reduce the wrong signal produced from impurities in the air.

The Reader-Analyser TLD RA'04 works in three modes, described below.

1. READER (measurement of the absorbed dose)

The thermoluminescent material is heated in a three-stage measuring cycle: pre-heating, readout stage, final heating. Temperatures and times of individual stages of the cycle are programmed, giving the possibility to adjust the measurement conditions to the type of material used.

2. XREADER (curve registration in three-stage heating)

During the three-stage heating cycle, the thermoluminescence curve is traced in time and is evaluated as a function of time with its simultaneous recording in memory and plotting on the PC monitor screen.

3. ANALYSER (registers the curve of lighting)

Materials are heated linearly with programmed speed, until the maximum temperature, set by the operator, is reached. The system records the luminescence curve of the material under test as the function of temperature simultaneously storing the results in memory and performing on-line visualisation on a PC monitor [76]. Fig. 6.3 illustrates the Reader-Analyser RA'04.

This device is highly specialised. It has an automatic system for a compensation of the sensitivity of the measuring path and the dark current level of the photomultiplier. It is adapted to work with PCs. It has programmed conditions and measurement parameters. The software enables the analysis of glow curves; particularly, the glow peaks can be fully or partially resolved.

Fig. 6.3: Laboratory Reader Analyser RA'04

The most important technical parameters of this reader are mentioned below [76].

1. Accuracy: ± 2 % for repeated reading of the detector.
2. Stability: better than ± 2 % during 8 hours of work.
3. Sensitivity: variable reading regulated by the number of recorded counts from the reference light source.
4. Duration of measuring: mode READER: (3–180) s; standard 22 s,
   mode ANALYSER: (25–4000) s,
   mode XREADER: max. 45 s (the sum of three stages).
5. Three-stage heating: temperature from 40 °C to 400 °C in each stage,
   time of each stage (1–60) s.
6. Range of linear heating programmed: (0.1–10) °C/s.
7. Maximum programming temperature: (40–400) °C.
8. Highly stable platinum alloy heater.
9. High voltage: adjusted automatically.

6.1.5. Magma MT 1105 Therm-E4 Annealing Furnace

The Magma MT 1105 Therm-E4 annealing furnace (Fig. 6.4) is specifically developed for the thermal treatment (annealing process) of TLDs. Its operational programme is designed for annealing of TLD type MTS-N before irradiation. Thermoluminescence detectors are placed on the shelf inside the furnace, using TLD plate with a capacity of 120 TLDs (Fig. 6.5). The heating rate is set in the range (5–25) °C/min, final temperature is precisely controlled with an accuracy of ±1 °C and highest achievable temperature is equal 950 °C [77]. The annealing furnace also includes a built-in fan that distributes the heat evenly though the interior volume of the furnace during the annealing process.

Fig. 6.4: Annealing furnace MT 1105-E4.

Fig. 6.5: Plate with the TLDs type MTS-N prepared to annealing.

6.1.6. TLD Annealing Furnace SUP-18 W (Drier)

The device is designed for very precise and reproducible temperature treatment of TLD material, including preheating after irradiation for X-ray and UV and before reading by a TLD reader (programme for MCP-N). The highest achievable temperature is equal 250 °C; the time it takes to reach this temperature does not exceed 30 minutes, and the accuracy of temperature stabilisation is in the range ± 0.2 °C [78].

For annealing the TLDs were put on copper trays with the same plate as shown in Fig. 6.5. The TLD annealing furnace SUP-18 W is shown in Fig. 6.6.

Fig. 6.6: Laboratory dryer SUP-18 W.

6.1.7. UV LMS-38 8W Lamp and HC 17.5D Heating Plate

The UV lamp allows the irradiation of detectors with ultraviolet radiation in three wavelengths: 254 nm, 302 nm and 365 nm. Fig. 6.7 shows a UV lamp and a heating plate with a plate filled with thermoluminescent detectors placed thereon.

The heating plate HC17.5D is a device allowing a heating of plates with dimensions up to 125 mm × 125 mm with a temperature range up to 500 °C. It is used for heating the detectors during their irradiation with ultraviolet radiation [79].

Fig. 6.7: UV LMS-38 8W lamp with HC 17.5D heating plate
and TL detectors arranged on it.

6.1.8. Barracuda X-ray Multimeter

The Barracuda is an ‘all-in-one’ X-ray multimeter for all types of X-ray systems. It is the most versatile device available and it has set the standard for the latest generation of X-ray multimeters using solid-state technology. Barracuda with the multi-purpose detector MPD was used for the dose and kilovoltage measuring during TLD exposure on the beam produced by X-ray unit. Fig. 6.8 shows Barracuda X-ray multimeter device.

The Barracuda is designed to make it quick and easy to measure on such systems. Dose and kVp measurements are very accurate due to the automatic compensation feature.

Fig. 6.8: Barracuda X-ray multimeter device.

The measuring range fully covers the requirements for important parameters of TLD exposure at this work. For the MPD detector the measuring range in the Radiography, Fluoroscopy and Dental mode is as follows:

- X-ray tube voltage (kVp): (35–155) kV, inaccuracy: ± 1.5 %,
- air kerma (dose): 15 nGy – 1000 Gy, inaccuracy: ± 1.5 %,
- air kerma rate (dose rate): 15 nGy/s – 450 mGy/s, inaccuracy: ± 5 % or ± 7 nGy/s,
- irradiation time: 0.1 ms – 2000 s [80].

6.2. Cycle of Measurements

During this work two types of detectors: MTS-N (LiF:Mg,Ti) and MCP-N (LiF:Mg,Cu,P) were used. Experiments were performed using in total 100 MTS-N and 120 MCP-N detectors. All the detectors were used many times.

6.2.1. Handling of MTS-N Detectors

The 100 detectors were chosen from the group of 120 ones which were selected in order to choose detectors with similar performance before starting my measurements. The first step of my experimental work consisted of the division of 100 detectors into 5 groups, intended for measurements at 5 different doses. All detectors were numbered.

The procedure was performed in the following way:

1) detectors were annealed,
2) detectors were irradiated with linear accelerator of electrons,
3) detectors were subjected to post-irradiation annealing,
4) detectors were read,
5) for each dose, groups of 10 detectors were irradiated with UV and simultaneously heated for attain the PTTL effect,
6) second readout (PTTL) was carried out.

After determining the optimal temperature, the measurements were carried out with 9 values of UV exposure (and heating) time.

Ad 1: Annealing

The annealing of all MTS-N pellets was carried out in accordance with the manufacturer's instructions:

- first stage: at 400 °C within 1 h in the furnace Magma MT1105 Therm-E4 and after that cooling on the aluminium pad,
- second stage: annealing using drier/furnace SUP-18W within 2 h at the temperature 100 °C and cooling again on the aluminium pad.

Failure to comply with these conditions may result in measurement errors and even irreversible changes in the properties of phosphors.

Ad 2: Irradiation

Detectors were exposed to a beam of electromagnetic radiation at CLINAC accelerator using doses of (100, 300, 500, 700 and 1000) mGy. Absorbed doses were set using the software controlling the accelerator. Additionally, to determine the background the measurements were performed without irradiation.

Ad 3: Post-irradiation annealing

The post-exposure annealing of all MTS-N pellets was carried out using a furnace/dryer SUP-18W in accordance with the manufacturer's instructions: at the temperature 100 °C within 10 minutes and cooling on metal pad.

Ad 4: First readout

MTS-N type detectors were read using Reader-Analyser RA'04 in the XREADER mode in argon atmosphere. The three-stage heating consists of:

- heating I: at 155 °C within 5 seconds,
- heating II: at 290 °C within 15 seconds,
- heating III: at 295 °C within 5 seconds.

In the first stage of heating low energy traps (not used in dosimetry) are emptied. During the second stage of heating a thermoluminescence peak is acquired, whose area, under appropriate calibration, allows us to obtain information about the dose to which the detector was exposed. Third stage of heating finalises the detection.

Ad 5: UV irradiation and heating

The UV irradiation was carried out with LMS-38 8W UV lamp using a wavelength of 254 nm. During irradiation, TL detectors were heated on the HC17.5D heating plate. Initially, groups of 10 detectors were irradiated with UV radiation within 2 h and simultaneously heated at temperature (33, 40, 60, 70, 80, 100, 120 and 140) °C.

When the optimal temperature has been determined (80 °C), the irradiation was carried out at this temperature with following values of UV exposure (and heating) time: (0.5, 1, 2, 3, 4, 5, 6, 7 and 8) h.

Ad 6: Second readout

After UV irradiation, the detectors were read again in the Reader-Analyser RA'04, in the same conditions as during first reading. This readout delivers the information about PTTL efficiency, what is a main topic of this work.

Figure 6.9 shows the set of configuration parameters of TLD reader used with MTS-N type detectors.

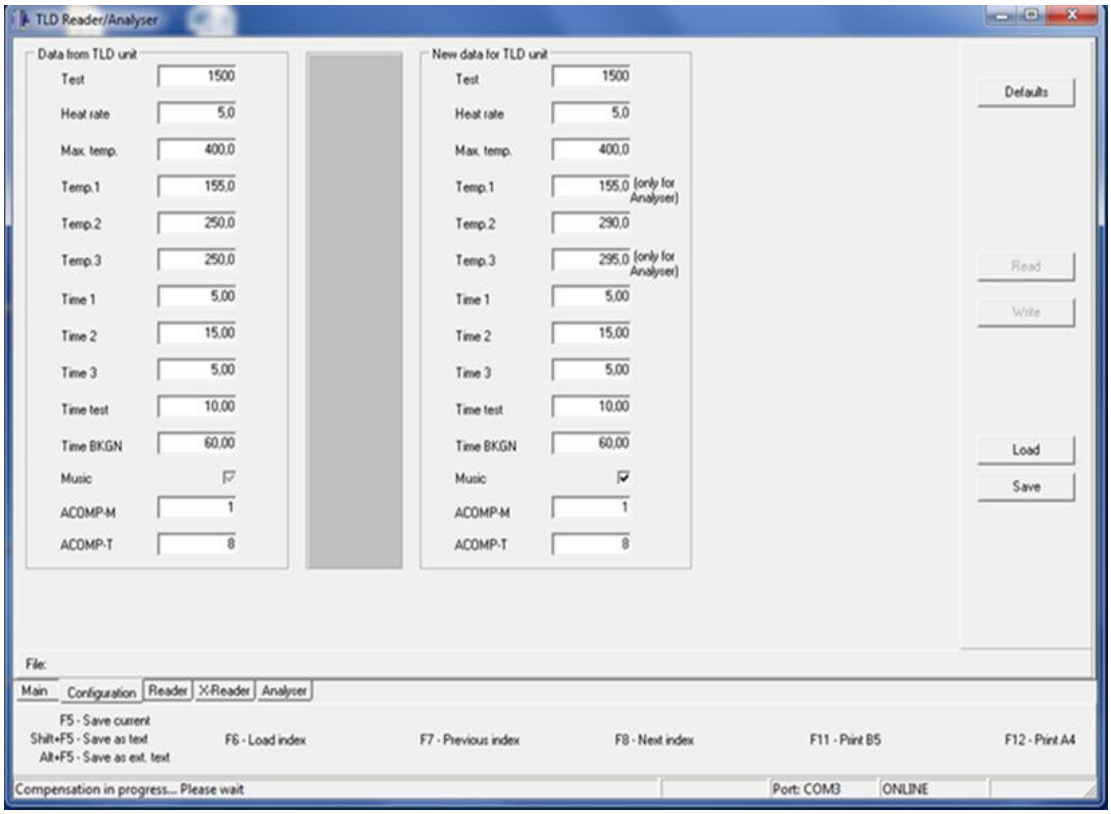

Fig. 6.9: Configuration parameters of TLD reader used with MTS-N type detectors.

Scheme of the procedure of PTTL measurements is presented in Fig. 6.10. In some cases, after the second readout there was performed additional third readout to check the emptying of the traps.

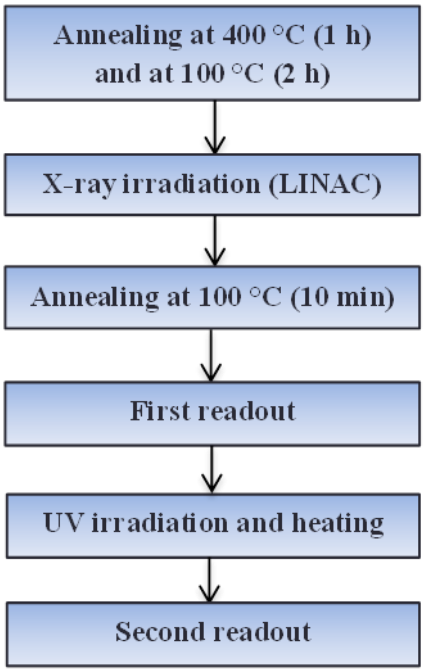

Fig. 6.10: Scheme of PTTL measurement cycle of MTS-N detectors.

6.2.2. Handling of MCP-N Detectors

Handling of MCP-N detectors was generally similar to the handling of MTS-N ones, but there are some differences regarding the annealing and reading procedures. All the 120 detectors were selected before starting my measurements. The detectors were used repeatedly.

The procedure was performed in the following way:

1) detectors were annealed,
2) detectors were irradiated with X-ray unit,
3) detectors were subjected to post-irradiation annealing,
4) detectors were read,
5) for each dose, groups of 10 or 5 detectors were irradiated with UV and simultaneously heated for attain the PTTL effect,
6) detectors were subjected to post-UV irradiation annealing,
7) second readout (PTTL) was carried out.

After determining the optimal temperature, the measurements were carried out with 10 values of UV exposure (and heating) time.

Ad 1: Pre-irradiation annealing

The first annealing of all MCP-N pellets was carried out in the furnace/dryer SUP-18W in accordance with the manufacturer's instructions: at 240 °C within 10 minutes and after that cooling on the aluminium pad.

Ad 2: Irradiation

Detectors were exposed on the beam of electromagnetic radiation at X-ray mobile radiography unit Intermedical Basic 4003 using doses of (0.5, 1, 2, 5, 10 and 25) mGy. Absorbed doses were measured with Barracuda X-ray multimeter. Additionally, to determine the background the measurements were performed without irradiation.

Ad 3: Post-irradiation annealing

The post-exposure annealing of all MCP-N pellets was carried out in the furnace/dryer SUP-18W in accordance with the manufacturer's instructions: at the temperature 100 °C within 10 minutes and cooling on metal pad.

Ad 4: First readout

MCP-N type detectors were read using Reader-Analyser RA'04 in the XREADER mode in argon atmosphere. The three-stage heating is different as for MTS-N detectors and it consists of:

- heating I: at 155 °C within 5 seconds,
- heating II: at 250 °C within 15 seconds,
- heating III: at 250 °C within 5 seconds.

Ad 5: UV irradiation and heating

The UV irradiation was carried out with LMS-38 8W UV lamp using a wavelength of 254 nm. During irradiation, TL detectors were heated on the HC17.5D heating plate. Initially, groups of 10 or 20 or 5 detectors were irradiated with UV radiation within 2 h and simultaneously heated at temperature (30, 40, 50, 60, 70, 80, 90, 100, 110 and 120) °C.

When the optimal temperature has been determined (80 °C), the irradiation was carried out at this temperature with following values of UV exposure (and heating) time: (10, 20, 30, 40, 50, 60, 70, 80, 90, 100 and 110) min and (2, 2.5, 3, 3.5 and 4) h.

Ad 6: Post-UV irradiation annealing

The post-exposure annealing of all MCP-N pellets was carried out in the furnace/dryer SUP-18W using the same conditions as in previous annealing: at the temperature of 100 °C within 10 minutes and cooling on metal pad.

Ad 7: Second readout

Finally, the detectors were read again in the Reader-Analyser RA'04, in the same conditions as during first reading. This readout delivers the information about PTTL efficiency.

Configuration parameters of the TLD reader used with MCP-N type detectors are shown in Fig. 6.11.

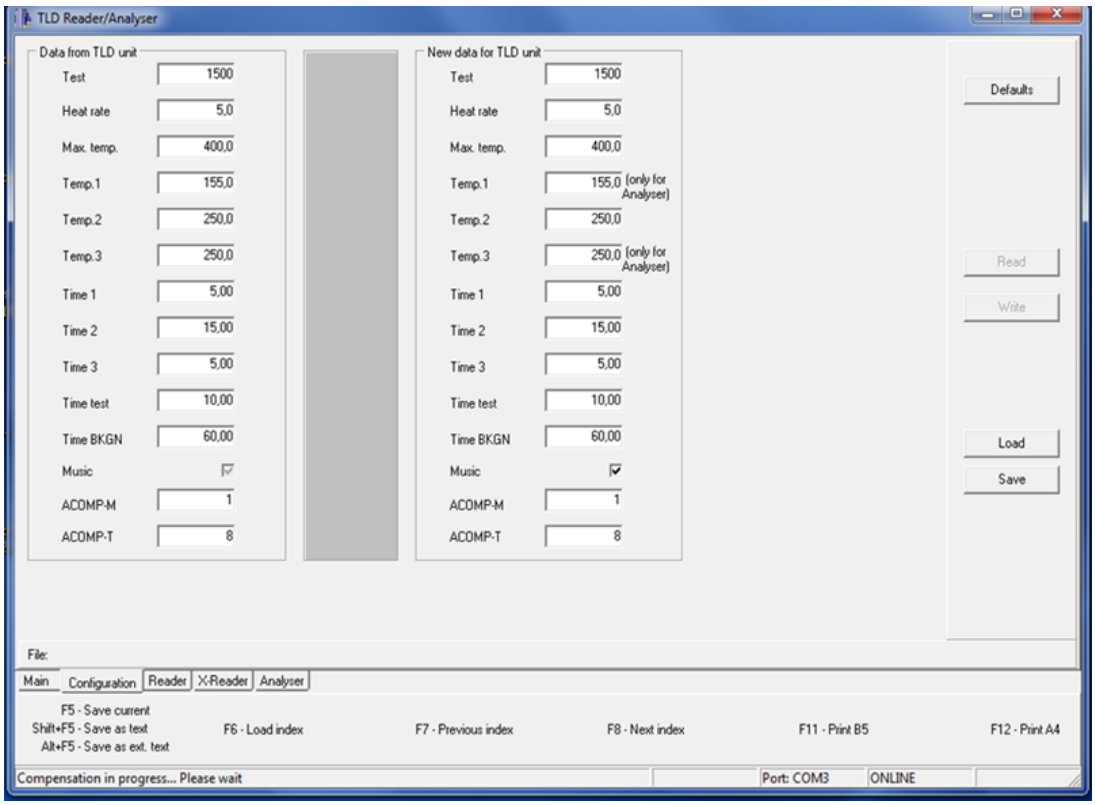

Fig. 6.11: Configuration parameters of TLD reader used with MCP-N type detectors.

Scheme of the procedure of PTTL measurements is presented in Fig. 6.12.

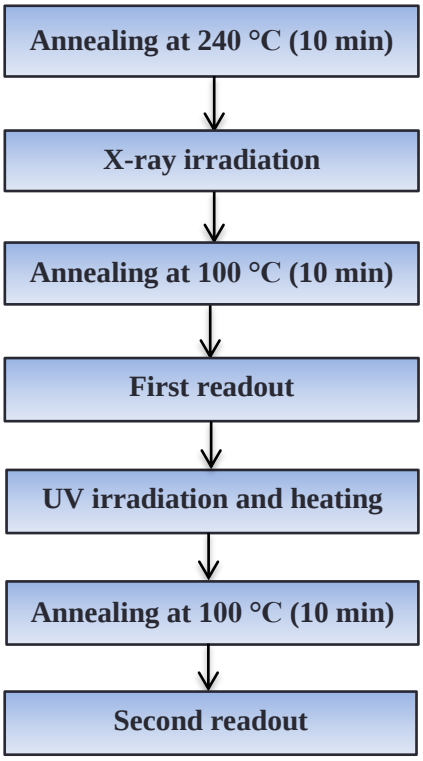

Fig. 6.12: Scheme of PTTL measurement cycle of MCP-N detectors.

7. Results and Discussion

The possibility of implementing this method to dose reassessment for individual dosimetry has been checked in the range up to 1000 mGy for MTS-N detectors and (0–25) mGy for MCP-N detectors.

7.1. Preliminary Measurements

7.1.1. Choice of Test Parameter for TLD Reading

One of parameters adjusted at the reading of TLDs in a Reader-Analyser RA'04 is the so called Test parameter (see Fig. 6.9 and 6.11). This parameter is set by the operator as number of counts to be recorded from a calibration light source during the self-calibration procedure. The values of the Test parameter belong within the range of 100 to 9000. During the reading TLD exposed for the same dose, the number of counts is roughly proportional to Test value. So the Test parameter is closely related to the sensitivity of the detection.

The study has been carried out with MTS-N dosimeters exposed to the dose of 1000 mGy, using 7 groups of 10 dosimeters. For each group of dosimeters a different Test parameter value was set. The Test parameter values and number of counts registered are shown in the table below.

Table 7.1: Test parameter and average number of counts at the dose of 1000 mGy.

Test parameter	300	500	1000	1500	2000	2500	3000
Average number of counts	43 962	65 187	127 725	197 597	261 007	331 162	415 112

As one could be expected, the number of counts is roughly proportional to the Test parameter: the quotient of number of counts and Test parameter is approximately constant (Tab. 7.2).

Table 7.2: Quotient of number of counts and Test parameter at the dose of 1000 mGy.

Test parameter	300	500	1000	1500	2000	2500	3000
Average number of counts per Test parameter	146.5	130.4	127.7	131.7	130.5	132.5	138.4

Assuming, in simplification, the proportionality between the dose and number of counts, the calibration coefficient a can be calculated:

$$D = a \cdot N, \tag{7.1}$$

where D is an absorbed dose, N – number of pulses and a – calibration coefficient. Values of this coefficient, calculated based on Eq. (7.1), are listed in the Tab. 7.3 and shown in the Fig. 7.1.

Table 7.3: Test parameter and calibration coefficient.

Test parameter	300	500	1000	1500	2000	2500	3000
Calibration coefficient, mGy/pulses	0.0227	0.0153	0.0078	0.0051	0.0038	0.0030	0.0024

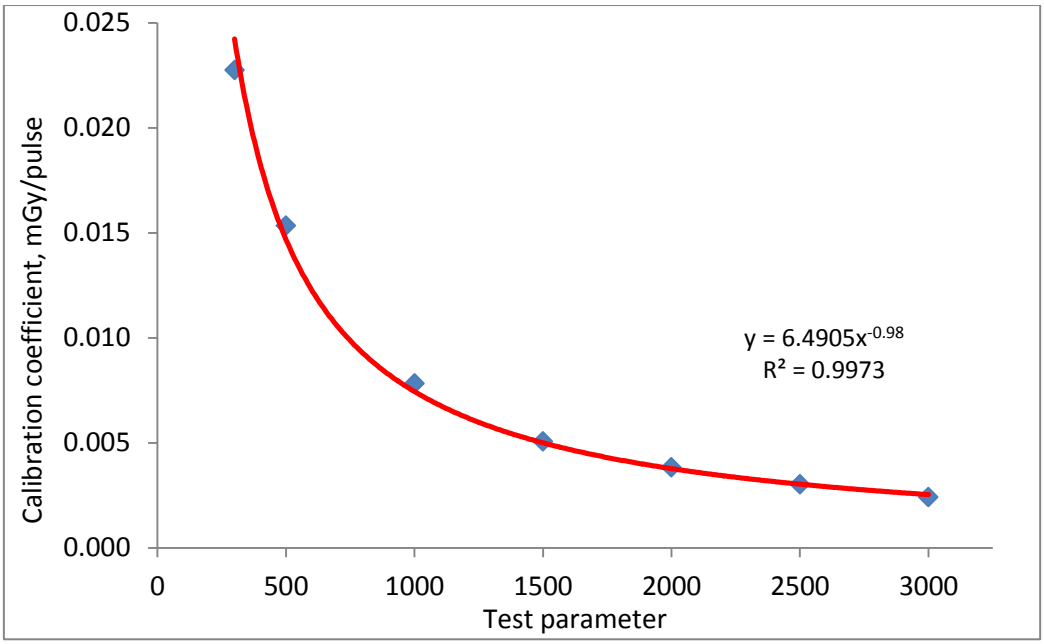

Fig. 7.1: Simplified calibration coefficient as a function of Test parameter and a fit of this dependence with power function.

For further analysis, the Test parameter was chosen as 1500, in order to work with relatively large number of pulses, but and at the same time avoiding pulses superimposition.

7.1.2. Choosing UV wavelength

One of the first issues in PTTL measurements was choosing the optimal UV wavelength. Three wavelengths were available: 254, 302 and 365 nm. Set of MCP-N dosimeters has been divided into 3 groups of 35 for each wavelength. All dosimeters were irradiated with X-ray with different doses up to 25 mGy, at the same conditions inside each group. Next all detectors were subjected to the first reading, later to UV exposure (each group with different wavelength) with heating within 2 hours at 80 °C and finally to re-reading.

Average numbers of counts for three wavelengths doses are shown in Tab. 7.4—7.6 and in Fig. 7.2—7.4 as functions of dose.

The biggest PTTL yield and the biggest directional coefficient have been obtained at the UV wavelengths equal 254 nm, thus the wavelength of 254 nm has been considered optimal.

Table 7.4: Absorbed dose and PTTL counts after the UV exposure with λ = 254 nm.

Dose, mGy	Average count
0	267 ± 87
0.5	288 ± 38
1	298 ± 69
2	350 ± 79
5	403 ± 66
10	552 ± 100
25	1285 ± 446

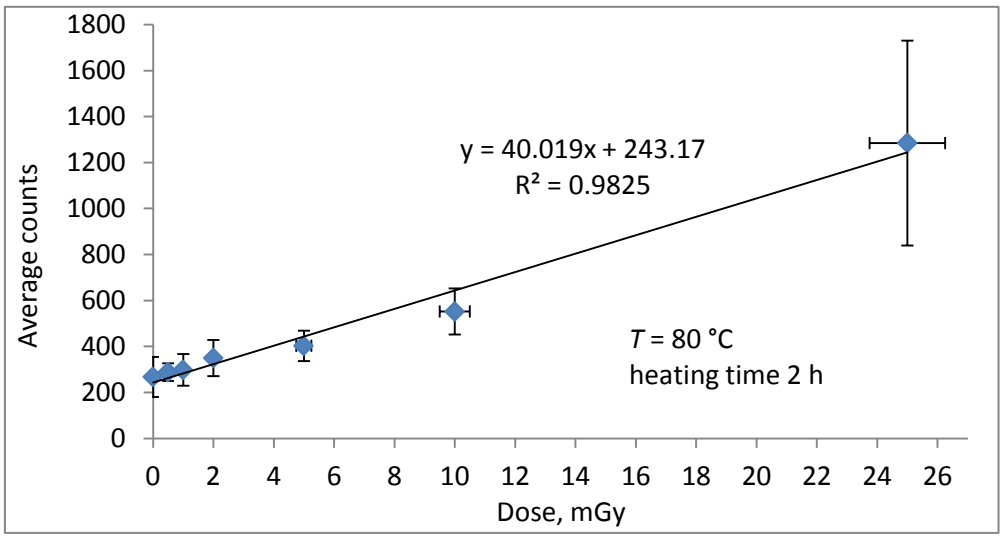

Fig. 7.2. The PTTL signal versus dose after the UV exposure with λ = 254 nm.

Table 7.5: Absorbed dose and PTTL counts after the UV exposure with λ = 302 nm.

Dose, mGy	Average count
0.5	319 ± 63
1	273 ± 35
2	321 ± 63
5	259 ± 28
10	380 ± 73
25	517 ± 108

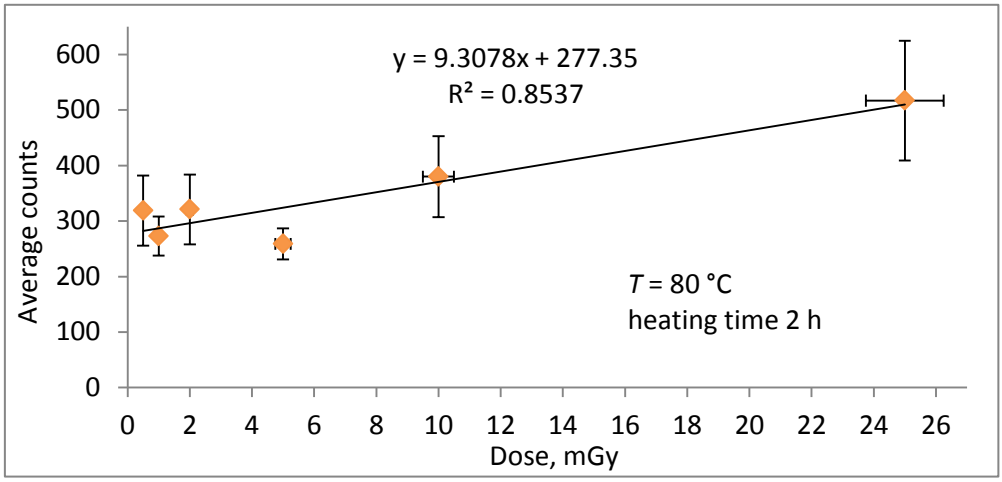

Fig. 7.3. The PTTL signal versus dose after the UV exposure with λ = 302 nm.

Table 7.6: Absorbed dose and PTTL counts after the UV exposure with λ = 365 nm.

Dose, mGy	Average count
0.5	252 ± 53
1	245 ± 67
2	474 ± 104
5	253 ± 51
10	287 ± 63
25	423 ± 91

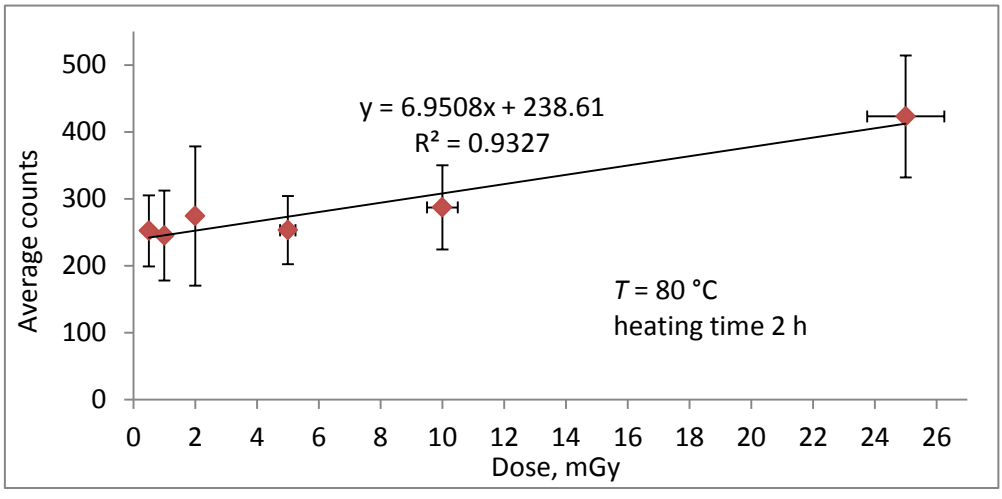

Fig. 7.4. The PTTL signal versus dose after the UV exposure with λ = 365 nm.

The coefficients describing the slope of linear dependence of counts vs. dose are obtained as followed: 40.0/mGy for λ = 254 nm, 9.3/mGy for λ = 302 nm and 7.0/mGy for λ = 365 nm. Comparison of these three slope values leads us to the unquestionable conclusion that among the three wavelengths tested the best results are obtained for λ = 254 nm. Therefore, this wavelength was chosen for further measurements.

7.2. First and Second Readout of MTS-N Dosimeters

7.2.1. Linearity of TL Detectors at First Readout

In order to make sure that the measuring equipment was working properly, the dose vs. average number of counts from 10 MTS-N detectors read in the Reader--Analyser RA'04 had been studied. The measurements have been performed with 10 dosimeters at every dose value. Results are summarised in the Tab. 7.7.

Table 7.7: Dose and average number of counts after irradiation

Dose, mGy	Average count
0	2 346 ± 497
100	22 244 ± 908
300	61 763 ± 2 773
500	97 247 ± 5 355
700	135 529 ± 6 071
1000	197 597 ± 11 266

Because one should expect a linear relationship between dose and number of counts, this relationship, also named 'calibration curve', can be described by the formula more advanced than shown in Eq. (7.1):

$$D = a \cdot N + b, \tag{7.2}$$

where:

D: absorbed dose (mGy),

a and b: calibration coefficients (mGy/pulse and mGy, respectively),

N: number of counts.

The calibration coefficients were calculated with the linear regression method. Their values are as follows: $a = (5.17 \pm 0.06) \times 10^{-3}$ mGy/pulse and $b = (-12 \pm 6)$ mGy.

Uncertainty of dose measurement was estimated as 2 % of dose. Calibration curve is shown in the Fig. 7.5. The graph shows experimental data for the first readout and their linear fit. Value of the square of correlation coefficient, $R^2 = 0.9995$, indicates accurate linearity of the relationship studied.

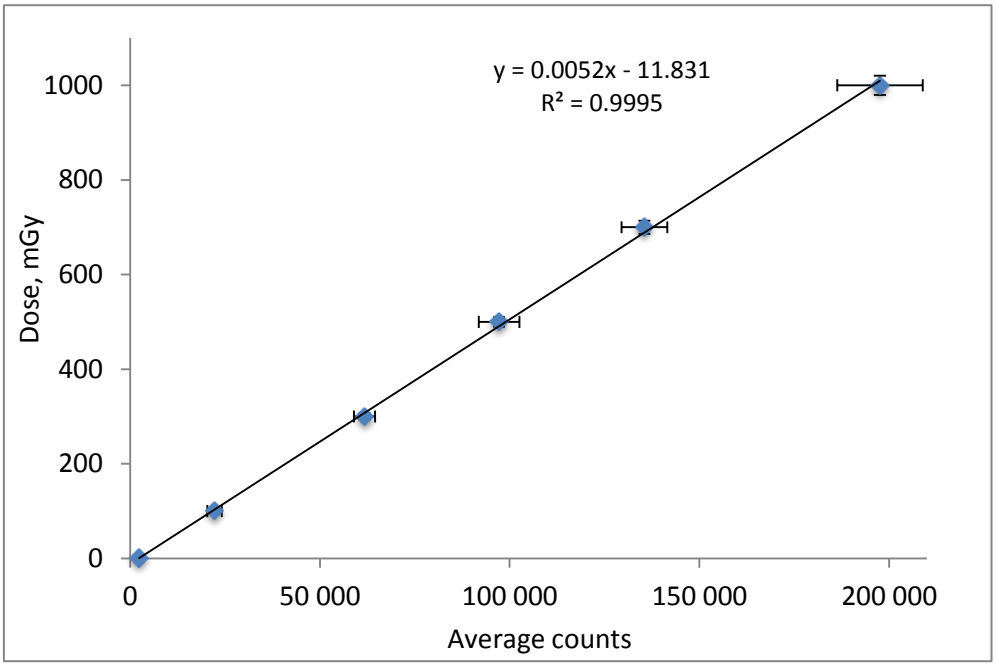

Fig. 7.5: Calibration curve for MTS-N thermoluminescence detector describing the relationship between the dose and number of pulses received during detector's first readout.

The procedure of measurements is generally described in chapter 6.2.1. There are depicted only the parts of the measuring cycle relating to PTTL survey. At first, groups of 10 dosimeters were exposed at CLINAC accelerator with the dose of (100, 300, 500, 700 and 1000) mGy and subjected to reading at the Reader--Analyser RA'04. Additionally, to determine the background, the group of non--irradiated dosimeters was involved.

Then the dosimeters were irradiated with UV radiation with a wavelength of $\lambda = 254$ nm and simultaneously heated. The second readout was performed at the same Reader-Analyser in XREADER mode. In this mode three-step heating is applied and the glow curve is registered as a number of counts obtained in short time intervals vs. time. Because parameters of the second readout are the same as in first readout, it is possible to compare both glow curves. Sum of counts obtained during the reading in XREADER mode enables calculation of the PTTL efficiency.

The first set of measurements was performed with UV irradiation within 2 h, at temperature (33, 40, 60, 70, 80, 100, 120 and 140) °C.

After determination of optimal temperature, the irradiation was carried out at temperature 80 °C with following values of UV exposure (and heating) time: (0.5, 1, 2, 3, 4, 5, 6, 7 and 8) h.

7.2.2. Examples of TL Glow Curves

The figures below shown the TL glow curves, obtained at the first readout (green) and second readout (blue) of dosimeters exposed at CLINAC accelerator. Third curve (brown) in these figures is a glow curve, obtained after the second readout of dosimeter. This measurement has been added for verification, to what extent the traps are emptied during the second readout.

All the examples shown in the Fig. 7.6—7.15 refer to the second readout carried out after UV irradiation with heating at 80 °C within 2 hours.

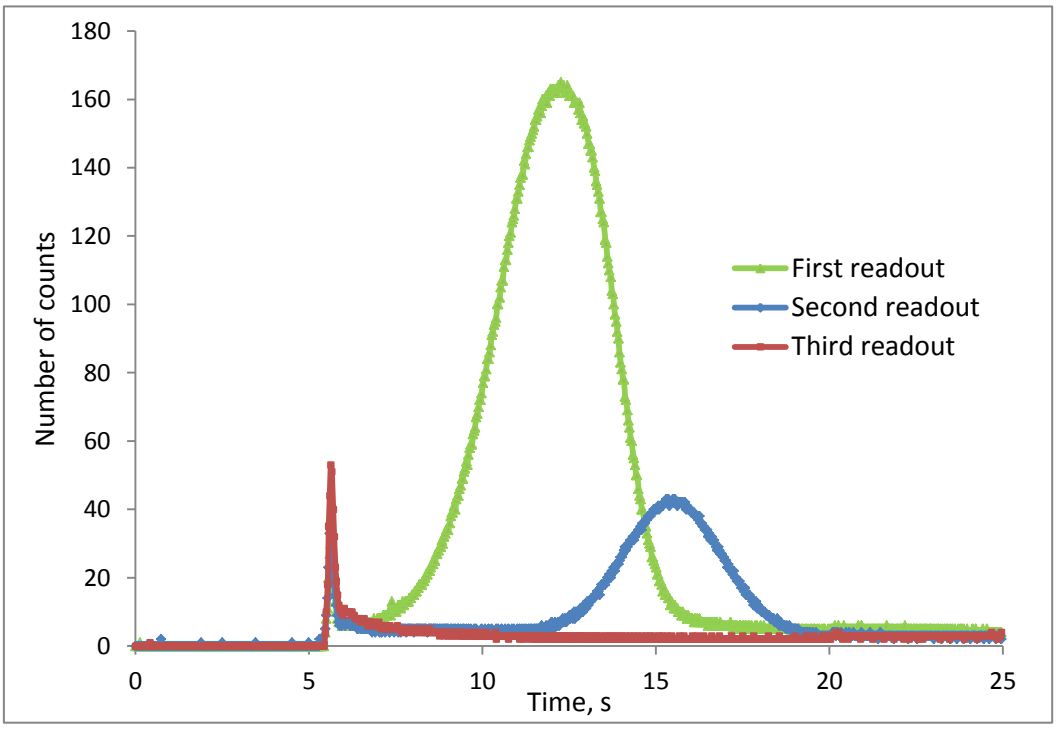

Fig. 7.6: TL curves obtained as a result of reading the detector number 59 at dose 100 mGy.

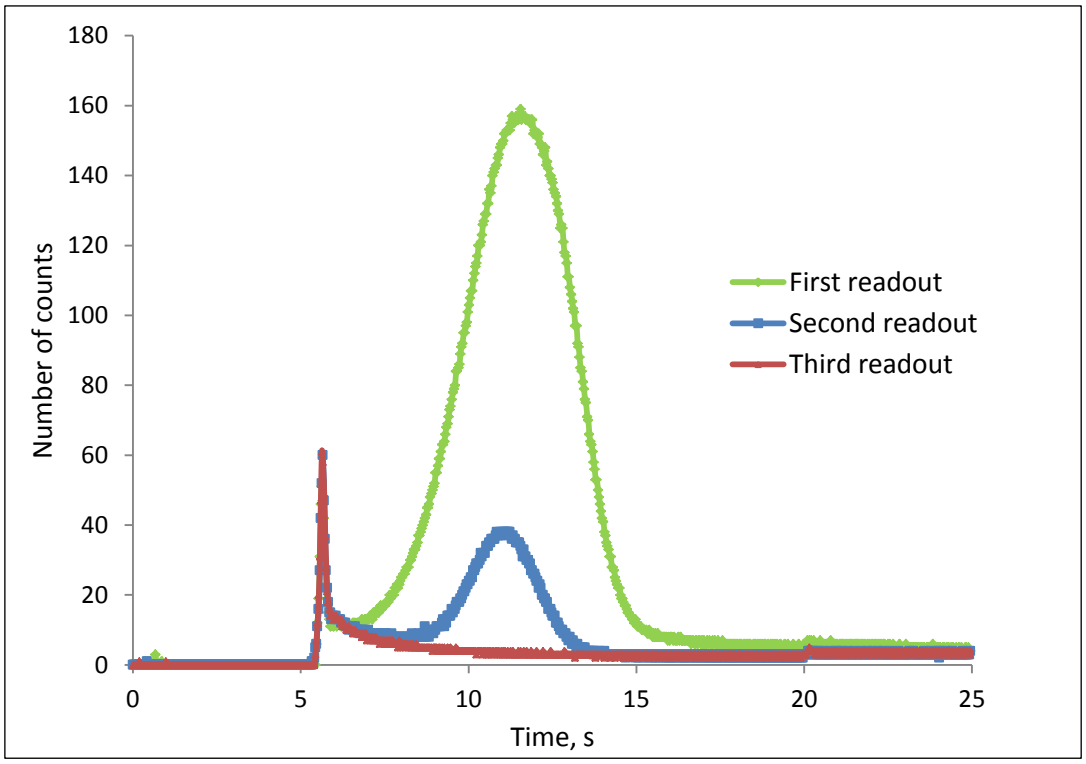

Fig. 7.7: TL curves obtained as a result of reading the detector number 44 at dose 100 mGy.

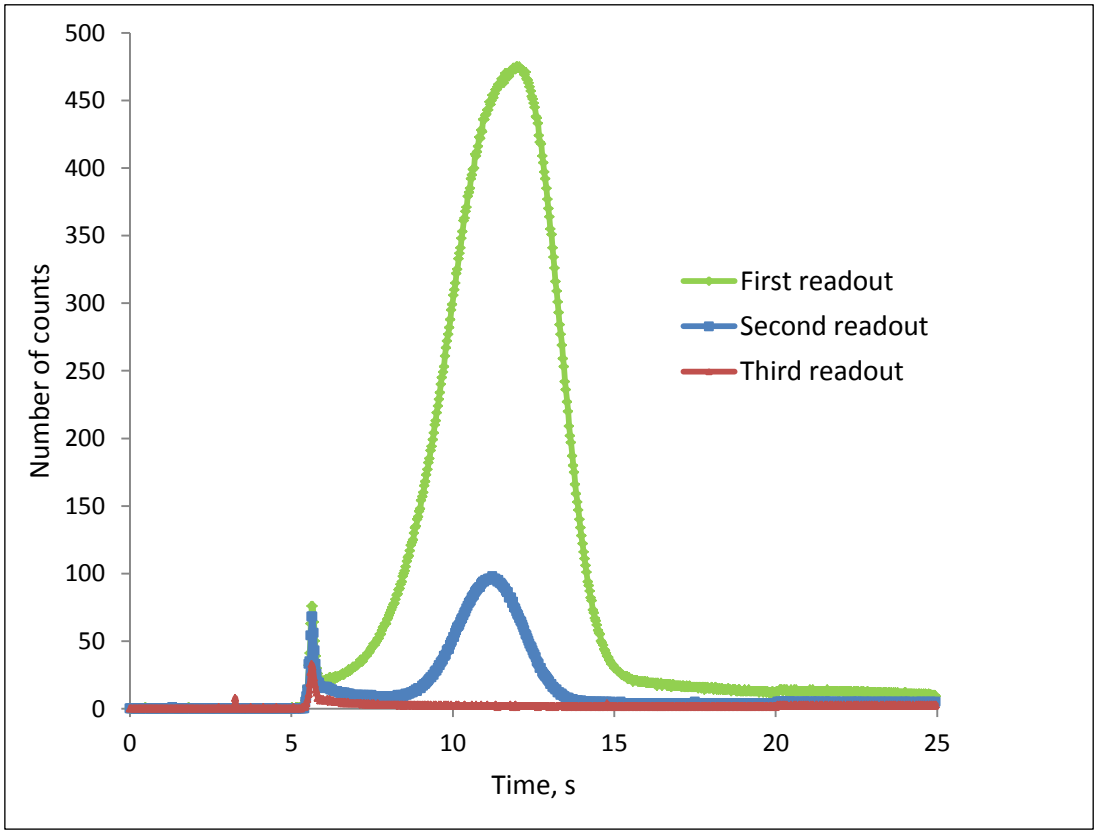

Fig. 7.8: TL curves obtained as a result of reading the detector number 69 at dose 300 mGy.

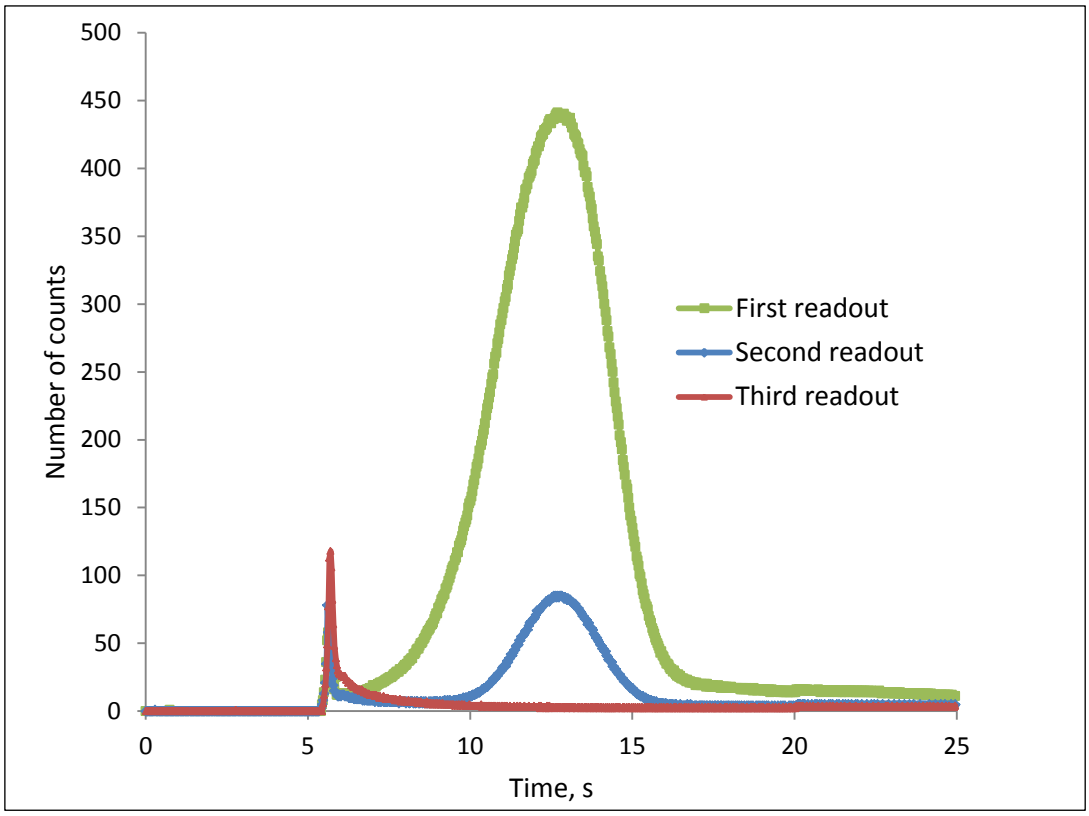

Fig. 7.9: TL curves obtained as a result of reading the detector number 23 at dose 300 mGy.

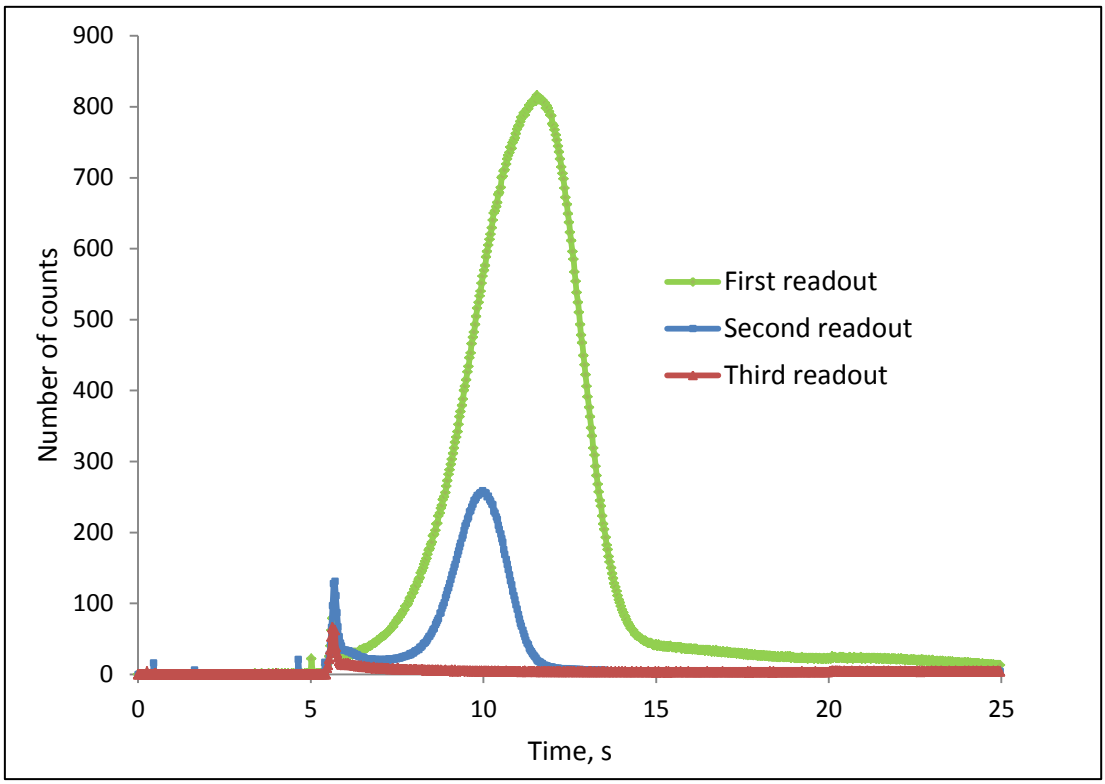

Fig. 7.10: TL curves obtained as a result of reading the detector number 150 at dose 500 mGy.

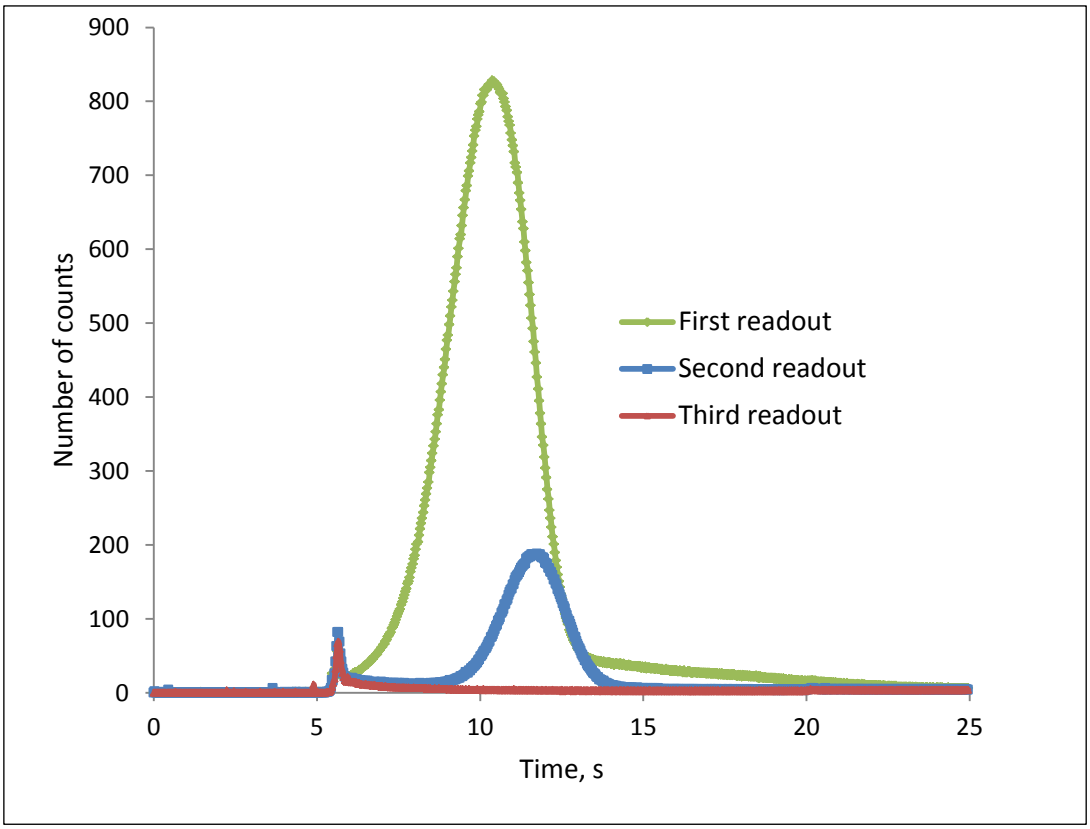

Fig. 7.11: TL curves obtained as a result of reading the detector number 149 at dose 500 mGy.

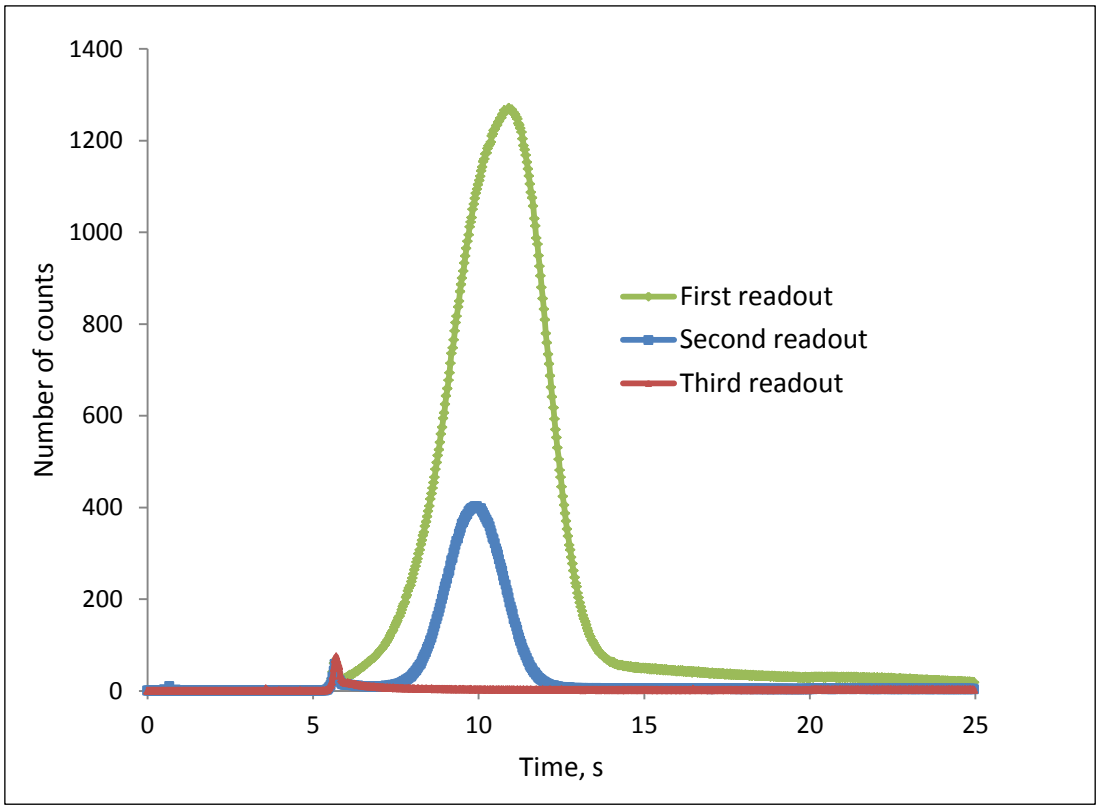

Fig. 7.12: TL curves obtained as a result of reading the detector number 155 at dose 700 mGy.

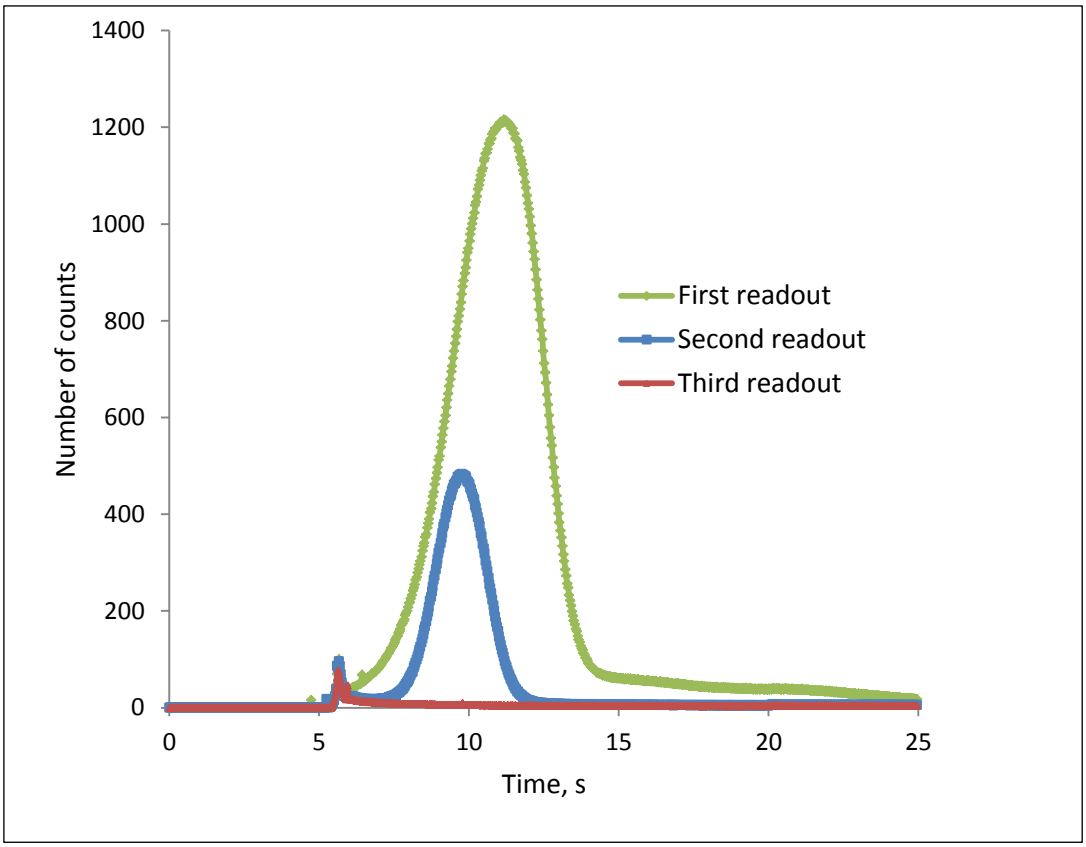

Fig. 7.13: TL curves obtained as a result of reading the detector number 147 at dose 700 mGy.

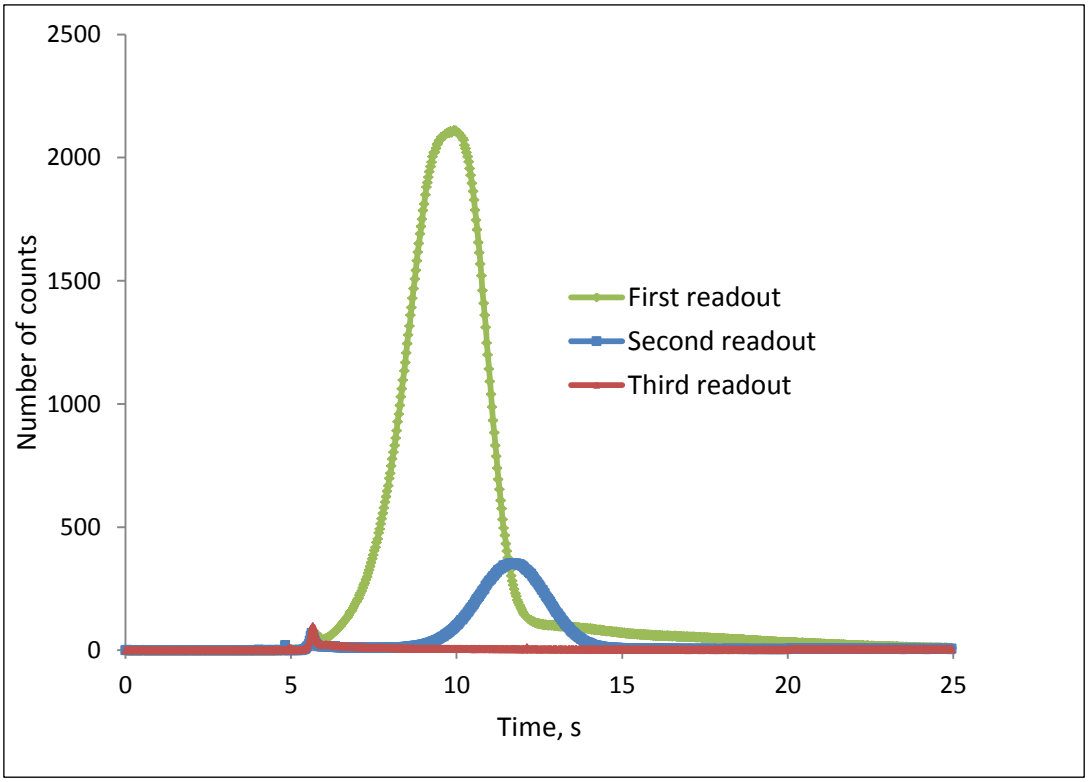

Fig. 7.14: TL curves obtained as a result of reading the detector number 193 at dose 1000 mGy.

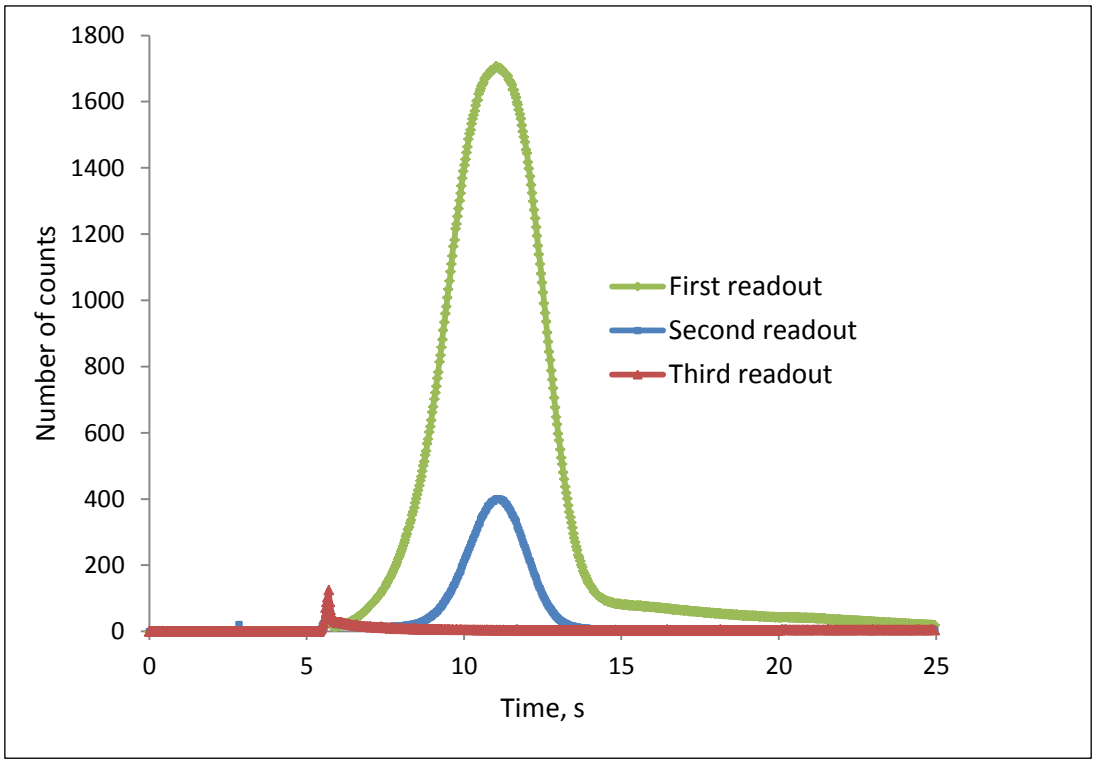

Fig. 7.15: TL curves obtained as a result of reading the detector number 151 at dose 1000 mGy.

7.2.3. PTTL Yield at Different Conditions of UV Exposure and Heating

The measurements were performed with the same wavelength of UV radiation (λ = 254 nm) and the exposure time of 2 hours, using heating temperatures (33, 40, 60, 70, 80, 100, 120 and 140) °C. Values of doses applied were (100, 300, 500, 700, and 1000) mGy.

Tables 7.8—7.15 illustrate experimental results: number of counts during second readout, after applying UV radiation within 2 hours. In these tables the value marked ‘Det’ is the detector number, ‘Counts’ is the number of counts obtained at the second readout and ‘No’ is the consecutive number of a measurement. The time interval of counting has been set from 6 to 16 seconds after start the reading. For some detectors, in justified cases only, its upper limit has been shifted to 20 seconds.

Table 7.8: Number of counts at second readout after 2-hours UV exposure at 33 °C.

Dose	100 mGy		100 mGy		300 mGy		500 mGy		700 mGy	
No	Det	Counts	Det	Counts	Det	Counts	Det	Counts	Det	Counts
1	30	3324	91	3755	69	6026	18	10316	155	14307
2	171	3065	66	3725	168	6342	57	10980	65	11847
3	188	3385	5	4257	31	4880	55	10419	195	10416
4	15	4113	24	3762	178	6079	2	10517	169	11648
5	28	3146	37	4198	94	5727	43	9992	82	15708
6	58	3832	26	2819	54	7209	149	8099	12	13808
7	60	4022	104	4476	42	5883	75	11188	93	12522
8	145	3803	1	3358	7	5789	78	10240	154	15204
9	45	4889	151	3223	148	5478	29	10242	92	11691
10	173	4287	36	2009	23	5866	6	10322		
Average		3787 ± 571		3558 ± 741		5928 ± 597		10231 ± 831		13017 ± 1814

Table 7.9: Number of counts at second readout after 2-hours UV exposure at 40 °C.

Dose	100 mGy		100 mGy		300 mGy		500 mGy		700 mGy	
No	Det	Counts	Det	Counts	Det	Counts	Det	Counts	Det	Counts
1	159	3575	70	2948	143	7861	49	13140	99	15903
2	59	4889	47	5494	183	8567	88	12088	35	13114
3	156	4992	95	3817	53	9361	56	10468	157	10851
4	74	4451	19	4986	172	7778	46	11907	189	13161
5	81	4805	71	5217	192	9368	17	9395	16	14307
6	68	4806	167	5585	164	6146	150	11212	179	16169
7	79	5007	62	4342	14	7624	174	13557	147	15255
8	36	4356	27	2419	105	8188	86	9003	83	16287
9	44	3313	22	3107	98	6238	13	9525	144	15453
10	191	4231	10	3693	146	7973	67	13175	25	14132
Average		4442 ± 593		4160 ± 1135		7910 ± 1093		11347 ± 1690		14463 ± 1720

Table 7.10: Number of counts at second readout after 2-hours UV exposure at 60 °C.

Dose	100 mGy		300 mGy		500 mGy		700 mGy		1000 mGy	
No	Det	Counts	Det	Counts	Det	Counts	Det	Counts	Det	Counts
1	159	4876	27	8341	150	14142	189	19584	66	18893
2	45	4207	54	6878	57	11308	157	13800	5	19195
3	79	8120	70	8513	56	15671	35	17140	146	23215
4	30	3760	167	12024	67	10305	147	19466	192	21755
5	60	3684	148	17205	88	14064	169	16446	24	22072
6	15	9920	62	10441	29	9782	82	19305	1	18280
7	81	10330	168	8306	75	13371	179	15744	143	21658
8	171	7165	47	9358	55	9334	65	17017	164	20588
9	156	3993	22	8406	6	9566	93	18285	151	20429
10	191	13335	94	6848	49	14038	83	12139	104	20243
Average		6939 ± 3397		9632 ± 3079		12158 ± 2343		16892 ± 2481		20632 ± 1559

Table 7.11: Number of counts at second readout after 2-hours UV exposure at 70 °C.

Dose	100 mGy		300 mGy		500 mGy		700 mGy		1000 mGy	
No	Det	Counts	Det	Counts	Det	Counts	Det	Counts	Det	Counts
1	45	5138	10	14444	78	17275	35	23990	5	26295
2	59	5735	69	19616	86	13996	82	25605	37	26824
3	81	8264	27	17664	67	18699	12	24652	151	25647
4	173	8741	95	15776	17	22173	16	19595	98	26994
5	63	14161	22	16944	57	18409	155	23832	36	23219
6	145	12913	70	13293	149	17361	83	19260	143	25196
7	171	11423	31	10366	2	14671	169	22549	192	30524
8	79	14709	7	13438	29	16831	154	20028	104	28790
9	191	8251	42	22444	13	18120	157	22425	183	24864
10	188	14497			150	17485			26	23247
Average		10383 ± 3625		15998 ± 3646		17502 ± 2243		22437 ± 2326		26160 ± 2288

Table 7.12: Number of counts at second readout after 2-hours UV exposure at 80 °C.

Dose	100 mGy		300 mGy		500 mGy		700 mGy		1000 mGy	
No	Det	Counts	Det	Counts	Det	Counts	Det	Counts	Det	Counts
1	68	6301	19	18126	149	16361	99	29806	38	33592
2	74	8871	167	12221	29	17665	92	22598	17	25590
3	159	9792	148	18662	67	20191	155	28229	193	30951
4	58	10652	178	15049	86	15476	144	25282	159	26929
5	60	9909	71	12211	88	21283	25	24643	151	31810
6	15	10814	94	11221	75	21123	154	27699	84	24012
7	28	9567	168	11416	18	22688	83	27901	57	26706
8	44	12916	54	12832	55	17857	147	33933	12	27901
9	156	13016	62	15731	78	21383	65	24624	49	27620
10	30	10115			150	18586	179	22525	13	21655
Average		10195 ± 1930		14163 ± 2844		19261 ± 2412		26724 ± 3520		27677 ± 3627

Table 7.13: Number of counts at second readout after 2-hours UV exposure at 100 °C.

Dose	100 mGy		300 mGy		500 mGy		700 mGy		1000 mGy	
No	Det	Counts	Det	Counts	Det	Counts	Det	Counts	Det	Counts
1	58	4097	71	8714	43	15428	12	17986	53	33550
2	63	5135	95	8924	18	15397	92	19797	105	27328
3	74	5270	10	9521	17	9482	155	16735	183	30973
4	145	3757	42	8610	13	9466	99	17709	98	16525
5	44	3744	19	8499	149	6898	195	12604	37	19234
6	28	5062	69	6218	46	10070	154	10802	26	19315
7	59	3797	178	8246	174	9799	25	13189	172	23558
8	173	2909	31	6196	86	7989	144	14196	36	21618
9	188	2917	23	6272	78	11362	16	11138	14	15522
10	68	4519	7	7682	2	9407			91	24008
Average		4121 ± 862		7888 ± 1236		10530 ± 2833		14906 ± 3248		23163 ± 5983

Table 7.14: Number of counts at second readout after 2-hours UV exposure at 120 °C.

Dose	100 mGy		300 mGy		500 mGy		700 mGy		1000 mGy	
No	Det	Counts	Det	Counts	Det	Counts	Det	Counts	Det	Counts
1	45	2998	10	9352	55	9464	179	12627	66	21710
2	59	4492	69	6581	18	7393	92	11344	172	19290
3	81	3298	27	5320	49	8424	189	6678	1	13570
4	173	4621	95	5435	56	7535	195	7691	53	13393
5	63	3516	22	5257	46	7605	25	7986	164	12194
6	145	3632	23	5680	75	7393	65	6864	105	11719
7	171	4566	70	3436	6	5934	93	6971	146	11333
8	79	4730	31	4256	43	7392	144	8815	14	12720
9	191	4675	7	4408	88	8303	99	8092	24	14766
10	188	4943	42	7636	174	7123	147	9963	91	15721
Average		4147 ± 705		5736 ± 1737		7657 ± 928		8703 ± 2010		14642 ± 3410

Table 7.15: Number of counts at second readout after 2-hours UV exposure at 140 °C.

Dose	100 mGy		300 mGy		500 mGy		700 mGy		1000 mGy	
No	Det	Counts	Det	Counts	Det	Counts	Det	Counts	Det	Counts
1	68	2478	19	5051	78	5172	35	7948	5	11821
2	74	2752	167	3052	86	4205	82	5994	37	8377
3	159	3005	148	4680	67	4925	12	4462	151	9555
4	58	3619	178	3956	17	4079	16	5406	98	8227
5	60	2898	71	4528	57	5125	155	5872	36	7619
6	15	2716	94	3367	149	4126	83	5501	143	6432
7	28	2382	168	2595	2	5576	169	4534	192	8970
8	44	3813	47	2335	29	4460	154	5290	104	8041
9	156	4427	54	3216	13	4808	157	4838	183	10455
10	30	5566	62	4509	150	5967			26	10828
Average		3366 ± 1007		3729 ± 945		4844 ± 637		5538 ± 1053		9032 ± 1637

When the TL glow curves of TLD after different temperature of UV exposure (33, 40, 60, 70, 80, 100, 120 and 140) °C are placed together, a clear example of PTTL can be observed. The thermally stimulated transfer of electronic charge causes this from deep traps to shallow traps, and results in the generation of thermoluminescence peaks at low temperatures.

Increasing temperature during UV exposure (up to ~80 °C) causes an increase of the PTTL signal. With a further increase of temperature, the PTTL signal decreases. The optimal temperature for UV irradiation has been found as 80 °C.

Figure 7.16 shows the PTTL yield after UV exposure applied to detectors that have been previously exposed to X-ray from linear accelerator with dose range of (100–1000) mGy.

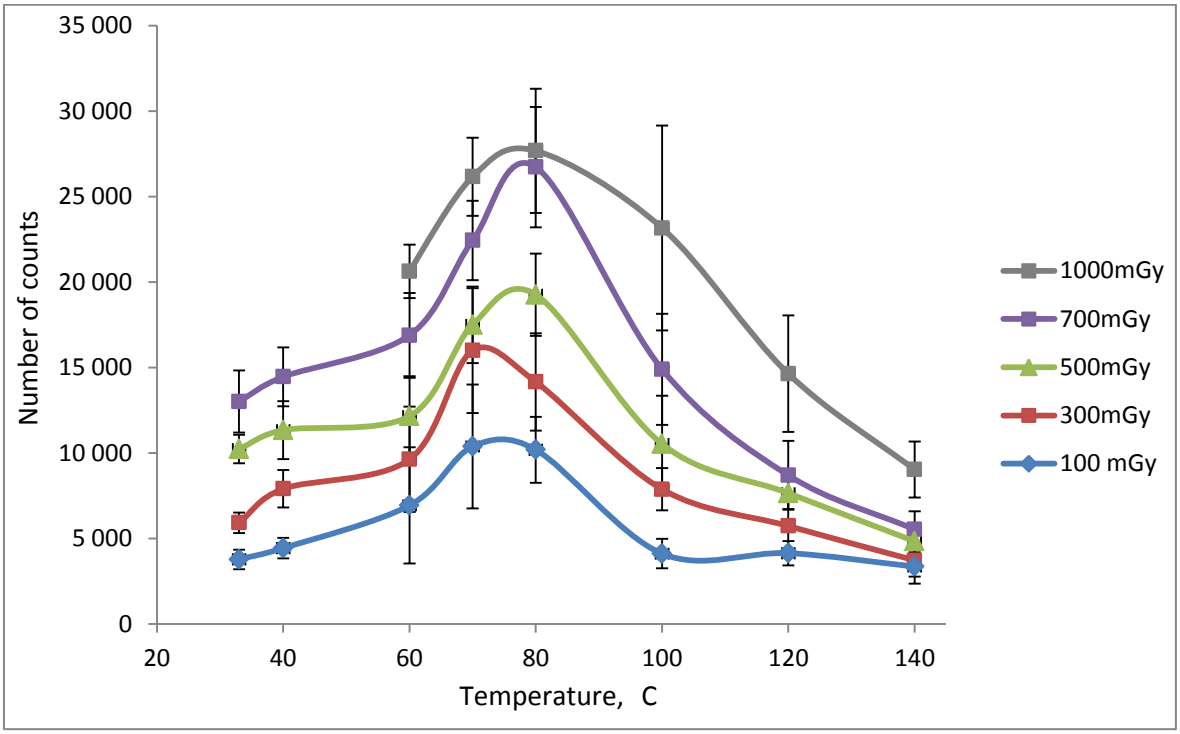

Fig. 7.16. PTTL signal of (100, 300, 500, 700 and 1000) mGy irradiated MTS-N detectors, after UV irradiation for 2 hours at temperatures (33, 40, 60, 70, 80, 100, 120, 140) °C.

The next measurements were carried out using different heat time (0.5, 1, 2, 3, 4, 5, 6, 7 and 8) hours, the same wavelength λ = 254 nm, and temperature 80 °C. Additionally, TLD elaboration was performed using dark room to prevent any influence of light. Results are shown in Tab. 7.16—7.24.

Table 7.16: Number of counts at second readout after 0.5-hour UV exposure at 80 °C.

Dose	100 mGy		300 mGy		500 mGy		700 mGy		1000 mGy	
No	Det	Counts	Det	Counts	Det	Counts	Det	Counts	Det	Counts
1	45	4148	10	11765	55	16464	179	24678	66	29440
2	59	5556	69	10449	18	20360	92	22219	172	29248
3	81	5089	27	10353	49	20455	189	19839	1	26209
4	173	5694	95	11706	56	18034	195	20264	53	31166
5	63	5665	22	12409	46	17498	25	23710	164	29869
6	145	5592	23	11167	75	16250	65	22192	105	27753
7	171	6975	70	10732	6	15117	93	23931	146	26289
8	79	5359	31	8800	43	17209	144	22543	14	28865
9	191	5743	7	7377	88	17983	99	23119	24	26621
10	188	7301	42	10169	174	17125	147	22619	91	22376
Average		5712 ± 890		10543 ± 1378		17650 ± 1691		22511 ± 1524		27784 ± 2520

Table 7.17: Number of counts at second readout after 1-hour UV exposure at 80 °C.

Dose	100 mGy		300 mGy		500 mGy		700 mGy		1000 mGy	
No	Det	Counts	Det	Counts	Det	Counts	Det	Counts	Det	Counts
1	68	5804	19	11303	78	17707	35	18427	5	23582
2	74	6708	167	10864	86	16495	82	19985	37	23673
3	159	5689	148	10847	67	19600	12	19515	151	24100
4	58	6431	178	10410	17	15136	16	20898	98	27090
5	60	6105	71	9733	57	17512	155	21269	36	26504
6	15	7189	94	9175	149	15681	83	20766	143	25530
7	28	7090	168	11688	2	17312	169	22390	192	29339
8	44	7643	47	12965	29	17838	154	21602	104	26609
9	156	6817	54	12163	13	16607	157	19461	183	28274
10	30	6354	62	12163	150	15775			26	25452
Average		6583 ± 626		114047 ± 1115		16966 ± 1310		20479 ± 1236		26015 ± 1930

Table 7.18: Number of counts at second readout after 2-hour UV exposure at 80 °C.

Dose	100 mGy		300 mGy		500 mGy		700 mGy		1000 mGy	
No	Det	Counts	Det	Counts	Det	Counts	Det	Counts	Det	Counts
1	68	4539	19	13841	78	17617	35	20278	5	25956
2	74	7264	167	14747	86	16137	82	23827	37	30479
3	159	5873	148	14312	67	18383	12	16752	151	25663
4	58	8553	178	15430	17	15953	16	19520	98	26685
5	60	8352	71	15583	57	16414	155	21275	36	26608
6	15	7391	94	13208	149	16319	83	19623	143	26524
7	28	6770	168	8077	2	15138	169	21394	192	29970
8	44	7684	47	9682	29	19870	154	23529	104	28929
9	156	7209	54	9148	13	20009	157	18497	183	30489
10	30	7210	62	11901	150	17038			26	21151
Average		7085 ± 1170		12593 ± 2743		17288 ± 1662		20522 ± 2277		27245 ± 2863

Table 7.19: Number of counts at second readout after 3-hour UV exposure at 80 °C.

Dose	100 mGy		300 mGy		500 mGy		700 mGy		1000 mGy	
No	Det	Counts	Det	Counts	Det	Counts	Det	Counts	Det	Counts
1	45	6491	10	13956	55	18706	179	23199	66	27504
2	59	7624	69	15180	18	17428	92	24269	172	29895
3	81	9196	27	15459	49	19703	189	18324	1	31666
4	173	10944	95	16985	56	20859	195	19241	53	31078
5	63	8417	22	14414	46	20190	25	26727	164	28679
6	145	6798	23	14719	75	21905	65	21296	105	27981
7	171	10331	70	10837	6	18263	93	21303	146	30126
8	79	11461	31	11599	43	18012	144	28035	14	28756
9	191	9414	7	15172	88	25093	99	32825	24	31443
10	188	8727	42	15583	174	21051	147	27747	91	31449
Average		8940 ± 1674		14390 ± 1863		20121 ± 2277		24297 ± 4533		29858 ± 1547

Table 7.20: Number of counts at second readout after 4-hour UV exposure at 80 °C.

Dose	100 mGy		300 mGy		500 mGy		700 mGy		1000 mGy	
No	Det	Counts	Det	Counts	Det	Counts	Det	Counts	Det	Counts
1	68	12216	19	16772	78	19040	35	18962	5	30813
2	74	9676	167	14857	86	22079	82	18898	37	27819
3	159	11117	148	18743	67	21363	12	18457	151	30927
4	58	15029	178	15649	17	17070	16	19595	98	30219
5	60	10677	71	10233	57	18118	155	21912	36	25094
6	15	11895	94	10097	149	17643	83	21473	143	25479
7	28	12268	168	12712	2	13202	169	23588	192	27332
8	44	17535	47	17186	29	16300	154	18153	104	24246
9	156	12721	54	17033	13	16955	157	18390	183	24801
10	30	9743	62	21922	150	19096			26	23946
Average		12288 ± 2419		15520 ± 3707		18086 ± 2542		19936 ± 1920		27068 ± 2764

Table 7.21: Number of counts at second readout after 5-hour UV exposure at 80 °C.

Dose	100 mGy		300 mGy		500 mGy		700 mGy		1000 mGy	
No	Det	Counts	Det	Counts	Det	Counts	Det	Counts	Det	Counts
1	45	8581	10	11149	55	13804	179	18202	66	20831
2	59	8921	69	13887	18	20338	92	20554	172	24047
3	81	7879	27	10120	49	16468	189	23491	1	14652
4	173	8563	95	16361	56	11007	195	15788	53	19945
5	63	8729	22	14584	46	19880	25	17810	164	19631
6	145	8091	70	15646	75	14626	65	13535	105	18249
7	171	12213	31	8725	6	12716	93	16891	146	25114
8	79	9494	7	10270	43	14457	144	17523	14	24047
9	191	15311	42	15516	88	18967	99	20537	24	25143
10	188	12685			174	15480	147	17144	91	17019
Average		10047 ± 2484		12918 ± 2857		15774 ± 3117		18148 ± 2789		20868 ± 3453

Table 7.22: Number of counts at second readout after 6-hour UV exposure at 80 °C.

Dose	100 mGy		300 mGy		500 mGy		700 mGy		1000 mGy	
No	Det	Counts	Det	Counts	Det	Counts	Det	Counts	Det	Counts
1	68	6701	19	12937	78	17762	35	18486	5	17249
2	74	7105	167	15671	86	13220	82	21313	37	16043
3	159	7978	148	16034	67	16208	12	10223	151	18054
4	58	11394	178	9934	17	11444	16	12113	98	19972
5	60	11405	71	10001	57	20636	155	13976	36	15736
6	15	11895	94	13786	149	17807	83	16705	143	15270
7	28	10204	168	6432	2	14633	169	21097	192	19652
8	44	11853	47	9535	29	13696	154	15490	104	20535
9	156	13396	54	10680	13	11874	157	17126	183	21214
10	30	14972	62	13274	150	15442			26	15013
Average		10690 ± 2704		11828 ± 3023		15272 ± 2898		16281 ± 3780		17874 ± 2336

Table 7.23: Number of counts at second readout after 7 hours UV exposure at 80 °C.

Dose	100 mGy		300 mGy		500 mGy		700 mGy		1000 mGy	
No	Det	Counts	Det	Counts	Det	Counts	Det	Counts	Det	Counts
1	68	9091	167	15778	78	13447	35	17698	5	18076
2	74	7733	148	15736	86	13651	82	17839	37	15578
3	159	8664	178	13021	67	12788	12	13663	151	17760
4	58	13873	71	13318	17	12568	16	12455	98	18053
5	60	9978	94	13361	57	14153	155	15096	36	18562
6	15	9869	168	13814	149	13587	83	15177	143	15112
7	28	11863	47	8373	2	11615	169	13235	192	22066
8	44	17722	54	9257	29	12099	154	16248	104	20988
9	156	9892	62	11535	13	12192	157	12355	183	22090
10	30	11103			150	12407			26	17642
Average		10979 ± 2935		12688 ± 2569		12851 ± 819		14863 ± 2096		18593 ± 2436

Table 7.24: Number of counts at second readout after 8-hour exposure at 80 °C.

Dose	100 mGy		300 mGy		500 mGy		700 mGy		1000 mGy	
No	Det	Counts	Det	Counts	Det	Counts	Det	Counts	Det	Counts
1	45	4926	10	11697	55	13634	179	21221	66	16544
2	59	6067	69	9250	18	17499	92	20557	172	22121
3	81	13379	27	11492	49	15474	189	9017	1	17254
4	173	12944	95	11245	56	13304	195	16792	53	18967
5	63	6869	22	10194	46	13967	25	11751	164	24351
6	145	7981	70	13729	75	13100	65	15621	105	21007
7	171	12078	31	6878	6	11602	93	16236	146	20759
8	79	14795	7	11583	43	14731	144	16129	14	13155
9	191	7793	42	11934	88	13486	99	14348	24	16699
10	188	10913	19	13539	174	10574	147	19182	91	16412
Average		9775 ± 3459		11154 ± 2009		13737 ± 1928		16085 ± 3778		18727 ± 3333

Figure 7.17 presents the relation between average value of PTTL signal and UV irradiation time. It can be seen that exposure time exceeding 4 hours leads to deterioration of results.

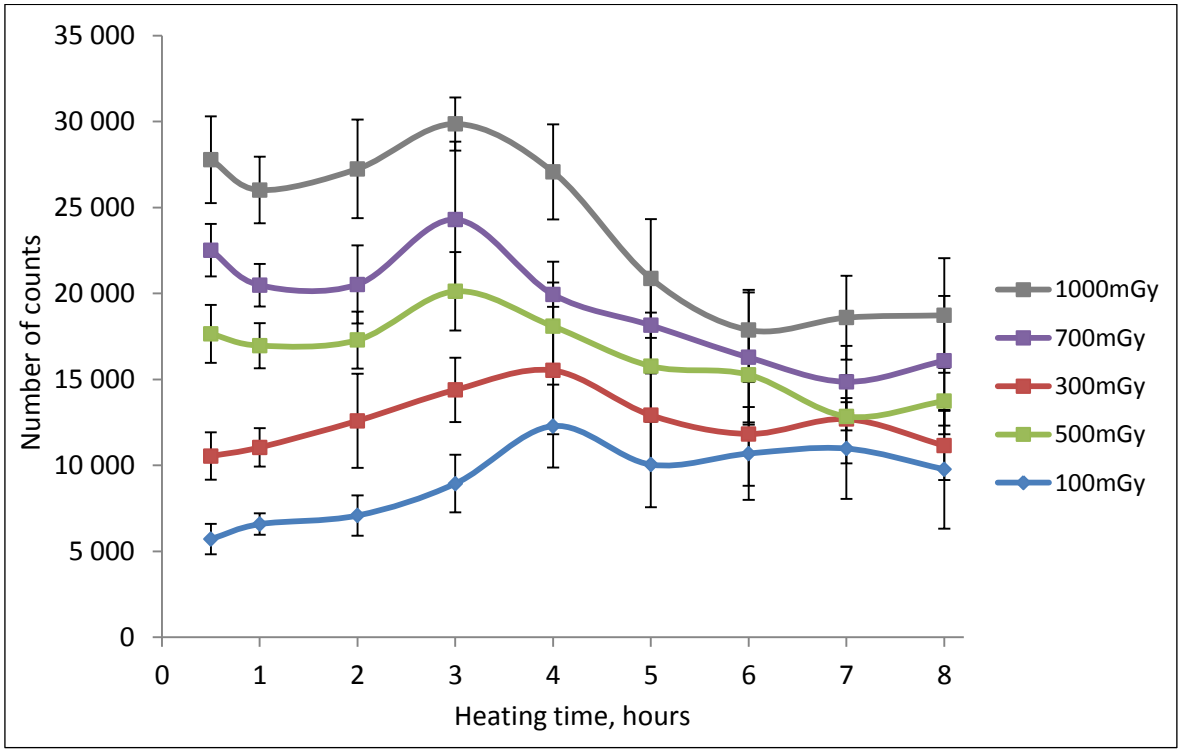

Fig. 7.17. PTTL signal of (100, 300, 500, 700 and 1000) mGy irradiated MTS-N detectors, after UV irradiation at the temperature 80 °C for (0.5, 1, 2, 3, 4, 5, 6, 7 and 8) hours.

7.2.4. PTTL Signal Linearity

In the right conditions of PTTL measurement this signal may be sufficient to allow re-evaluation of the dose obtained in a previous TL readout. It is desirable to use dosimeters with linear dependence between counts and dose.

The signal linearity can be examined using a set of data noted in the chapter 7.2.1 (Tab. 7.16—7.24, Fig. 7.17). As an example, there are shown results of PTTL signal reading after the UV irradiation with a wavelength of λ = 254 nm, lasting from 30 minutes to 4 hours, performed at temperature of 80 °C.

Figures 7.18—7.22 show the relation between average value of PTTL counts corresponding to these data and absorbed dose. It can be noted, that at considered time of UV exposure the PTTL signal linearity is fully acceptable.

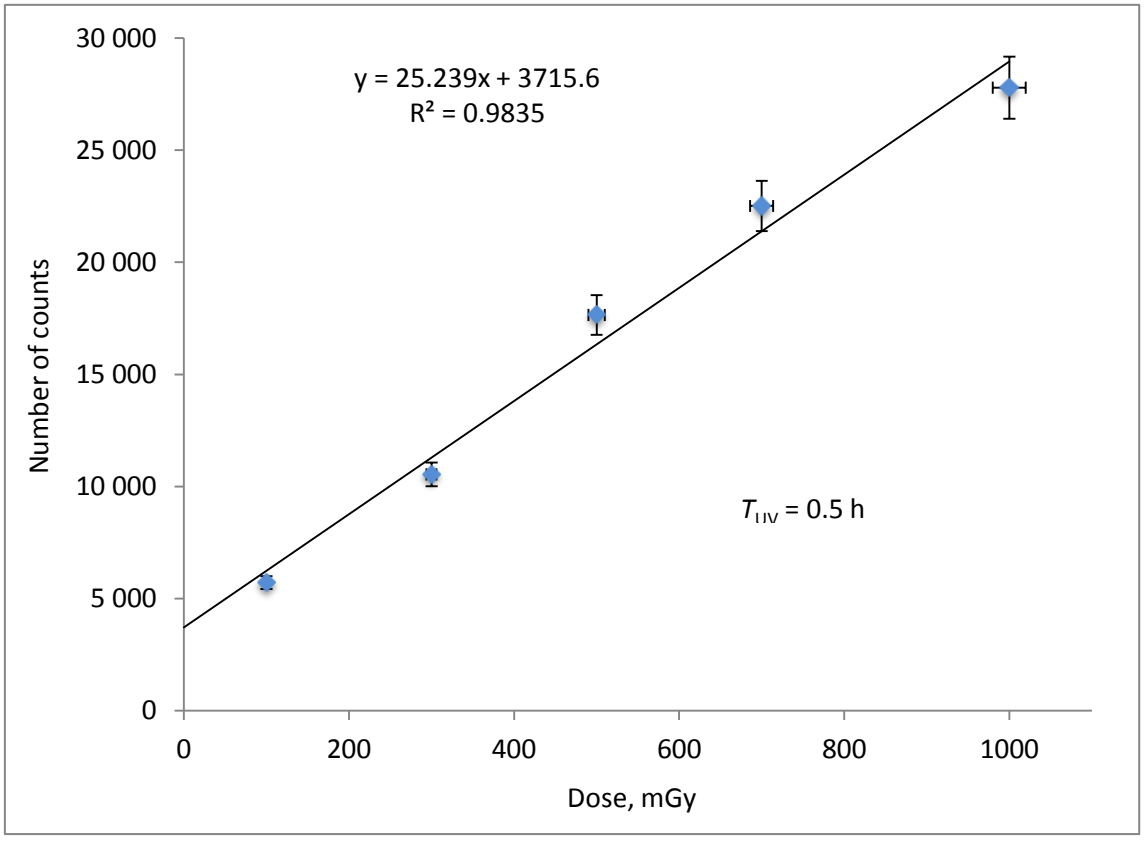

Fig. 7.18. PTTL signal versus dose after 30-minute UV irradiation at 80 °C.

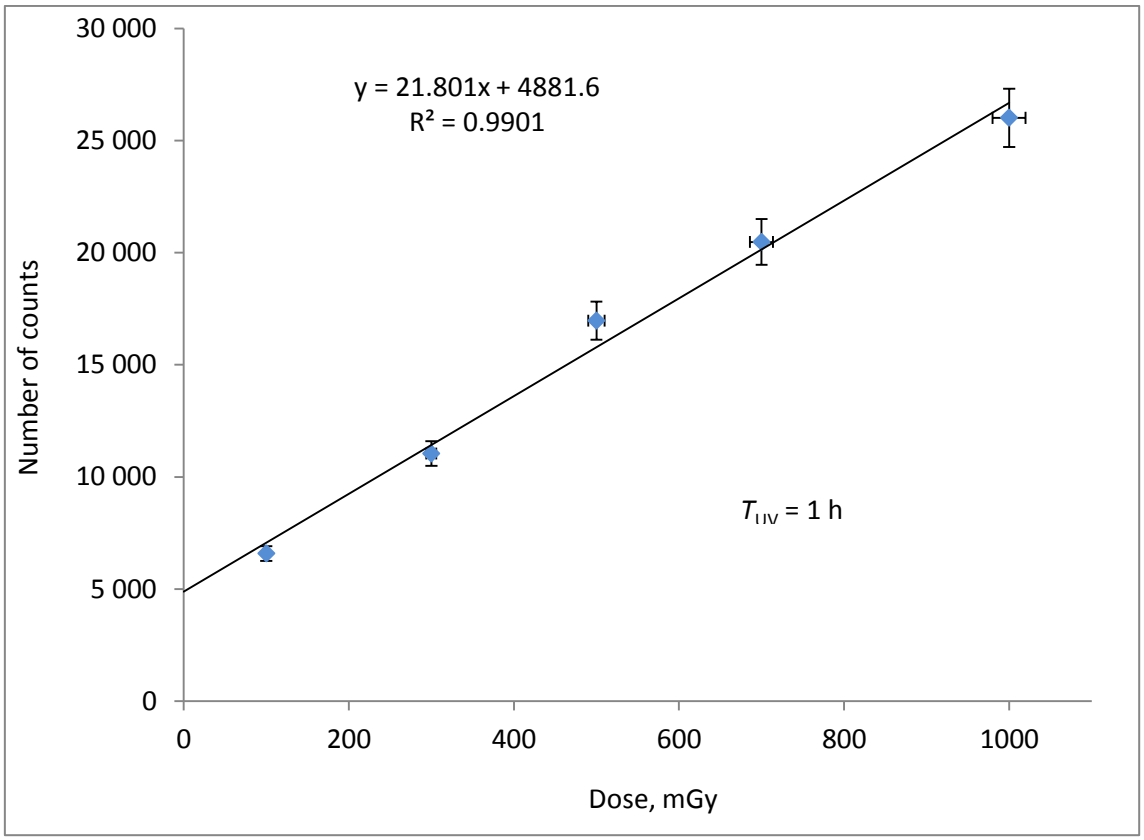

Fig. 7.19. PTTL signal versus dose after 1-hour UV irradiation at 80 °C.

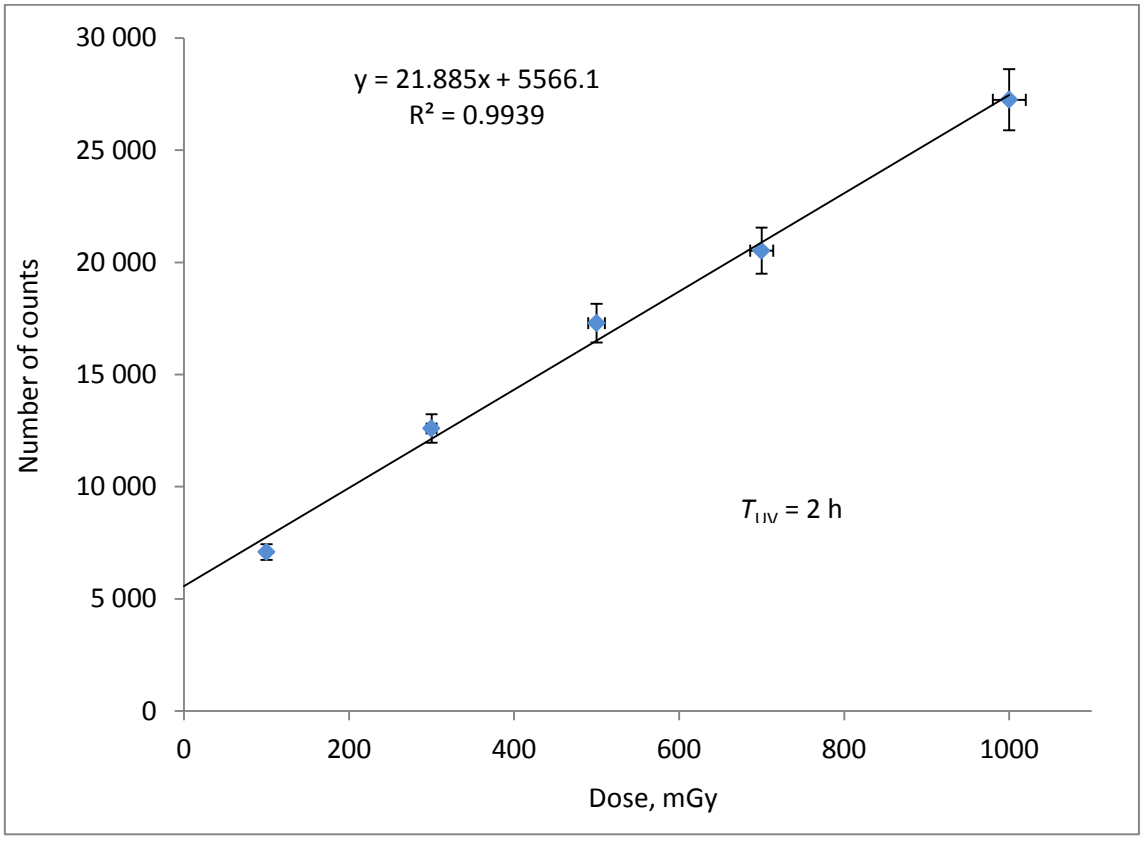

Fig. 7.20. PTTL signal versus dose after 2-hour UV irradiation at 80 °C.

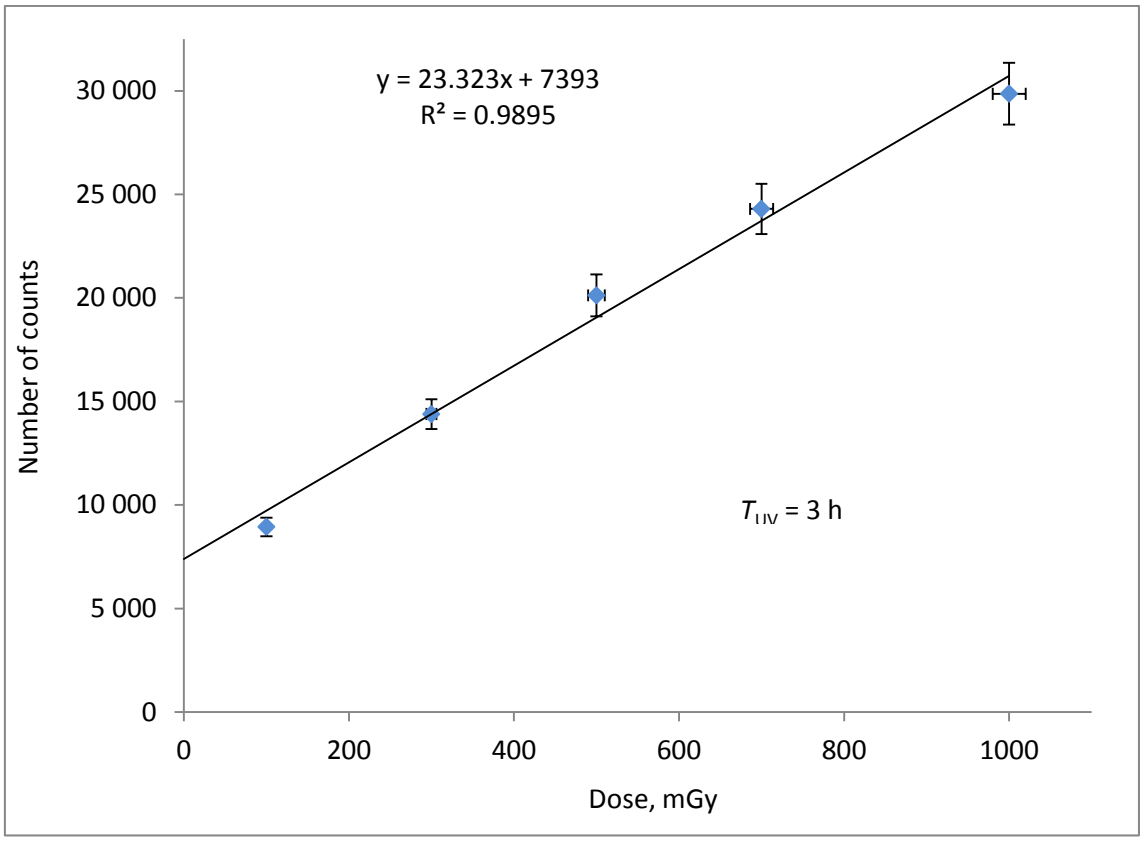

Fig. 7.21. PTTL signal versus dose after 3-hour UV irradiation at 80 °C.

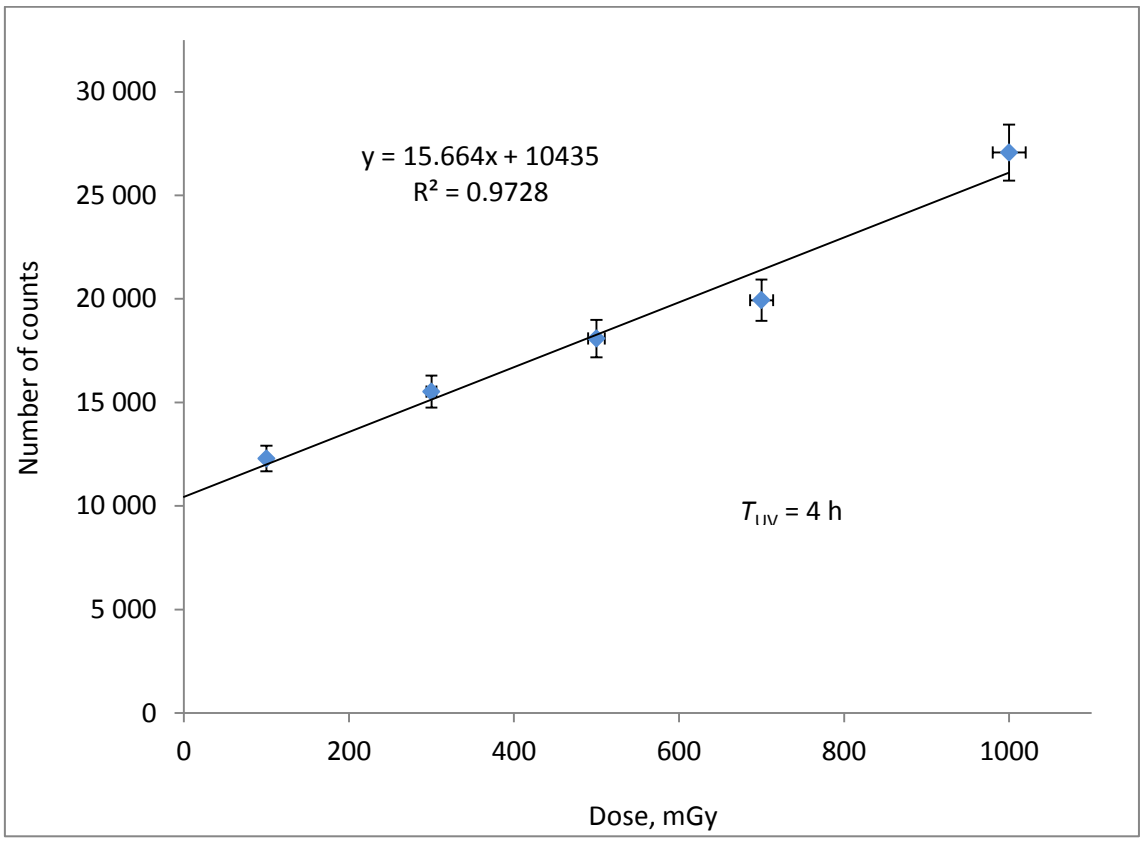

Fig. 7.22. PTTL signal versus dose after 4-hour UV irradiation at 80 °C.

7.2.5. Efficiency of PTTL Method

The relative efficiency of The PTTL method should not be calculated as a simple comparison of the number of counts in first and second readout. This is due to specific properties of the relationship between the counts number and dose. Analysing this function in the dose range up to 1000 mGy it can be seen that in the first readout this dependence is roughly proportional. If we take into account the data from the table 7.5, the linear approximation of this function is described by the formula

$$N = a\,D + b,$$

where a = (193.4 ± 2.2) mGy^{-1} and b = (2.3 ± 1.2) × 10^3. So the component b is equivalent to the change of counts which is corresponding to dose change of 12 mGy. This is equal only to 1.2 % of examined dose range.

Unlike, the PTTL yield in the same dose range shows a significant deviation from proportionality. For example, in the case of the 2-hours UV exposure at the temperature of 80 °C (Tab. 7.12) coefficients a and b are equal as follows: a = (21.1 ± 3.3) mGy^{-1} and b = (8.6 ± 2.0) × 10^3. Similar results were obtained in the second series of measurements (Tab. 7.18, Fig. 7.20): a = (21.9 ± 1.0) mGy^{-1} and b = (5.6 ± 0.60) × 10^3. Therefore, in the second reading the component b is equivalent to the change of counts which is corresponding to dose change of (260–410) mGy, i.e. between 26 % and 41 % of examined dose range.

In summary, to estimate the relative efficiency of the PTTL method in relation to routine measurement the ratio of slope coefficients is taken. Under the conditions mentioned above (2-hours UV exposure at 80 °C), the efficiency thus defined reaches 11%. Considering all measurements, the largest efficiency value obtained for MTS-N detectors is approximately equal 13 %.

7.3. First and Second Readout of MCP-N Dosimeters

7.3.1. Linearity of TL Detectors at First Readout

Before irradiation the detectors were annealed in accordance with the procedure described in the chapter 6. Then the detectors were irradiated with X-rays. Parameters of TLD exposure are shown in Table 7.25 below.

Table 7.25: Parameters of exposure.

Dose, mGy	Distance between X-ray tube focal spot and detector, cm	X-Ray tube high voltage, kV	Current-time product, mAs
1	100	80	20
2	80	90	20
5	100	87	80
10	80	100	80
25	65	100	130

Table 7.26 illustrates dose and average number of counts obtained at the TLD reading after X-ray exposure. This dependence is shown in Fig 7.23.

Table 7.26: Dose and average number of counts after exposure.

Dose, mGy	Average count
0	500 ± 154
0.5	3 110 ± 333
1	5 587 ± 716
2	10 297 ± 1 188
5	23 228 ± 3 607
10	51 171 ± 5 353
25	114 287 ± 10 340

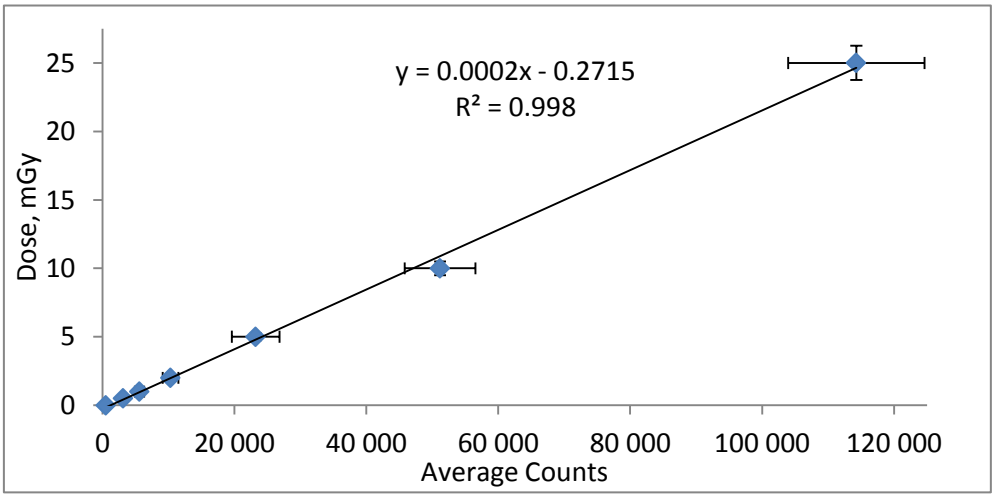

Fig. 7.23: Calibration curve for MCP-N thermoluminescence detector describing the relationship between the dose and number of pulses received during detector's first readout.

7.3.2. Examples of TL Glow Curves

The figures below show the TL glow curves, obtained at the first readout (green) and second readout (blue) of dosimeters exposed at X-ray with doses of (0.5, 1, 2, 5, 10 and 25) mGy.

All the examples shown in the Fig. 7.24—7.29 refer to second readout carried out after UV irradiation with a UV wavelength of 254 nm with heating at 80 °C within 2 hours.

Unfortunately, comparing both curves in each of the graphs it is visible that the yield of PTTL phenomenon at low doses is negligible.

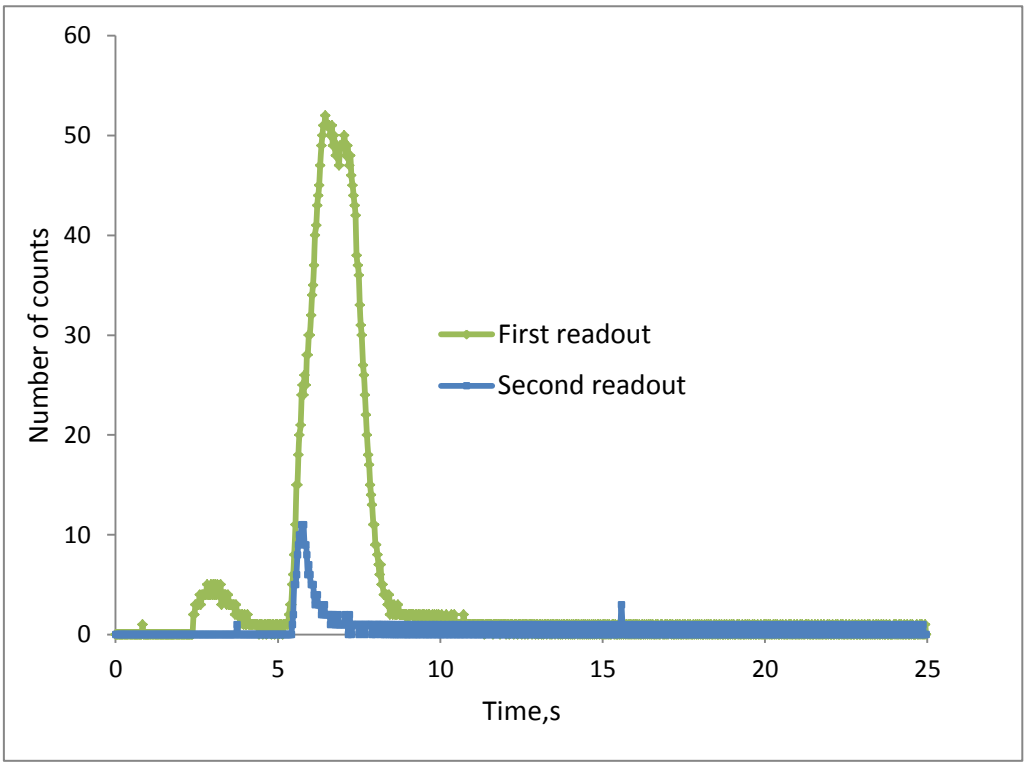

Fig. 7.24: TL curves obtained as a result of reading the detector at dose 0.5 mGy.

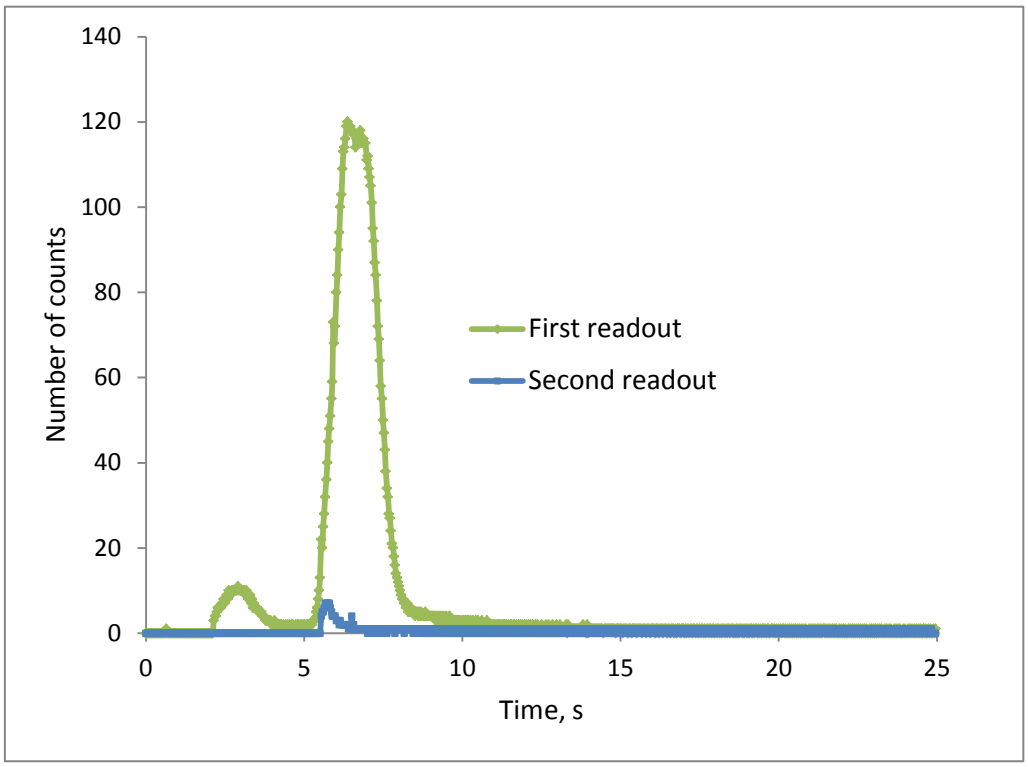

Fig. 7.25: TL curves obtained as a result of reading the detector at dose 1 mGy.

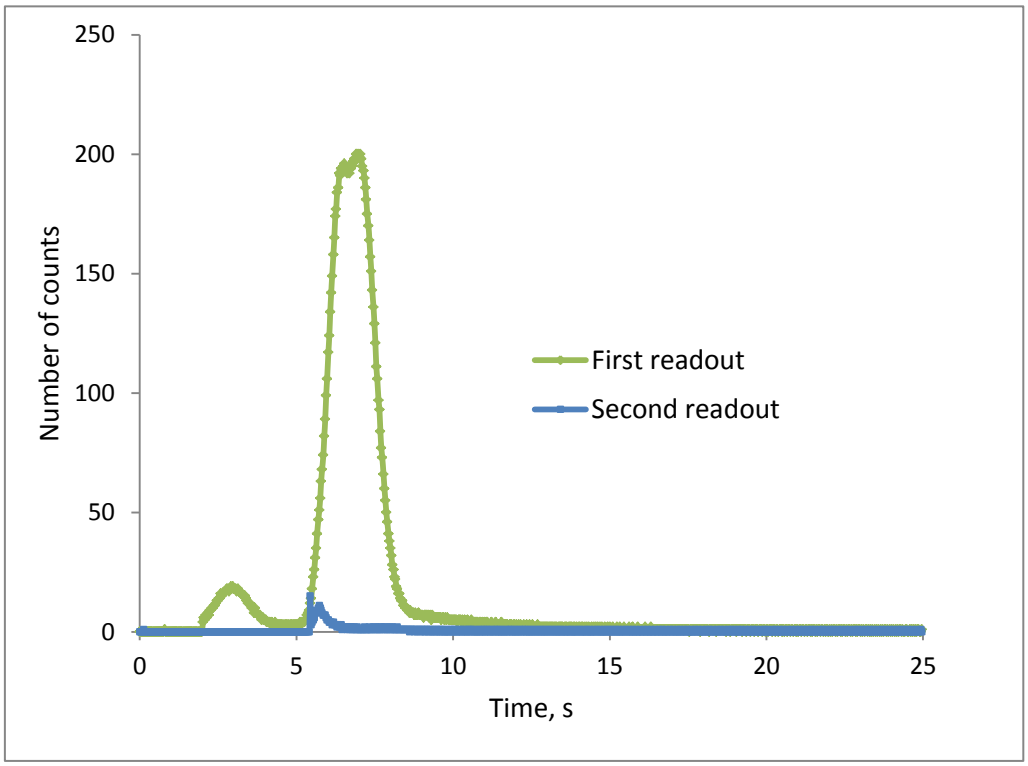

Fig. 7.26: TL curves obtained as a result of reading the detector at dose 2 mGy.

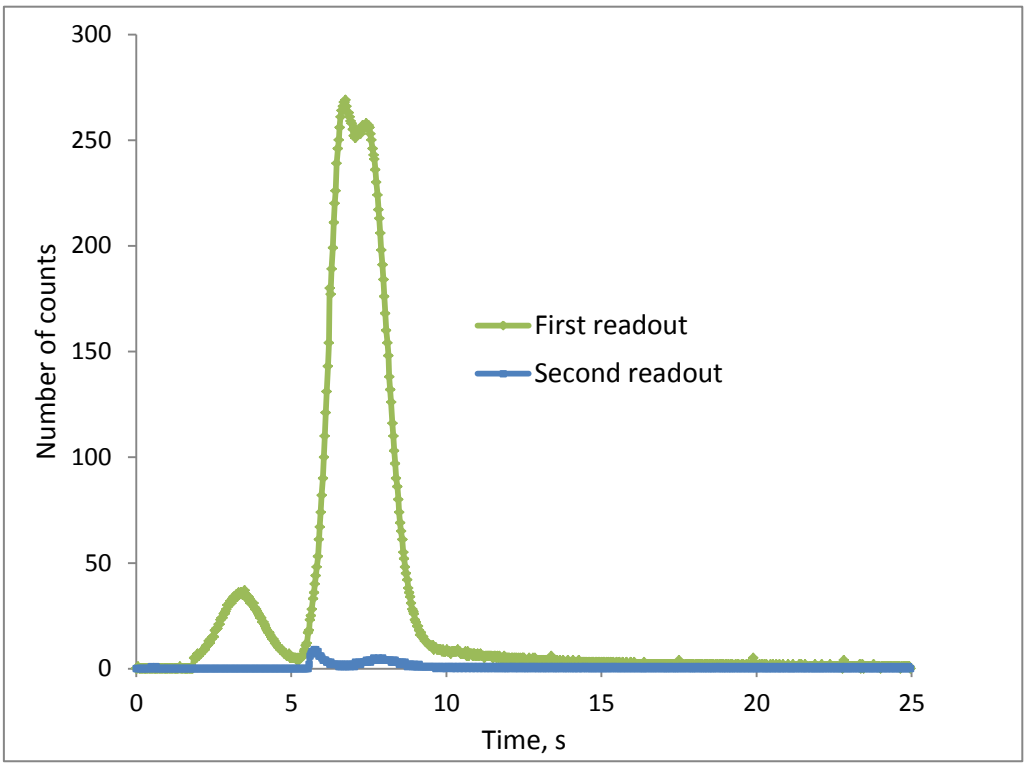

Fig. 7.27: TL curves obtained as a result of reading the detector at dose 5 mGy.

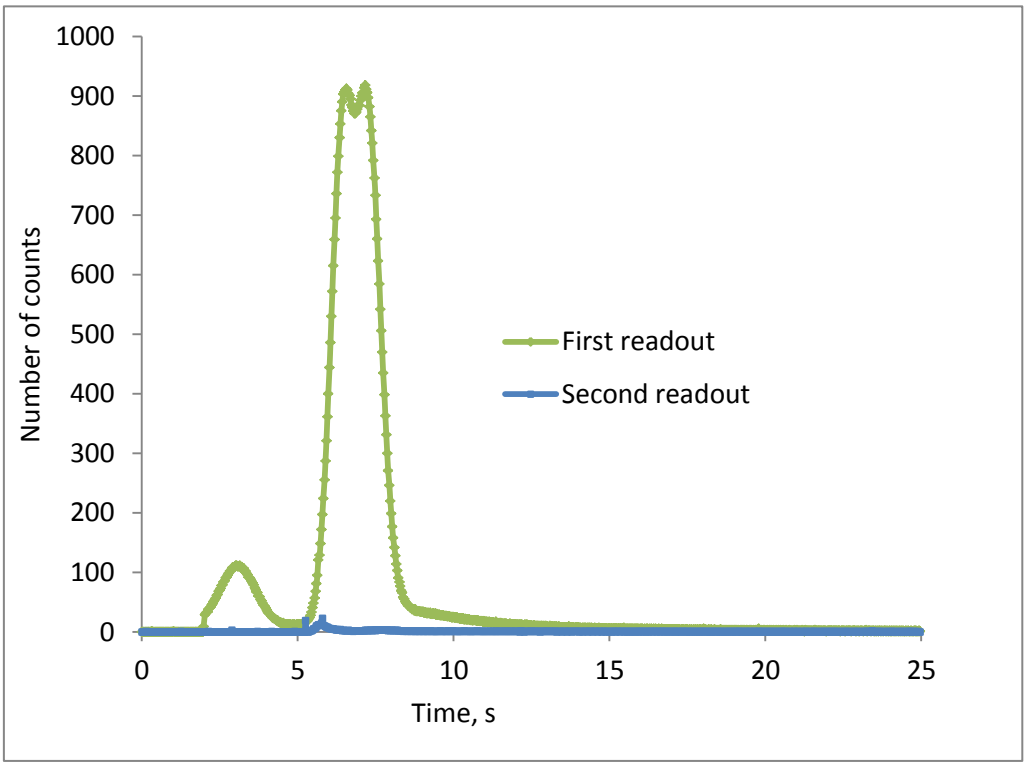

Fig. 7.28: TL curves obtained as a result of reading the detector at dose 10 mGy.

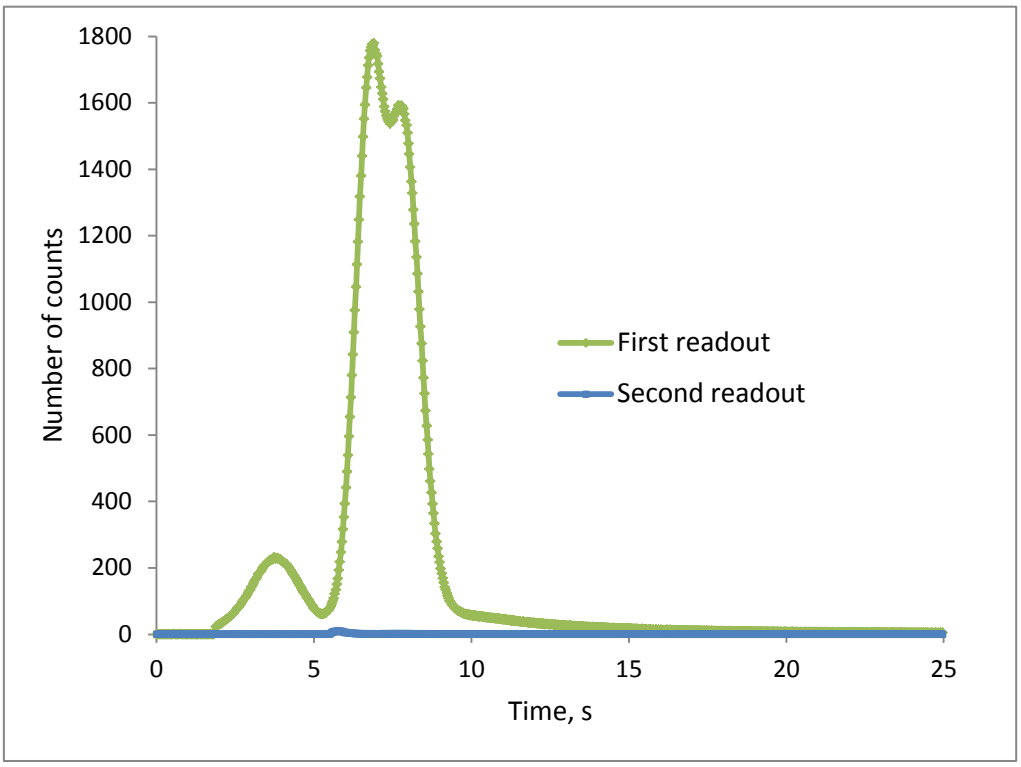

Fig. 7.29: TL curves obtained as a result of reading the detector at dose 25 mGy.

7.3.3. PTTL Yield at Different Conditions of UV Exposure and Heating

1. Measurements with UV exposure and heating within 2 hours

The measurements were performed using temperatures (30, 40, 50, 60, 70, 80, 90, 100, 110 and 120) °C for the same wavelength of UV radiation (λ = 254 nm) at the heating and exposure time of 2 hours. Values of absorbed doses were (0.5, 1, 2, 5, 10 and 25) mGy. For each temperature 30 detectors were applied, with 5 detectors for each dose.

Tables 7.27—7.36 illustrate experimental results: number of counts during second readout, after applying UV radiation. In these tables the value marked 'Counts' is the number of counts obtained at the second readout of the detector, and 'No' is the consecutive number of measurement.

Table 7.27: Number of counts at second readout after 2-hours UV exposure at 30 °C.

Dose	0 mGy	0.5 mGy	1 mGy	2 mGy	5 mGy	10 mGy	25 mGy
No	Counts	Counts	Counts	Counts	Counts	Counts	Counts
1	166	347	370	210	579	712	777
2	249	328	355	199	385	503	1004
3	146	217	393	263	391	724	550
4	256	258	123	310	108	808	914
5	344	213	329	350	232	703	1586
Average	232 ± 79	273 ± 62	314 ± 109	266 ± 65	339 ± 178	690 ± 113	966 ± 386

Table 7.28: Number of counts at second readout after 2-hours UV exposure at 40 °C.

Dose	0 mGy	0.5 mGy	1 mGy	2 mGy	5 mGy	10 mGy	25 mGy
No	Counts	Counts	Counts	Counts	Counts	Counts	Counts
1	189	384	224	544	553	466	395
2	252	297	286	290	492	555	709
3	374	304	335	260	473	395	936
4	233	358	351	294	528	482	992
5	346	351	458	346	453	467	1243
Average	279 ± 69	339 ± 37	331 ± 87	347 ± 115	500 ± 41	473 ± 57	855 ± 320

Table 7.29: Number of counts at second readout after 2-hours UV exposure at 50 °C.

Dose	0 mGy	0.5 mGy	1 mGy	2 mGy	5 mGy	10 mGy	25 mGy
No	Counts	Counts	Counts	Counts	Counts	Counts	Counts
1	166	391	286	423	338	475	533
2	223	504	378	321	484	387	713
3	337	456	381	417	424	315	447
4	252	490	448	213	618	582	654
5	420	437	487	271	367	640	575
Average	280 ± 100	456 ± 45	396 ± 77	329 ± 92	446 ± 111	480 ± 134	584 ± 104

Table 7.30: Number of counts at second readout after 2-hours UV exposure at 60 °C.

Dose	0 mGy	0.5 mGy	1 mGy	2 mGy	5 mGy	10 mGy	25 mGy
No	Counts	Counts	Counts	Counts	Counts	Counts	Counts
1	100	478	327	488	515	570	887
2	211	598	479	226	650	518	2071
3	359	451	535	313	489	452	1165
4	225	560	527	289	548	514	1216
5	230	516	421	643	634	595	989
Average	225 ± 92	521 ± 60	458 ± 86	392 ± 171	567 ± 72	530 ± 55	1266 ± 469

Table 7.31: Number of counts at second readout after 2-hours UV exposure at 70 °C.

Dose	0 mGy	0.5 mGy	1 mGy	2 mGy	5 mGy	10 mGy	25 mGy
No	Counts	Counts	Counts	Counts	Counts	Counts	Counts
1	172	422	344	541	356	410	569
2	281	326	362	261	384	463	953
3	269	298	344	221	423	519	834
4	420	374	354	433	545	437	550
5	255	325	383	403	470	545	928
Average	279 ± 89	349 ± 49	357 ± 16	372 ± 131	436 ± 75	475 ± 56	767 ± 194

Table 7.32: Number of counts at second readout after 2-hours UV exposure at 80 °C.

Dose	0 mGy	0.5 mGy	1 mGy	2 mGy	5 mGy	10 mGy	25 mGy
No	Counts	Counts	Counts	Counts	Counts	Counts	Counts
1	247	329	251	522	379	725	2123
2	290	247	363	341	432	561	1467
3	365	246	215	336	314	584	1232
4	323	277	214	348	414	586	1107
5	198	328	362	295	532	406	1031
Average	285 ± 65	285 ± 41	281 ± 76	368 ± 88	412 ± 77	572 ± 113	1392 ± 441

Table 7.33: Number of counts at second readout after 2-hours UV exposure at 90 °C.

Dose	0 mGy	0.5 mGy	1 mGy	2 mGy	5 mGy	10 mGy	25 mGy
No	Counts	Counts	Counts	Counts	Counts	Counts	Counts
1	228	546	310	342	741	653	525
2	272	280	404	222	710	777	1060
3	212	341	455	434	516	1168	567
4	295	481	435	507	332	778	781
5	398	461	450	474	798	586	2120
Average	281 ± 73	422 ± 109	411 ± 60	396 ± 115	619 ± 192	792 ± 226	1011 ± 655

Table 7.34: Number of counts at second readout after 2-hours UV exposure at 100 °C.

Dose	0 mGy	0.5 mGy	1 mGy	2 mGy	5 mGy	10 mGy	25 mGy
No	Counts	Counts	Counts	Counts	Counts	Counts	Counts
1	269	296	332	347	439	822	538
2	105	345	366	103	321	714	537
3	272	470	329	306	387	658	640
4	458	322	386	415	283	644	1029
5	407	483	482	257	397	679	675
Average	302 ± 138	383 ± 87	379 ± 62	286 ± 117	365 ± 63	703 ± 71	684 ± 202

Table 7.35: Number of counts at second readout after 2-hours UV exposure at 110 °C.

Dose	0 mGy	0.5 mGy	1 mGy	2 mGy	5 mGy	10 mGy	25 mGy
No	Counts	Counts	Counts	Counts	Counts	Counts	Counts
1	233	245	243	129	228	295	311
2	256	242	282	192	220	344	667
3	325	309	228	173	252	280	607
4	451	292	173	299	237	266	644
5	446	263	248	250	288	255	389
Average	342 ± 103	270 ± 29	334 ± 40	209 ± 67	245 ± 27	288 ± 35	524 ± 162

Table 7.36: Number of counts at second readout after 2-hours UV exposure at 120 °C.

Dose	0 mGy	0.5 mGy	1 mGy	2 mGy	5 mGy	10 mGy	25 mGy
No	Counts	Counts	Counts	Counts	Counts	Counts	Counts
1	237	322	435	532	576	1267	967
2	390	393	495	303	591	935	2628
3	217	443	436	373	413	727	1096
4	393	464	505	263	394	720	1882
5	287	208	466	378	633	825	2095
Average	305 ± 83	366 ± 104	467 ± 32	370 ± 103	521 ± 110	895 ± 226	1734 ± 698

Figure 7.30 presents experimental results for the evaluation of the PTTL signal with UV irradiation time at different temperatures of heating. As might be expected from the glow curves, the results are unsatisfactory.

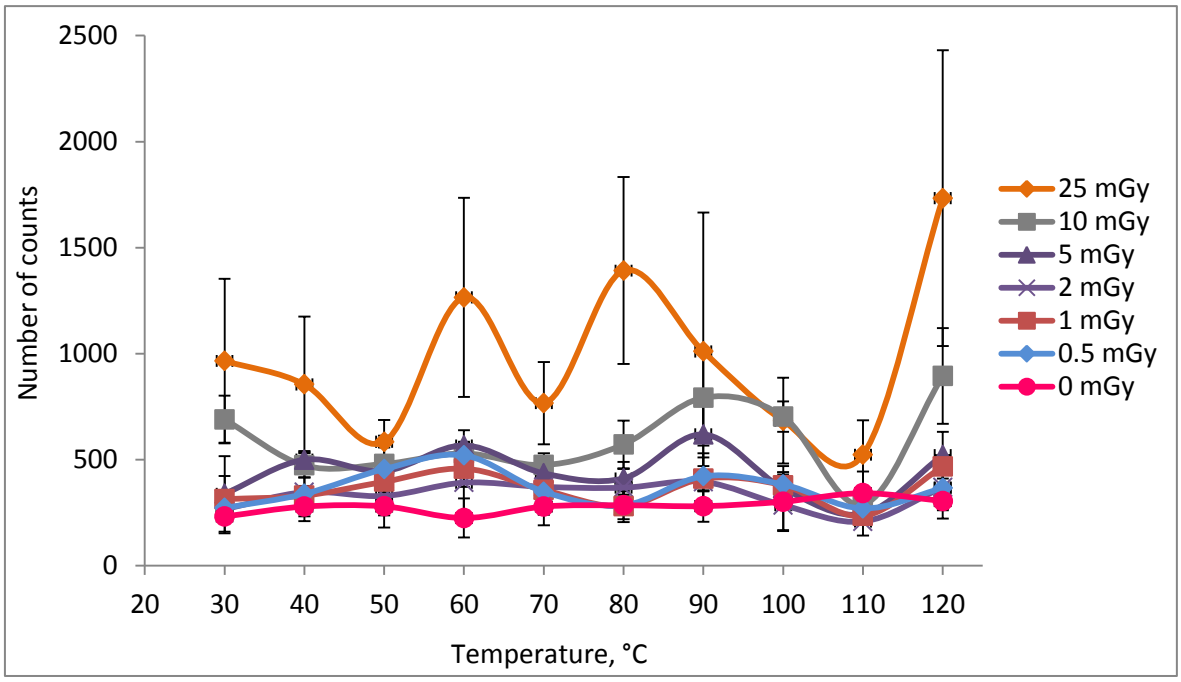

Fig. 7.30: PTTL signal of (0, 0.5, 1, 2, 5, 10 and 25) mGy irradiated MCP-N detectors after UV irradiation for 2 hours at temperatures (30, 40, 50, 60, 70, 80, 90, 100, 110 and 120) °C.

2. Measurements with UV exposure and heating within 1 hour in the darkroom

The next measurements were performed using the same doses, temperatures and the same wavelength of UV radiation, but at the heat time equal 1 hour. Second difference between the previous and these measurements was the carrying out the TLD handling in darkroom. The results are shown in Tab. 7.37—7.46.

Table 7.37: Number of counts at second readout after 1-hour UV exposure at 30 °C.

Dose	0.5 mGy	1 mGy	2 mGy	5 mGy	10 mGy	25 mGy
No	Counts	Counts	Counts	Counts	Counts	Counts
1	181	511	381	366	517	1189
2	305	551	407	451	441	1335
3	453	384	448	513	406	803
4	303	484	426	403	570	916
5	335	429	494	473	313	703
Average	315 ± 97	472 ± 66	431 ± 43	441 ± 58	449 ± 100	989 ± 265

Table 7.38: Number of counts at second readout after 1-hour UV exposure at 40 °C.

Dose	0.5 mGy	1 mGy	2 mGy	5 mGy	10 mGy	25 mGy
No	Counts	Counts	Counts	Counts	Counts	Counts
1	284	412	455	455	268	1066
2	374	432	171	316	388	319
3	410	420	247	444	504	508
4	389	440	349	537	428	519
5	372	546	367	445	298	893
Average	366 ± 48	450 ± 55	318± 110	439 ± 79	377 ± 96	661 ± 308

Table 7.39: Number of counts at second readout after 1-hour UV exposure at 50 °C.

Dose	0.5 mGy	1 mGy	2 mGy	5 mGy	10 mGy	25 mGy
No	Counts	Counts	Counts	Counts	Counts	Counts
1	317	224	261	344	226	574
2	252	232	115	164	300	484
3	268	233	193	196	316	152
4	309	294	196	230	399	411
5	288	301	234	218	309	208
Average	287 ± 27	257 ± 37	200 ± 55	230 ± 68	310 ± 61	366 ± 180

Table 7.40: Number of counts at second readout after 1-hour UV exposure at 60 °C.

Dose	0.5 mGy	1 mGy	2 mGy	5 mGy	10 mGy	25 mGy
No	Counts	Counts	Counts	Counts	Counts	Counts
1	405	397	238	585	327	203
2	332	471	244	600	462	686
3	404	464	263	532	451	1008
4	367	402	342	493	901	837
5	443	484	290	440	647	949
Average	390 ± 42	444 ± 41	275 ± 42	530 ± 66	558 ± 223	737 ± 322

Table 7.41: Number of counts at second readout after 1-hour UV exposure at 70 °C.

Dose	0.5 mGy	1 mGy	2 mGy	5 mGy	10 mGy	25 mGy
No	Counts	Counts	Counts	Counts	Counts	Counts
1	283	272	455	654	508	432
2	375	389	200	541	686	947
3	346	285	308	616	735	642
4	323	335	276	490	559	1122
5	341	362	270	434	711	1337
Average	334 ± 34	329 ± 50	302 ± 94	547 ± 90	640 ± 100	896 ± 363

Table 7.42: Number of counts at second readout after 1-hour UV exposure at 80 °C.

Dose	0.5 mGy	1 mGy	2 mGy	5 mGy	10 mGy	25 mGy
No	Counts	Counts	Counts	Counts	Counts	Counts
1	394	346	494	626	563	287
2	514	401	290	534	782	643
3	357	353	330	583	610	490
4	432	538	384	599	1043	622
5	435	531	388	574	672	827
Average	426 ± 58	434 ± 94	377 ± 77	583 ± 34	734 ± 191	574 ± 200

Table 7.43: Number of counts at second readout after 1-hour UV exposure at 90 °C.

Dose	0.5 mGy	1 mGy	2 mGy	5 mGy	10 mGy	25 mGy
No	Counts	Counts	Counts	Counts	Counts	Counts
1	367	337	280	394	356	816
2	364	366	260	410	423	768
3	352	339	241	235	462	645
4	351	279	458	255	621	688
5	417	351	214	345	467	834
Average	370 ± 27	334 ± 33	291 ± 97	328 ± 80	467 ± 97	750 ± 82

Table 7.44: Number of counts at second readout after 1-hour UV exposure at 100 °C.

Dose	0.5 mGy	1 mGy	2 mGy	5 mGy	10 mGy	25 mGy
No	Counts	Counts	Counts	Counts	Counts	Counts
1	419	380	257	349	626	608
2	430	483	281	277	590	620
3	336	460	258	463	506	1698
4	413	398	407	458	450	1001
5	350	321	377	413	484	873
Average	390 ± 43	408 ± 65	316 ± 71	392 ± 79	531 ± 74	960 ± 445

Table 7.45: Number of counts at second readout after 1-hour UV exposure at 110 °C.

Dose	0.5 mGy	1 mGy	2 mGy	5 mGy	10 mGy	25 mGy
No	Counts	Counts	Counts	Counts	Counts	Counts
1	240	356	395	531	549	353
2	318	327	216	418	462	509
3	200	283	398	432	512	429
4	220	263	276	370	567	510
5	280	383	295	414	623	1353
Average	252 ± 47	322 ± 50	316 ± 79	433 ± 59	543 ± 60	631 ± 409

Table 7.46: Number of counts at second readout after 1-hour UV exposure at 120 °C.

Dose	0.5 mGy	1 mGy	2 mGy	5 mGy	10 mGy	25 mGy
No	Counts	Counts	Counts	Counts	Counts	Counts
1	253	256	370	305	353	289
2	355	270	150	285	390	520
3	329	276	296	327	270	534
4	348	407	215	438	327	488
5	350	332	208	288	529	551
Average	327 ± 43	308 ± 62	248 ± 86	329 ± 63	374 ± 97	476 ± 107

The results presented in Tab. 7.37—7.46 are shown in Fig. 7.31. However, also in this case, the results leave a lot to be desired despite all the operation of the detectors was carried out in the darkroom.

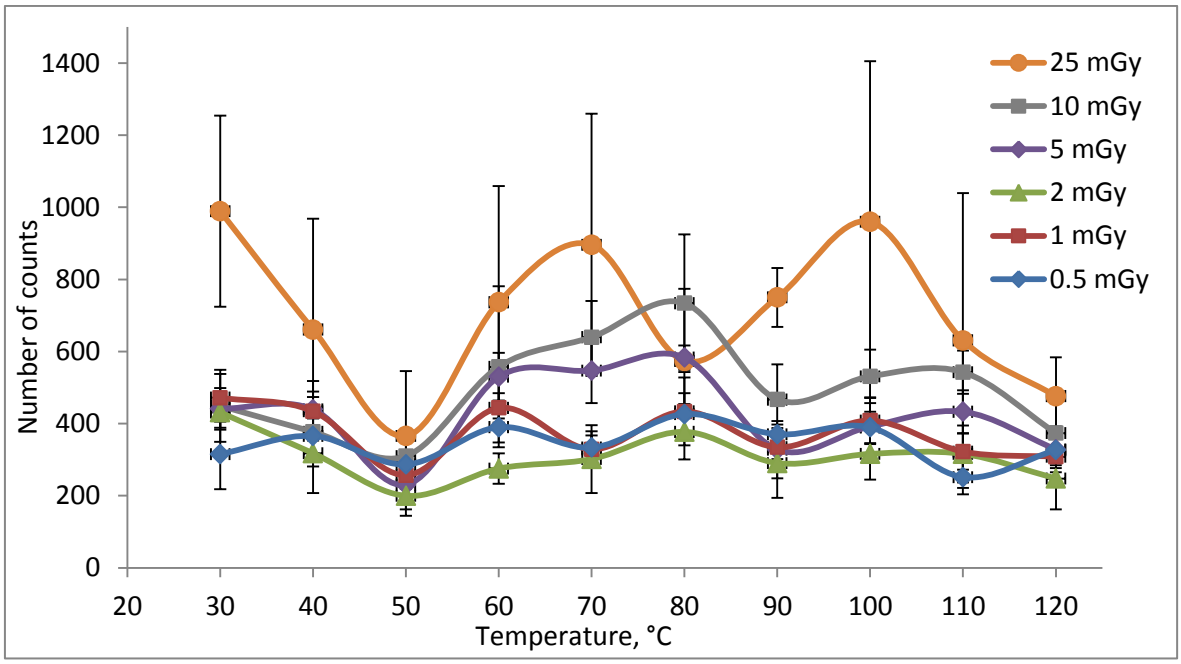

Fig. 7.31: PTTL signal of (0.5, 1, 2, 5, 10, 25) mGy irradiated MCP-N detectors after UV irradiation for 1 hour at temperatures (30, 40, 50, 60, 70, 80, 90, 100, 110, 120) °C.

3. Measurements with UV exposure at temperature of 80 °C and different heating time

In this series the irradiation was carried out at temperature 80 °C with following values of UV exposure (and heating) time: (10, 20, 30, 40, 50, 60, 70, 80, 90, 100, 110, 120, 135, 150, 165, 180, 195, 210, 225 and 240) minutes with UV wavelength λ = 254 nm. Also in this case the results showed that PTTL signal is not enough to calculate and reassessment the dose.

PTTL counts with different heat time are shown in Tab. 7.47—7.66.

Table 7.47: Number of counts at second readout after 10 min UV exposure at 80 °C.

Dose	0 mGy	1 mGy	2 mGy	5 mGy	10 mGy	25 mGy
No	Counts	Counts	Counts	Counts	Counts	Counts
1	137	190	361	243	570	325
2	241	197	260	302	462	476
3	252	386	391	419	640	630
4	325	434	363	398	509	719
5	435	312	478	477	757	613
Average	278 ± 110	304 ± 110	371 ± 78	368 ± 94	588 ± 116	553 ± 154

Table 7.48: Number of counts at second readout after 20 min UV exposure at 80 °C.

Dose	0 mGy	1 mGy	2 mGy	5 mGy	10 mGy	25 mGy
No	Counts	Counts	Counts	Counts	Counts	Counts
1	584	487	489	407	586	712
2	465	343	191	550	195	482
3	453	380	295	481	405	730
4	345	498	409	408	376	620
5	407	453	391	556	489	652
Average	451 ± 88	432 ± 68	355 ± 115	480 ± 73	410 ± 145	639 ± 98

Table 7.49: Number of counts at second readout after 30 min UV exposure at 80 °C.

Dose	0 mGy	1 mGy	2 mGy	5 mGy	10 mGy	25 mGy
No	Counts	Counts	Counts	Counts	Counts	Counts
1	246	394	506	512	235	301
2	290	403	535	535	526	720
3	415	378	334	447	582	543
4	361	442	608	462	616	858
5	306	507	505	419	514	894
Average	324 ± 66	425 ± 52	498 ± 105	475 ± 48	495 ± 151	663 ± 245

Table 7.50: Number of counts at second readout after 40 min UV exposure at 80 °C.

Dose	0 mGy	1 mGy	2 mGy	5 mGy	10 mGy	25 mGy
No	Counts	Counts	Counts	Counts	Counts	Counts
1	573	502	253	554	346	589
2	396	370	320	747	344	963
3	193	266	464	366	531	632
4	365	268	441	337	600	726
5	448	353	444	317	518	642
Average	395 ± 138	352 ± 97	384 ± 93	464 ± 184	468 ± 116	710 ± 150

Table 7.51: Number of counts at second readout after 50 min UV exposure at 80 °C.

Dose	0 mGy	1 mGy	2 mGy	5 mGy	10 mGy	25 mGy
No	Counts	Counts	Counts	Counts	Counts	Counts
1	284	431	507	861	619	811
2	333	429	543	531	508	803
3	435	443	584	564	532	913
4	336	519	269	353	588	821
5	496	373	330	382	764	923
Average	376 ± 87	439 ± 52	447 ± 139	538 ± 202	602 ± 101	854 ± 59

Table 7.52: Number of counts at second readout after 60 min UV exposure at 80 °C.

Dose	0 mGy	1 mGy	2 mGy	5 mGy	10 mGy	25 mGy
No	Counts	Counts	Counts	Counts	Counts	Counts
1	362	425	396	394	353	870
2	235	235	325	382	575	885
3	415	371	661	644	346	1020
4	314	474	613	497	453	554
5	362	613	507	401	399	735
Average	338 ± 68	424 ± 139	500 ± 142	464 ± 111	425 ± 94	813 ± 176

Table 7.53: Number of counts at second readout after 70 min UV exposure at 80 °C.

Dose	0 mGy	1 mGy	2 mGy	5 mGy	10 mGy	25 mGy
No	Counts	Counts	Counts	Counts	Counts	Counts
1	204	355	337	577	292	911
2	200	552	515	395	196	822
3	376	531	646	584	385	1202
4	316	404	316	520	497	740
5	153	380	509	249	518	1010
Average	250 ± 93	444 ± 91	465 ± 138	465 ± 143	378 ± 136	937 ± 179

Table 7.54: Number of counts at second readout after 80 min UV exposure at 80 °C.

Dose	0 mGy	1 mGy	2 mGy	5 mGy	10 mGy	25 mGy
No	Counts	Counts	Counts	Counts	Counts	Counts
1	419	526	394	469	623	1183
2	505	549	663	325	912	926
3	458	424	559	622	751	731
4	493	494	547	595	572	971
5	391	366	534	476	661	694
Average	453 ± 48	472 ± 76	539 ± 96	497 ± 118	704 ± 134	901 ± 198

Table 7.55: Number of counts at second readout after 90 min UV exposure at 80 °C.

Dose	0 mGy	1 mGy	2 mGy	5 mGy	10 mGy	25 mGy
No	Counts	Counts	Counts	Counts	Counts	Counts
1	432	232	503	247	506	926
2	307	255	289	586	645	1026
3	406	384	418	578	561	795
4	252	337	434	260	661	999
5	347	452	464	649	619	642
Average	349 ± 73	332 ± 91	422 ± 81	464 ± 194	598 ± 64	878 ± 159

Table 7.56: Number of counts at second readout after 100 min UV exposure at 80 °C.

Dose	0 mGy	1 mGy	2 mGy	5 mGy	10 mGy	25 mGy
No	Counts	Counts	Counts	Counts	Counts	Counts
1	233	395	668	582	563	891
2	154	382	107	590	631	370
3	390	461	359	562	548	1158
4	244	588	431	950	644	736
5	263	434	410	487	703	394
Average	257 ± 85	452 ± 82	395 ± 200	634 ± 181	618 ± 63	710 ± 335

Table 7.57: Number of counts at second readout after 110 min UV exposure at 80 °C.

Dose	0 mGy	1 mGy	2 mGy	5 mGy	10 mGy	25 mGy
No	Counts	Counts	Counts	Counts	Counts	Counts
1	555	459	354	698	581	504
2	272	470	583	599	487	947
3	321	434	383	565	713	388
4	514	515	322	595	680	1137
5	552	633	489	241	710	1498
Average	443 ± 136	502 ± 79	426 ± 108	540 ± 174	634 ± 98	895 ± 457

Table 7.58: Number of counts at second readout after 120 min UV exposure at 80 °C.

Dose	0 mGy	1 mGy	2 mGy	5 mGy	10 mGy	25 mGy
No	Counts	Counts	Counts	Counts	Counts	Counts
1	480	530	527	434	570	452
2	244	484	519	272	362	880
3	344	418	520	496	593	833
4	322	340	440	433	532	563
5	367	382	473	511	762	876
Average	351 ± 85	431 ± 77	496 ± 38	429 ± 95	564 ± 143	721 ± 199

Table 7.59: Number of counts at second readout after 135 min UV exposure at 80 °C.

Dose	0 mGy	1 mGy	2 mGy	5 mGy	10 mGy	25 mGy
No	Counts	Counts	Counts	Counts	Counts	Counts
1	248	196	268	274	714	784
2	307	408	456	357	485	839
3	131	376	566	548	431	682
4	373	473	609	605	664	603
5	403	430	577	560	393	840
Average	292 ± 108	377 ± 107	495 ± 139	469 ± 145	537 ± 143	750 ± 104

Table 7.60: Number of counts at second readout after 150 min UV exposure at 80 °C.

Dose	0 mGy	1 mGy	2 mGy	5 mGy	10 mGy	25 mGy
No	Counts	Counts	Counts	Counts	Counts	Counts
1	178	523	509	515	619	873
2	215	526	566	574	522	818
3	329	530	736	602	545	640
4	243	283	265	469	518	774
5	334	322	299	448	722	412
Average	260 ± 69	437 ± 123	475 ± 195	522 ± 66	585 ± 87	703 ± 184

Table 7.61: Number of counts at second readout after 165 min UV exposure at 80 °C.

Dose	0 mGy	1 mGy	2 mGy	5 mGy	10 mGy	25 mGy
No	Counts	Counts	Counts	Counts	Counts	Counts
1	319	405	432	534	547	679
2	229	507	327	447	377	616
3	209	409	350	420	626	906
4	383	372	435	500	539	572
5	286	414	314	470	359	1220
Average	285 ± 70	421 ± 51	372 ± 58	474 ± 45	490 ± 116	799 ± 268

Table 7.62: Number of counts at second readout after 180 min UV exposure at 80 °C.

Dose	0 mGy	1 mGy	2 mGy	5 mGy	10 mGy	25 mGy
No	Counts	Counts	Counts	Counts	Counts	Counts
1	436	559	371	494	333	809
2	544	298	172	527	418	1066
3	416	341	345	556	430	865
4	352	452	441	504	562	718
5	324	458	347	445	438	965
Average	414 ± 86	422 ± 104	335 ± 99	505 ± 41	436 ± 82	885 ± 135

Table 7.63: Number of counts at second readout after 195 min UV exposure at 80 °C.

Dose	0 mGy	1 mGy	2 mGy	5 mGy	10 mGy	25 mGy
No	Counts	Counts	Counts	Counts	Counts	Counts
1	298	502	336	540	561	1025
2	515	520	269	451	434	915
3	455	577	542	564	678	383
4	538	509	423	603	446	810
5	468	319	620	389	601	985
Average	455 ± 94	485 ± 98	438 ± 144	509 ± 87	544 ± 93	824 ± 259

Table 7.64: Number of counts at second readout after 210 min UV exposure at 80 °C.

Dose	0 mGy	1 mGy	2 mGy	5 mGy	10 mGy	25 mGy
No	Counts	Counts	Counts	Counts	Counts	Counts
1	377	521	430	580	669	684
2	374	539	368	670	646	242
3	382	557	446	364	497	693
4	507	537	413	536	431	1020
5	486	362	475	337	458	824
Average	425 ± 66	503 ± 80	426 ± 40	497 ± 143	540 ± 110	693 ± 286

Table 7.65: Number of counts at second readout after 225 min UV exposure at 80 °C.

Dose	0 mGy	1 mGy	2 mGy	5 mGy	10 mGy	25 mGy
No	Counts	Counts	Counts	Counts	Counts	Counts
1	266	392	377	441	650	823
2	287	484	387	561	614	878
3	434	270	441	539	555	727
4	327	474	471	493	633	1353
5	348	442	509	544	373	849
Average	332 ± 65	412 ± 87	437 ± 56	516 ± 49	565 ± 113	926 ± 245

Table 7.66: Number of counts at second readout after 240 min UV exposure at 80 °C.

Dose	0 mGy	1 mGy	2 mGy	5 mGy	10 mGy	25 mGy
No	Counts	Counts	Counts	Counts	Counts	Counts
1	346	433	611	664	349	639
2	465	514	510	599	706	777
3	161	554	744	639	574	700
4	153	519	601	425	473	905
5	224	700	335	413	355	491
Average	270 ± 134	544 ± 98	560 ± 151	548 ± 120	491 ± 152	702 ± 154

The results presented in Tab. 7.47—7.66 are shown in Fig. 7.32. And, also in this case, the results are not good enough, although all the detector service was carried out in the darkroom.

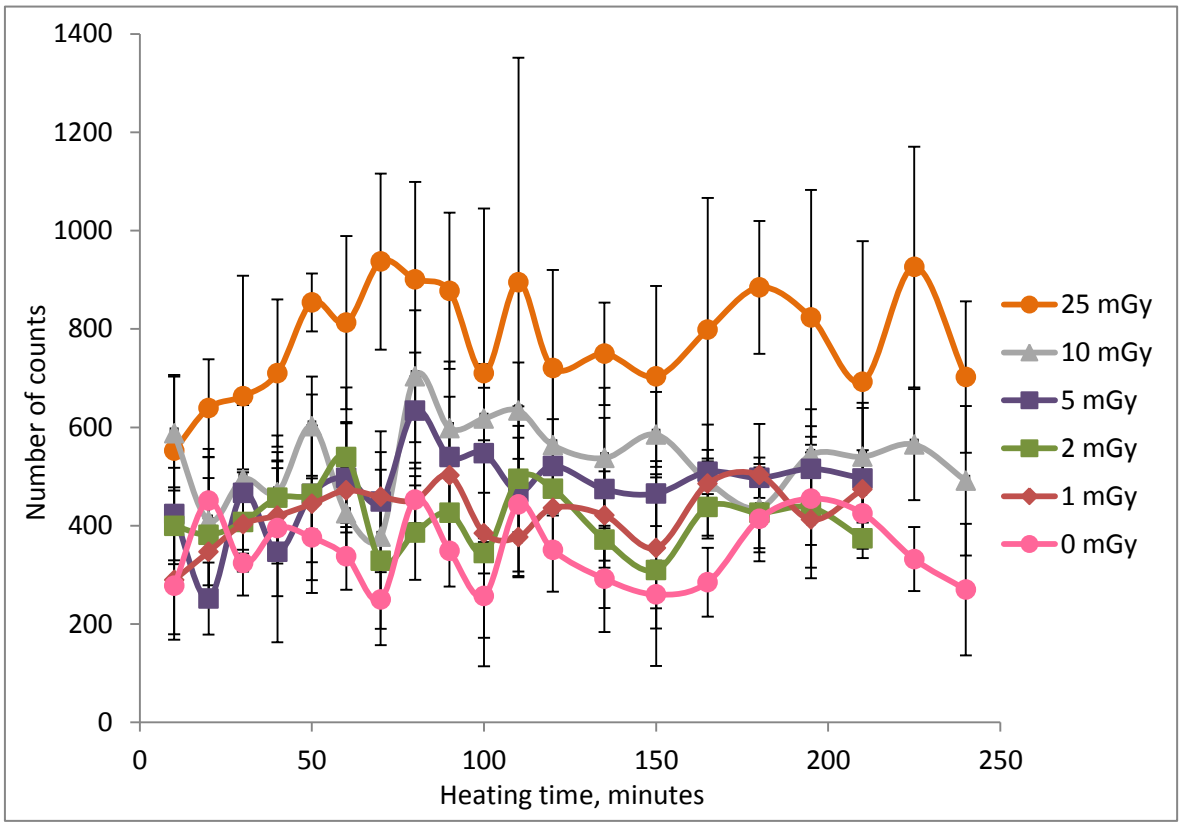

Fig. 7.32: PTTL signal of (0, 1, 2, 5, 10, 25) mGy irradiated MCP-N detectors obtained after UV irradiation with heating temperature of 80 °C at different time of heating and UV exposure.

7.3.4. PTTL Signal Linearity

The signal linearity was examined using the optimal wavelength λ = 254 nm and carried out with a set of data noted in chapter 7.3.1 (Tab. 7.47—7.66, Fig. 7.32). As an example, there are shown results of PTTL signal reading after the UV irradiation and lasting from 30 minutes to 4 hours, performed at temperature of 80 °C.

Figures 7.33—7.37 show the relation between the average value of PTTL counts corresponding to these data and absorbed dose.

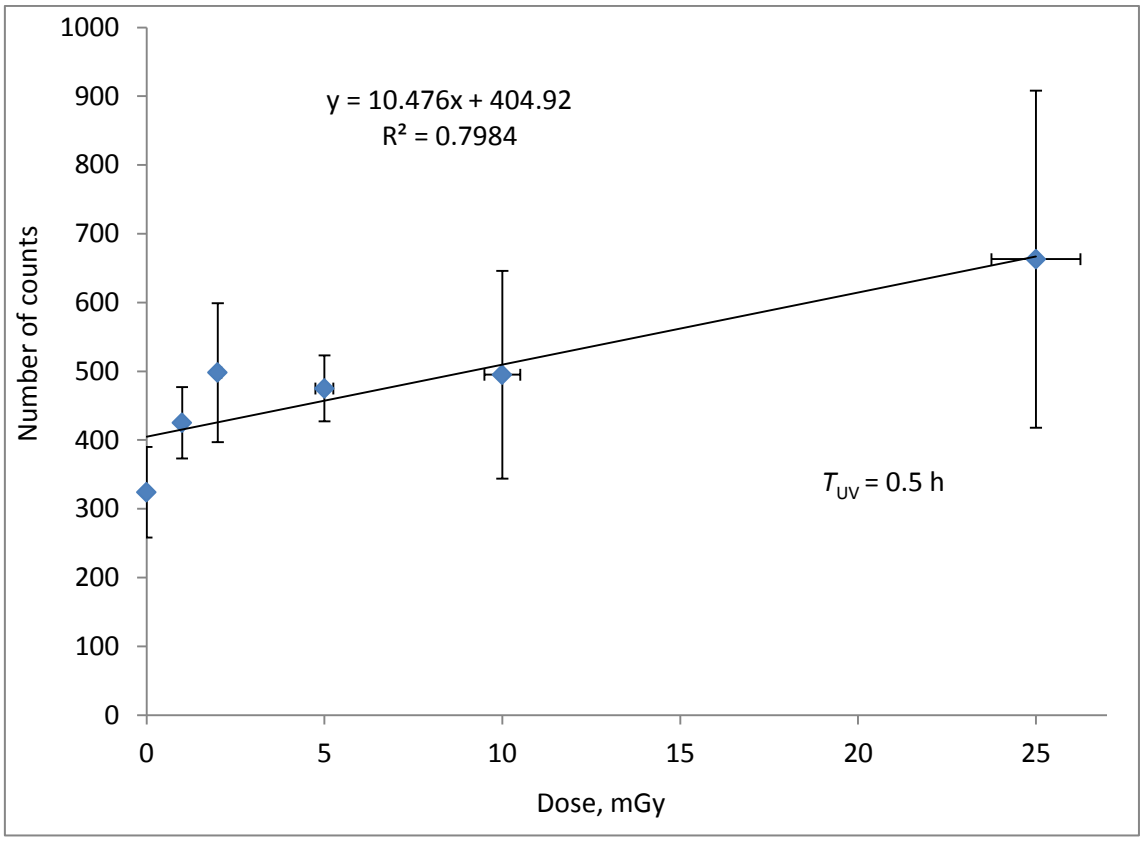

Fig. 7.33. PTTL signal versus dose after 30-minute UV irradiation at 80 °C.

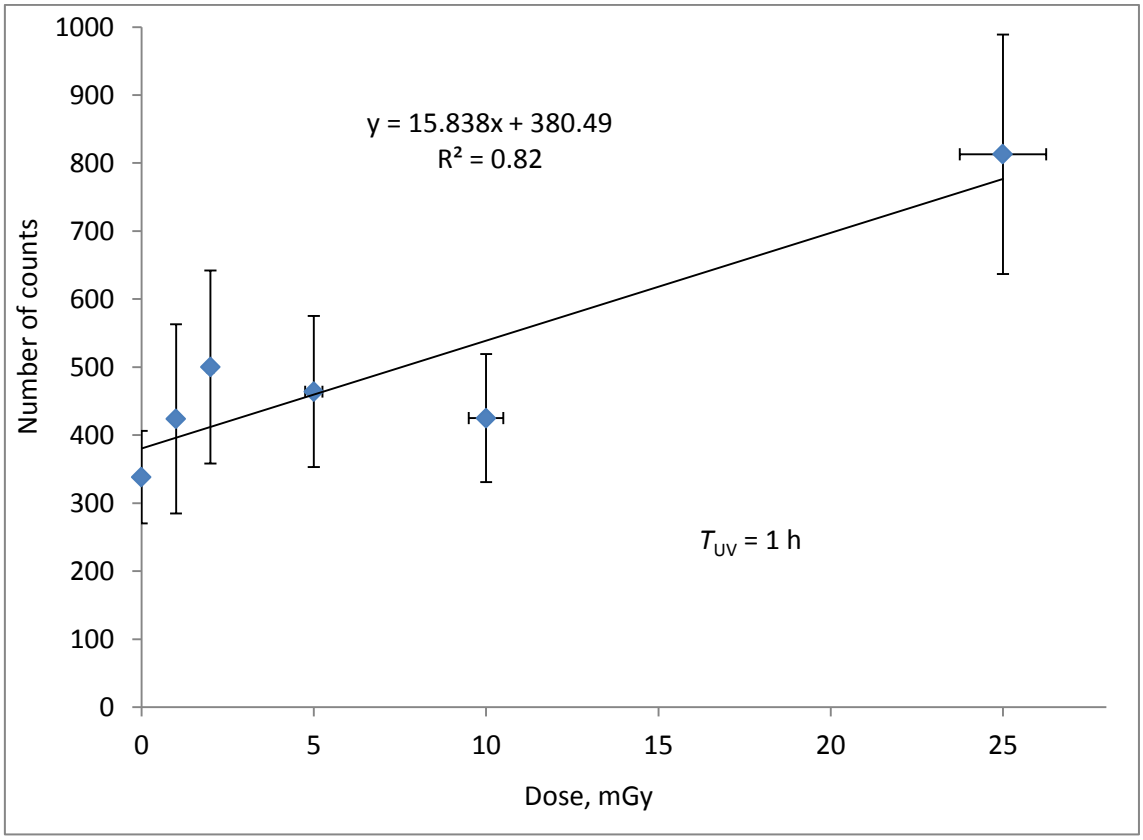

Fig. 7.34. PTTL signal versus dose after 1-hour UV irradiation at 80 °C.

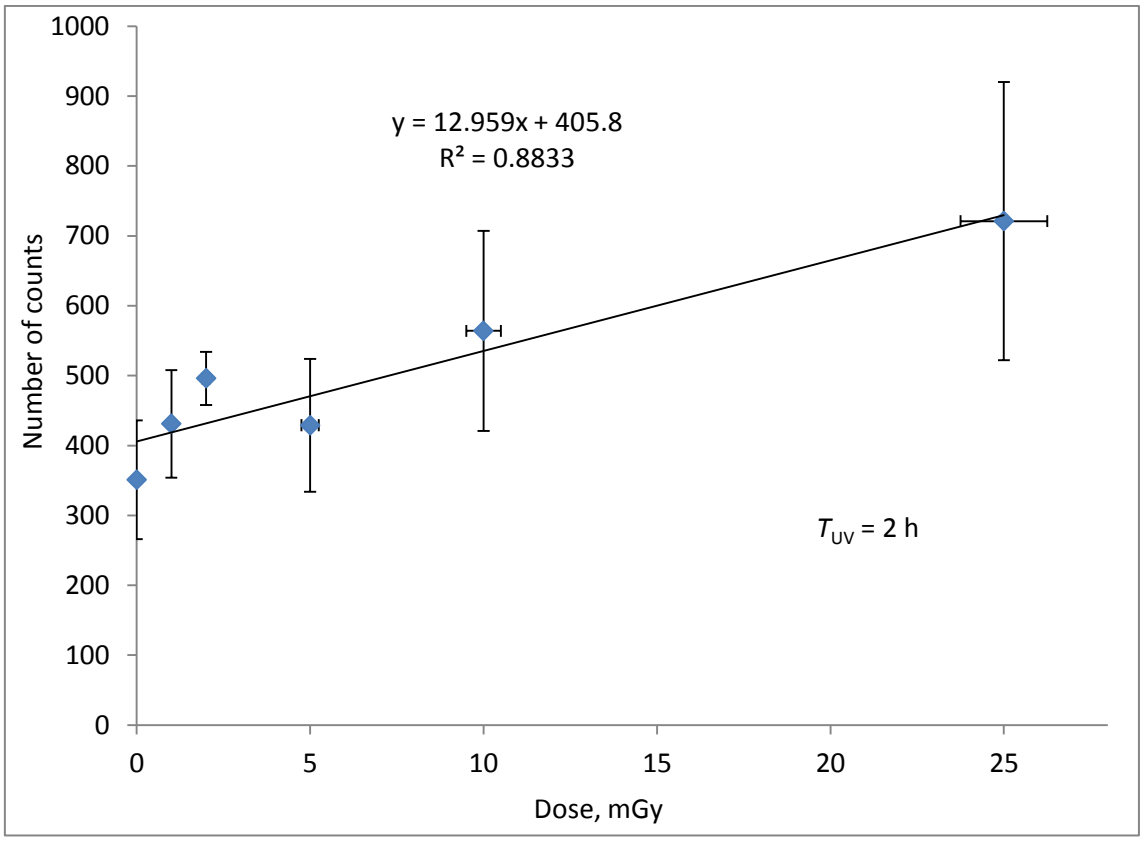

Fig. 7.35. PTTL signal versus dose after 2-hour UV irradiation at 80 °C.

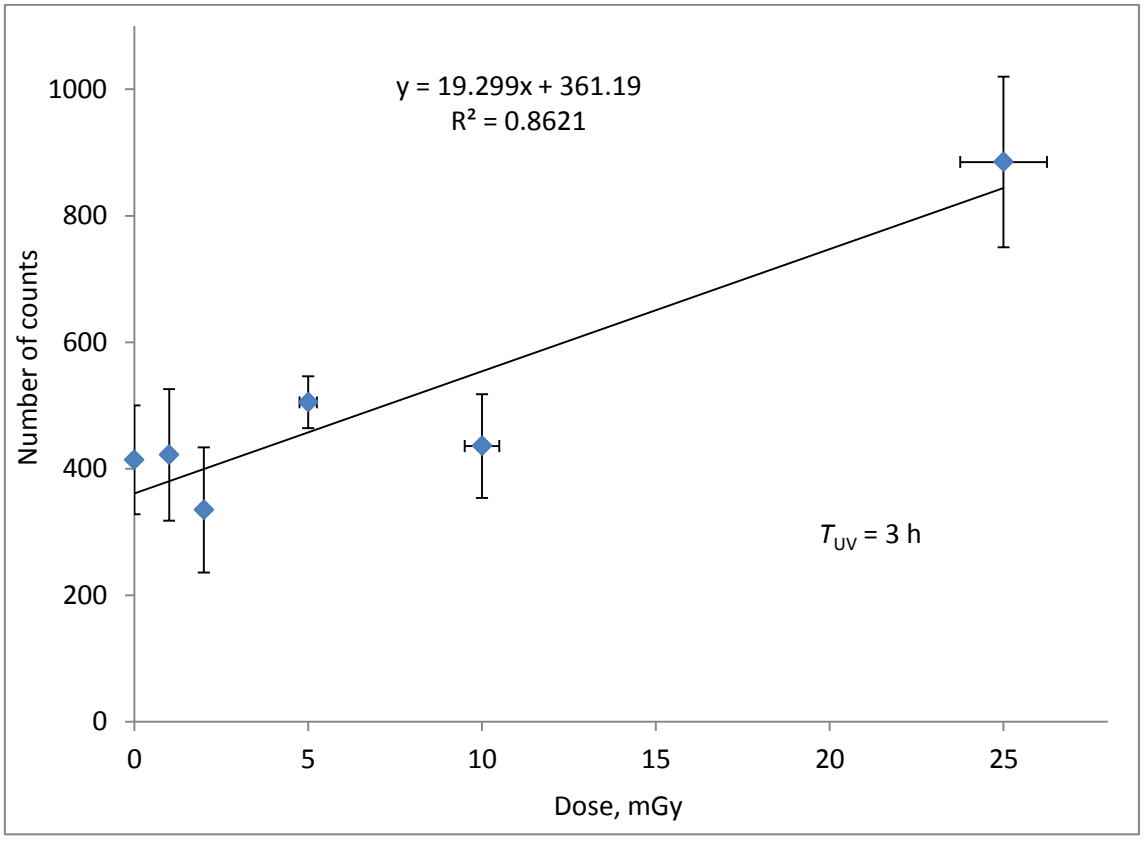

Fig. 7.36. PTTL signal versus dose after 3-hour UV irradiation at 80 °C.

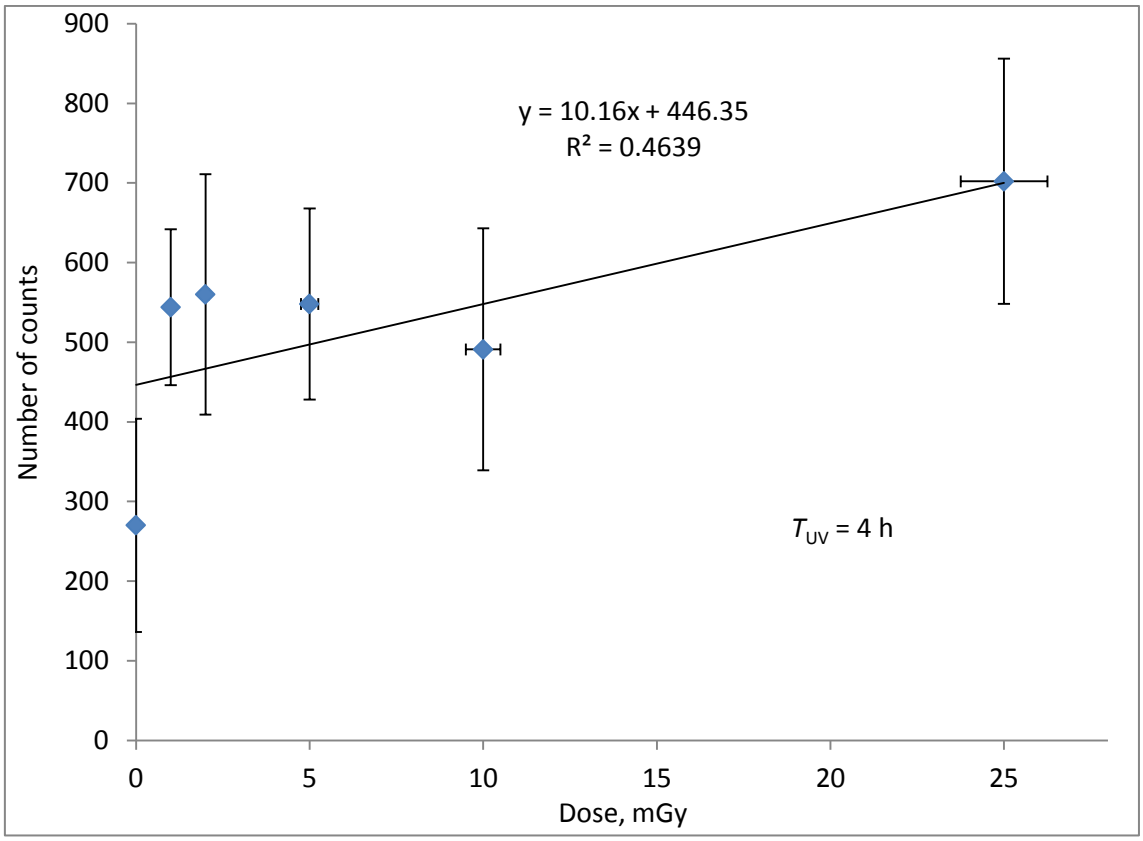

Fig. 7.37. PTTL signal versus dose after 4-hour UV irradiation at 80 °C.

It should be noted, that under the considered conditions of UV exposure and heating, in the dose range up to 25 mGy the PTTL signal linearity is not acceptable. As can be seen in the figures above, the R^2 values for MCP-N detectors are significantly lower than for MTS-N ones, shown in chapter 7.2.4. Moreover, the vertical error bars are relatively big comparing to the range of number of counts variation. The PTTL signal seems to be not sufficient to allow re-evaluation of the dose in the dose range used.

7.3.5. Efficiency of PTTL Method

Thermoluminescence detectors LiF:Mg,Cu,P have entirely different properties comparing to LiF:Mg,Ti ones. They are about 25–30 times more sensitive to photon irradiation than LiF:Mg,Cu,P [74, 83]. The efficiency measurements are described in this chapter using the same calculation methods as in chapter 7.2.5, basing on a relationship between the counts number and dose. The linear approximation of this function is described by the formula

$$N = a\,D + b,$$

where a = (4576 ± 93) mGy^{-1} and b = (1.3 ± 1.0) × 10^3. So the component b is equivalent to the change of counts which is corresponding to a dose change of 0.28 mGy. This is equal to only 1.1 % of the examined dose range.

The same as with MTS-N detectors, the PTTL yield of MCP-N detectors shows a significant deviation from proportionality. For example, in the case of the 2-hours UV exposure at the temperature of 80 °C (Tab. 7.4) coefficients a and b are equal as follows: a = (40 ± 3) mGy^{-1} and b = (0.24 ± 0.03) × 10^3. Similar results were obtained in the second series of measurements (Tab. 7.32, Fig. 7.2): a = (44 ± 3) mGy^{-1} and b = (0.24 ± 0.03) × 10^3. Therefore, in the second reading the intercept b is equivalent to the change of counts corresponding to dose change of about 5.7 mGy, i.e. approximately equal to 23 % of examined dose range.

Moreover, the relative PTTL yield of MCP-N detectors is unsteady. The stability and reproducibility of the LiF:Mg,Cu,P phosphor, despite its applicability in routine radiation protection, cannot fully compete with standard LiF:Mg,Ti phosphors under PTTL measurements. In the third series of measurements under the above-mentioned conditions (Tab. 7.58), significantly different results were obtained: a = (13 ± 3) mGy^{-1} and b = (0.4 ± 0.03) × 10^3. In this case the intercept b is equivalent to the change of counts corresponding to dose change of about 31 mGy, i.e. approximately equal to 125 % of examined dose range.

And finally, the relative efficiency of the PTTL method in relation to routine measurement of MCP-N detectors is very low. Taking into account values of PTTL slope between 13 and 44 per mGy, and 4576 mGy^{-1} at first readout, the relative efficiency is obtained as (0.28–0.96) % only. For comparing, analogous value for MTS-N detectors, given in chapter 7.2.5, reaches up to 13 %. A very large dispersion of results and a large value of measurement uncertainties does not allow the use of the PTTL method for re-evaluation of the dose in the dose range below 25 mGy using the MCP-N detectors.

8. Summary and Conclusions

This work is based on about two thousand readings of TL glow curves. Thermoluminescence detectors of MTS-N and MCP-N type were exposed to X-ray, after which they were subjected to routine reading in the Reader-Analyser RA'04. After the first readout the TL detectors were treated with UV radiation and heating, and then were read in the same Reader-Analyser for the study of PTTL effect. All readings were carried out in the XREADER mode. In this mode, in addition to glow curves the sum of the counts is obtained. Essentially, the data analysis was performed using a number of counts. Data summary, enclosed in chapter 7, is completed by some glow curves.

1. Relationship between number of counts and TL light intensity in the TLD Reader-Analyser RA'04

All TL detectors used were selected before onset of the measurements described in this paper. First, the characteristics of the RA'04 reader were examined: the number of counts from detectors exposed to the same dose as a function of the Test parameter [Chapter 7.1.1]. As a result of this study, the value of the Test parameter equal to 1500 was selected. This value was preserved in all subsequent measurements, hence the **conversion factor between TL light intensity and number of counts remained constant during all readings.** As a result, it is easy to compare the TL and PTTL light emission relative efficiency, defined as the quotient of the change in the number of counts and the dose change: $\Delta N/\Delta D$. For the linear approximation of the $N(D)$ function, this quotient is the slope.

2. Efficiency and linearity of MTS-N and MCP-N detectors at first readout

The PTTL phenomenon was studied using standard-sensitivity detectors (MTS-N) with doses up to 1000 mGy and high-sensitivity detectors (MCP-N) with doses up to 25 mGy. According to manufacturer data, the MCP-N detectors are 25–30 times more sensitive to gamma ray dose than MTS-N ones [74, 83].

The measurements presented in chapter 7 provide the opportunity to compare detection performance. Using linear approximation of the relationship between counts at first readout and a function of dose, the slope was determined as (4576 ± 93) mGy^{-1} for MCP-N detector [Tab. 7.26], and (193.4 ± 2.2) mGy^{-1} for MTS-N detector [Tab. 7.7]. The calculation of the quotient of these two quantities shows that the **efficiency of the MCP-N detector is 24 times greater than the efficiency of the MTS-N detector.** Considering the fact that the measurements were carried out at different X-ray energies, I assume that this result is consistent with the one provided by the manufacturer. Besides, in the paper of Bilski et al. [83] the LiF:Mg,Cu,P detectors are described as 25 times more sensitive to photon radiation than LiF:Mg,Ti. This ratio is almost the same as in this work.

It should be noted that in both cases the linearity of the discussed relationship is excellent: values of R^2 are equal 0.998 and 0.999, respectively. Moreover, both relationships are close to simple proportionality. The intercept is equal to 1303 pulses for MCP-N and 2332 pulses for MTS-N detector. This is equivalent to the dose of 0.28 mGy and 24 mGy, i.e. 1.1 % and 2.4 % of the entire dose range tested.

3. Optimisation of UV radiation wavelength for PTTL measurements

The UV irradiation of TL detectors was performed with UV source allowing irradiation in three wavelengths: 254 nm, 302 nm and 365 nm. A series of measurements was carried out in order to choosing the wavelength value providing the best PTTL yield. The results obtained under the same conditions of UV exposure time and heating temperature show a big difference between the three data sets for three wavelengths: the slope of linear dependence of counts vs. dose for λ = 254 nm is significantly greater than others. The values of coefficients for MCP-N dosimeters were determined as 40/mGy for λ = 254 nm, 9.3/mGy for λ = 302 nm and 7.0/mGy for λ = 365 nm. Due to these results, the main set of **PTTL measurements has been carried out with UV radiation with a wavelength of 254 nm** [chapter 7.1.2].

I suppose that the use of UV radiation with a shorter wavelength would give a better result. Unfortunately, I did not have the option of using a UV source with a different wavelength.

4. PTTL efficiency and linearity of MTS-N and MCP-N detectors

The majority of the measurements concerned the properties of the PTTL phenomenon. Upper limits of dose range were selected accordingly to efficiency of detectors, so at the first readout the counts corresponding to upper dose limit for MTS-N and MCP-N detectors were of the same order of magnitude (about 10^5). Moreover, in both cases the relationship between counts and dose was obtained as close to simple proportionality.

Unlike, the second readout has a different character:

- PTTL counts are significantly smaller than counts at first readout,
- the relationship between counts and dose differs significantly from simple proportionality,
- counts received in a series of measurements under identical conditions are widely scattered.

The PTTL readouts for MTS-N and MCP-N detectors are very different. They are described below.

■ MTS-N detectors (absorbed dose range up to 1000 mGy)

Results described in chapter 7.2 (see Fig. 7.16 and 7.17) indicate that the best conditions of heating and UV exposure for optimisation of PTTL yield are as follows: temperature 80 °C and duration of UV exposure and heating between 0.5 and 4 hours. Some relationships between the number of counts and the dose are presented in Fig. 7.18—7.22 and analysed in chapter 7.2.5. In order to compare the PTTL properties, the data has been collected in the table 8.1.

Table 8.1: Efficiency and R^2 for MTS-N detectors.

Time of UV exposure and heating, h	$\Delta N/\Delta D$ mGy^{-1}	R^2	Data source (Table)
First readout	193.4 ± 2.2	0.9995	7.7
Second readout (PTTL) after 80 °C heating			
0.5	25.2 ± 1.9	0.9835	7.16
1	21.8 ± 1.3	0.9901	7.17
2 (meas. 1)	21.1 ± 3.3	0.9308	7.12
2 (meas. 2)	21.9 ± 1.0	0.9939	7.18
3	23.3 ± 1.4	0.9895	7.19
4	15.7 ± 1.5	0.9728	7.20

Comparing the efficiency of second and first readout, the information that **for UV exposure time from 1 hour to 3 hours and heating at 80 °C, the relative PTTL reading performance reaches (11–13) % of the first reading** was obtained. For longer times of UV exposure the PTTL relative efficiency is smaller. It is worth checking. It is worth checking whether a shorter UV exposure time would allow for higher relative efficiency. In addition, it should be emphasized that high R^2 values were obtained in these measurements, so the linearity is at a satisfactory level. Generally, **the second readout of MTS-N detectors after heat treatment and UV exposure under optimal conditions enables a satisfactory dose reassessment for doses in the order of hundreds of mGy.**

- **MCP-N detectors (absorbed dose range up to 25 mGy)**

The analysis of the properties of MCP-N detectors is based on the data contained in chapter 7.3. A summary presentation of data representing number of PTTL counts (see Fig. 7.30, 7.31 and 7.32) indicate that **the counts are subjected to significant fluctuations.** Unlike MTS-N detectors, there is practically impossible to determine optimal conditions.

The first series of PTTL measurements was performed with UV exposure and heating within 2 hours, at the temperature range between 30 and 120 °C (Fig. 7.30). Because very large variation in results was noted, in the following series of measurements the conditions were changed: **the TL detectors treatment after first readout was carried out in a darkroom** and additionally time of heating was reduced to 1 hour. Unfortunately, the darkroom treatment did not improve the results: very **large variation in results was remained** (Fig. 7.31).

Likewise as in the case of MTS-N detectors, some data were collected in the table (Tab. 8.2).

Comparing the efficiency of second and first readout allows us to calculate that **the relative PTTL reading performance reaches only about 0.9 % of the first reading data**, which is a very bad result comparing to (11–13) % for MTS-N detectors.

Table 8.2: Efficiency and R^2 for MCP-N detectors.

Time of UV exposure and heating, h	$\Delta N/\Delta D$ mGy^{-1}	R^2	Data source (Table)
First readout	4576 ± 93	0.9980	7.26
Second readout (PTTL) after 80 °C heating			
0.5	10.5 ± 2.6	0.7984	7.49
1	15.8 ± 3.7	0.8200	7.52
2 (meas. 1)	40.0 ± 2.4	0.9825	7.4
2 (meas. 2)	44.1 ± 2.9	0.9784	7.32
2 (meas. 3)	13.0 ± 2.4	0.8833	7.58
3	19.3 ± 3.9	0.8621	7.62
4	10.2 ± 5.5	0.4639	7.20

Summarising:

- In routine TL readings the MCP-N detectors are 25–30 times more sensitive than MTS-N ones. But in a study of PTTL yield, their performance, regrettably, it turned out to be much worse: it is roughly the same as for MTS-N detectors.
- Experimental results show that applying UV radiation with a wavelength λ = 254 nm causes appearance of TL signal which is not enough to determine the dose of the previously read detectors in the dose range below 25 mGy in MCP-N detectors, so in this range the phenomenon of PTTL is not suitable for a dose reassessment. Furthermore, the standard deviation of the count numbers exceeds the coun difference corresponding to a dose difference of about a few mGy. In many cases, the number of PTTL counts decreases as the dose increases.
- The PTTL counts for a dose of 25 mGy are significantly bigger than the counts related to a smaller dose at all heating time values. It can be assumed that for the doses exceeding 25 mGy the relationship between the dose and PTTL counts may become appropriate to the dose reassessment. I assume that in the same dose range as in MTS-N measurements, i.e. of a few hundred mGy, it is possible to achieve satisfying results.

5. Final remarks

I would like to add that I am aware that there is still a lot to be done within the chosen topic. Unfortunately, the time limit for my studies is coming to an end. Unlike the MTS-N detectors, the high efficiency of MCP-N detectors is strongly reduced when the PPTL yield is examined. If I could continue the measurements, first of all I would study the PTTL yield in MCP-N detectors in the same dose range as MTS-N detectors.

References

[1] Radiation Protection and Safety for Industrial X-ray Equipment; Safety Code 34; Safe Environments Programme Healthy Environments and Consumer Safety Branch 03-HECS-333, 2003

[2] Introduction to Dosimetry; Canadian Nuclear Safety Commission, INFO-0827, February 2012

[3] T. Hargreaves, R. Moridi: X-Ray Safety Awareness Handbook; Radiation Safety Institute of Canada, February 16, 2010

[4] E.B. Podgoršak: Radiation Physics for Medical Physicist; Springer-Verlag Berlin Heidelberg 2006

[5] H. Stadtmann: Dose quantities in radiation protection and dosimeter calibration; Radiat. Prot. Dosim. 2001, Vol 96 (1–3)

[6] Fundamental Quantities and Units for Ionizing Radiation; J. ICRU Vol 11 (1), Report 85, April 2011

[7] A. Auvinen: Cancer risk from low doses of ionizing radiation; Finnish Centre for Radiation and Nuclear Safety, University of Tampere, School of Public Health; PhD thesis, Helsinki 1997

[8] Radiation Quantities and Units, ICRU Report 10a; National Bureau of Standards, Handbook 84, 1962

[9] The 2007 Recommendations of the International Commission on Radiological Protection; Annals of the ICRP, Publication 103; published for The International Commission on Radiological Protection by Elsevier, 2007

[10] Dose equivalent: Supplement to ICRU Report 19; ICRU Rep. No. 19S, ICRU, Washington D.C. 1973

[11] Quantities and Units in Radiation Protection Dosimetry, J. ICRU Vol os-26 (2), Report 51, September 1993

[12] Determination of dose equivalents resulting from external radiation sources; J. ICRU Vol os-20 (2), Report 39 Part 1, February 1985

[13] C.A. Carlsson, G.A. Carlsson, E. Lund, G. Matscheko, H.B.L. Pettersson: An Instrument for Measuring Ambient Dose Equivalent, $H^*(10)$; Radiat. Prot. Dosim. 1996, Vol 67 (1)

[14] J. Magill, J. Galy: Radioactivity·Radionuclides Radiation; Springer-Verlag Berlin Heidelberg and European Communities, 2005

[15] L. Munro: Basics of Radiation Protection — How to achieve ALARA: Working Tips and guidelines; World Health Organization, Geneva 2004

[16] IAEA: International Basic Safety Standards for Protection against Ionizing Radiation and for the Safety of Radiation Sources; Safety Series No. 115, Vienna 1996

[17] IAEA Safety Standards for protecting people and the environment: Radiation Protection and Safety in Medical Uses of Ionizing Radiation; Specific Safety Guide No. SSG-46, IAEA 2014

[18] Radiation Safety Training Module: Diagnostic Radiology; Radiation Protection in Diagnostic Radiology, Radiological Safety Division; Government of India, Atomic Energy Regulatory Board, 2017 (https://aerb.gov.in/images/PDF/DiagnosticRadiology/RADIATION-PROTECTION-IN-DIAGNOSTIC-RADIOLOGY.pdf)

[19] D.R. Dance, S. Christofides, A.D.A. Maidment, I.D. McLean, K.H. Ng (Eds.): Diagnostic Radiology Physics — A Handbook for Teachers and Students; IAEA, Vienna 2014

[20] M.J. Aitken: Thermoluminescence Dating; Academic Press, London 1985

[21] K.V.R. Murthy, H.S. Virk: Luminescence Phenomena: An Introduction; Defect and Diffusion Forum 2014, Vol 347

[22] S.W.S. McKeever: Thermoluminescence of Solids; Cambridge University press, 1985

[23] D.R. Vij (Ed.): Luminescence of Solids; Plenum Press, New York, 1998

[24] A.F. McKinley: Thermoluminescence dosimetry; Medical Physics Handbooks series 5, Adam Hilger Ltd., Bristol 1981

[25] M.O. Akpochafor, M.A. Aweda, Z.A. Ibitoye, S.O. Adeneye: Thermoluminescent dosimetry in clinical kilovoltage beams; Radiography 2013 Vol 19 (4)

[26] F.H. Attix: Introduction to radiological physics and radiation dosimetry; John Wiley and Sons, 1986, and Wiley VCH Verlag GmbH & Co. KGaA, Weinheim 2004

[27] J. Van Dam, G. Marinello: Methods for in vivo dosimetry in external radiotherapy; 2nd ed.; ESTRO, Brussels, 2006

[28] A.J.J. Bos: High sensitivity thermoluminescence dosimetry; Nucl. Instrum. Meth. B 2001, Vol 184 (1–2)

[29] R. Chen, S.W.S. McKeever: Theory of Thermoluminescence and Related Phenomena; World Scientific Publishing Co. Pte. Ltd., Singapore 1997

[30] C. Furetta: Handbook of Thermoluminescence; World Scientific Publishing Co. Pte. Ltd., Singapore 2009 [2003 1st ed.]

[31] S.W.S. McKeever, M. Moscovitch, P.D. Townsend: Thermoluminescence Dosimetry Materials: Properties and Uses; Ramtrans Publishing / Nuclear Technology Publishing, Ashford, England 1995

[32] H. Aboud, R. Hussin, H. Wagiran: Mechanism of Thermoluminescence International Journal of Scientific & Engineering Research, October-2012, Vole 3 (10)

[33] D. Schauer, A. Brodsky, J. Sayeg: Handbook of Radioactivity Analysis; Second Edition; Academic Press, Great Britain 2003

[34] A.J.J. Bos: Theory of Thermoluminescence; Radiat. Meas. 2007, Vol 41, Supplement 1

[35] J.T. Randall, M.H.F. Wilkins: Phosphorescence and Electron Traps. I. The Study of Trap Distributions; Proc. R. Soc. Lond. Ser-A 1945, Vol 184 (A999)

[36] J.T. Randall, M.H.F. Wilkins: Phosphorescence and Electron Traps. II. The Interpretation of Long-Period Phosphorescence; Proc. R. Soc. Lond. Ser-A 1945, Vol 184 (A999)

[37] D. A. Sono: Potential TLD materials for use as ultraviolet radiation dosimeters; Oklahoma State University, MSc thesis 2000

[38] A.P. Hufton (Ed.): Practical Aspects of Thermoluminescence Dosimetry; Proceedings of the Hospital Physicists' Association Meeting on Practical Aspects of TLD, held at the University of Manchester on 29th March, 1984; Conference Report Series 43, The Hospital Physicists' Association, London 1984

[39] J.F. Fowler, F.H. Attix: Solid State Integrating Dosimeters; In: F.H. Attix, W.C. Roesch (Eds.): Radiation Dosimetry, Vol 2: Instrumentation; 2nd ed., Chap 14; Academic Press, New York, London 1967

[40] G. Wilding: Linearity and residual dose correction of a LiF:Mg,Ti thermoluminescence dosimeter; Graz University of Technology, MSc thesis 2015

[41] P. Bilski, P. Olko, M. Puchalska, B. Obryk, M.P.R. Waligórski, J.L. Kim: High-dose characterization of different LiF phosphors; Radiat. Meas. 2007, Vol 42 (4–5)

[42] Y.S. Horowitz: Theory of thermoluminescence gamma dose response: The unified interaction model; Nucl. Instrum. Meth. B 2001,Vol 184 (1–2)

[43] J. Livingstone: Solid-state micro- and nano- dosimetry: theory and applications; University of Wollongong, PhD thesis; 2014

[44] G.F. Knoll: Radiation Detection and Measurement, 4th ed.; John Wiley and Sons, Inc., New York, 2010

[45] P.K. Papadogiannis: Dosimetry of upper extremities of personnel in nuclear medicine hot labs; University of Patra, School of Medicine, Department of Physics, 2012

[46] A.N. Al-Haj, C.S. Lagarde: Glow Curve Evaluation in Routine Personal Dosimetry; Health Phys. 86, Supplement 1, 2004

[47] RADAT — Dosimetry Laboratory Services, Turkey (https://www.radat.com.tr/index_en.php)

[48] Doğan Yaşar, Bayram Demir, Erol Kam, Gürsel Karahan, Murat Okutan: A New TLD Holder for External Radiotherapy Beam Audit; SDU Journal of Science (E-Journal), Turkey 2013, Vol 8 (1)

[49] M. Budzanowski: Ocena przydatności ultraczułych detektorów termoluminescencyjnych LiF:Mg,Cu,P (MCP-N) w dozymetrii promieniowania gamma w środowisku; IFJ Report, 1875/D, Institute of Nuclear Physics, Cracow 2001

[50] M. Oberhofer, A. Scharmann (Eds.): Applied Thermoluminescence Dosimetry; Adam Hilger Ltd., Bristol 1981

[51] T.H. Kirby, W.F. Hanson, D.A. Johnston: Uncertainty analysis of absorbed dose calculations from thermoluminescence dosimeters; Medical Physics. 1992, Vol 19 (6)

[52] P. Bilski: Lithium fluoride: From LiF:Mg,Ti to LiF:Mg,Cu,P; Radiat. Prot Dosim. 2002, Vol 100 (1–4)

[53] A. D. Herr: Phototransfer Thermoluminescence Applied to the Re-Estimation of Low Dose Levels of Ionizing Radiation for Personnel Dosimetry; Georgetown University, Washington D.C., MSc thesis, April 23, 2010

[54] P. Olko: Advantages and disadvantages of luminescence dosimetry; Radiat. Meas. 2010, Vol 45 (3–6)

[55] J.S. Nagpal: Ultraviolet Dosimetry using Thermoluminescent Phosphors — An Update; BARC/1998/E/007, Bhabha Atomic Research Centre, Mumbay 1998

[56] D. Hughes: Hazards of Occupational Exposure to Ultraviolet Radiation; British Occupational Hygiene Society, London; Monography, No: 1, University of Leeds, Industrial Services Ltd, Science Reviews; Northern Office, 1978

[57] Health and Environmental Effects of Ultraviolet Radiation; A Scientific Summary of Environmental Health Criteria 160; Ultraviolet Radiation; WHO/EHG/95.16; World Health Organization, Geneva, 1995

[58] C.G. Orton: Radiation Dosimetry — Physical and Biological Aspects; Plenum Press, New York and London; Springer Science+Bussiness Media, New York 1986

[59] H. Cember, T.E. Johnson: Introduction to Health Physics, Fourth Edition, , McGraw-Hill Education / Medical 2009

[60] A. Karpińska: Zastosowanie promieniowania UV w uzupełniającej ocenie dawki z zastosowaniem detektorów termoluminescencyjnych typu MTS-N; thesis, University of Łódź, 2016 a

[61] C.S. Alexander, S.W.S. McKeever: Phototransferred thermoluminescence; J. Phys. D: Appl. Phys. 1998, Vol 31

[62] T. Niewiadomski: Dozymetria termoluminescencyjna w praktyce; IFJ Report, 1550/D, Institute of Nuclear Physics, Cracow 1991

[63] A.G. Wintle, A.S. Murray: The relationship between quartz thermoluminescence, phototransferred thermoluminescence and optically stimulated luminescence; Radiat. Meas. 1997, Vol 27 (4)

[64] C.S. Alexander, M.F. Morris, and S.W.S. McKeever: The Time and Wavelength Response of Phototransferred Thermoluminescence in Natural and Synthetic Quartz; Radiat. Meas. 1997, Vol 27 (2)

[65] J.A. Nieto: Thermoluminescence Dosimetry (TLD) and its Application in Medical Physics; Eighth Mexican Symposium on Medical Physics; AIP Conference Proceedings Vol 724 (1), American Institute of Physics 2004

[66] F. Daniels, C.A. Boyd, D.F. Saunders: Thermoluminescence as a Research Tool; Science 1953, Vol 117 (3040)

[67] J. M. Oduko: Thermoluminescence: Materials and Applications; University of Surrey, Guildford, Surrey; PhD thesis, June 1992

[68] M. Ranogajec-Komor: Thermoluminescence Dosimetry — Application in Environmental Monitoring; Radiation Safety Management, Vol 2 (1) 2003

[69] DOE Fundamentals Handbook: Instrumentation and Control, Vol.2; U.S. Department of Energy, Washington D.C. 1992

[70] W.S.C. Williams: Nuclear and Particle Physics; Oxford University Press / Clarendon Press 1991

[71] R.R. Burn: Introduction to Nuclear Reactor Operation; Detroit Edison Company, University of Michigan, 1988

[72] E.B Podgorsak (Ed.): Radiation Oncology Physics: A Handbook for Teachers and Students; IAEA, Vienna, 2005

[73] User Manual of Mobile Radiographic Unit Basic 4003-4006, Italy 2011

[74] www.radcard.pl (TL detectors manufacturer's website)

[75] P. Bilski, P. Olko, M. Budzanowski, E. Ryba, M.P.R Waligórski: 10 Years of Experience with High-Sensitive LiF:Mg,Cu,P (MCP-N) Thermoluminescent Detectors in Radiation Dosimetry; Proc. of IRPA Regional Symp. on Radiation Protection in Neighbouring Countries of Central Europe 1997, Prague, Czech Republic, 8–12 September 1997; 1998

[76] Laboratoryjny czytnik/analizator materiałów termoluminescencyjnych RA'04 (User manual for the laboratory TLD Reader-Analyser RA'04); Mikrolab, Cracow 2011

[77] www.magmatherm.com (Magma MT 1105 Therm-E4 furnace manufacturer's website)

[78] Instrukcja użytkowania – suszarka uniwersalna z elektronicznym regulatorem temperatury SUP-18W (User manual for the laboratory annealing furnace/drier SUP-18W), Warsaw 2013

[79] Life Science Tools and Technology — Ultraviolet Products, Light Sources, Laboratory Products, BioImaging Systems; UVP An Analytic Jena Company; UVP, LLC 2014

[80] Barracuda & QABrowser Reference Manual, Version 4.3A, RTI 2012

[81] M. Budzanowski, A. Sas-Bieniarz, P. Bilski, A. Bubak, R. Kopeć: Dose reassessment by using PTTL method in MTS-N (LiF:Mg,Ti) thermoluminescent detectors; Proceedings of the 8th International Conference on Luminescent Detectors and Transformers of Ionizing Radiation LUMDETR 2012; Radiat. Meas. 2013, Vol 56

[82] J.L. Muñiz, V. Correcher, A. Delgado: PTTL Dose Re-estimation Applied to Quality Control in TLD-100 Based Personal Dosimetry; Radiat. Prot. Dosim. 1999, Vol 85 (1–4)

[83] P. Bilski, P. Olko, B. Burgkhardt, E. Piesch, M.P.R Waligórski: Thermoluminescence Efficiency of LiF:Mg,Cu,P (MCP-N) Detectors to Photons, Beta-Electrons, Alpha Particles and Thermal Neutrons; Radiat. Prot. Dosim. 1994, Vol 55 (1)

List of Publications

Publications in journals not included in thesis

1. Atheer Q. Mryoush, **Hiba M. Salim:** Determination of Uranium Concentration in Soil of Baghdad Governorate and its Effect on Mitotic Index Assay; Iraqi Journal of Science 2015, Vol 56, No. 1A, 140–146
2. Małgorzata Wrzesień, Łukasz Albiniak, **Hiba Al-Hameed:** MTS-6 detectors calibration by using ^{239}Pu-Be neutron source; Medycyna Pracy 2017, Vol 68 (6), 705–710
3. **Hiba M. Salim Al-Hameed:** Measurement of Radioactivity in Marsh Sediments of South Iraq; IOSR Journal of Applied Physics (IOSR-JAP), e-ISSN 2278--4861, Vol 10, Issue 3 Ver III May – June 2018, 43–49